MODELING UNCERTAINTY IN FISH POPULATION DYNAMICS

YAN JIAO

Your file Votre référence
ISBN: 0-612-99036-2
Our file Notre référence
ISBN: 0-612-99036-2

Modeling uncertainty in fish population dynamics

by

© Yan Jiao

A dissertation submitted to the School of Graduate Studies

in partial fulfillment of the

requirements for the degree of

Doctor of Philosophy

Department of Biology

Memorial University of Newfoundland

2004

St. John's Newfoundland Canada

ABSTRACT

Large uncertainties may exist in modeling various processes determining fisheries population dynamics. The uncertainties may come from various sources such as environmental variations (process errors), measurement errors, and model errors. In order to quantify the uncertainties, an understanding of the complex model error structure in the population dynamic models and how the model error structure affects the parameter estimation is important. In this study I evaluated and quantified the uncertainties in modeling various processes of fisheries population dynamics using Monte Carlo simulations and applied the proposed methods to Atlantic cod stocks.

The generalized linear model approach, which can readily deal with different error structures, were used to identify suitable model error structure in stock-recruitment modeling, stock biomass modeling, and age-structure population modeling. A simulation study was developed to evaluate the influence of stock mixing on the collection of fish growth data and estimation of growth parameters. The recent status of the Atlantic cod fishery in Divisions 2J3KL was evaluated using a composite risk assessment method which calculates the total risk of overexploitation in the cod fishery. I considered the uncertainties in both biological reference point and current fishing mortality estimates.

I recommend that the generalized linear model be used to identify appropriate model error structures in stock-recruitment modeling, stock biomass modeling, and age-structure population modeling. I also suggest that stock mixing be incorporated into stock assessment models to improve the estimation of growth parameters in stock assessment.

Uncertainty in both management reference points and in indicator reference points should be considered in evaluating stock status using the proposed composite risk assessment method.

ACKNOWLEDGEMENTS

First and foremost I would like to thank my supervisors, Dr. Joe Wroblewski of MUN and Dr. Yong Chen of the University of Maine, who during the course of my research and in a timely manner gave me encouragement and guidance. Their insightful understanding and care have made my study enjoyable and beneficial during the past three years.

I also wish to thank the members of my supervisory committee, Dr. Brad de Young of MUN and Dr. Noel Cadigan of DFO, for always making their time available when help was needed. I appreciate the help from Dr. David Schneider, Dr. Paul Peng and Dr. Chu-In Charles Li of MUN, who gave me valuable advice. The assistance of Dr. George Lilly and Dr. Peter Shelton of DFO was valuable. They provided me good advice and references on Atlantic cod.

I was generously supported by a CIDA/MUN (Canadian International Development Agency/Memorial University of Newfoundland) Marine Science Scholarship, the Royal Bank Fellowship in Marine Studies, and a SSHRCC-DFO Ocean Management Network Sustainability Group Graduate Student Research Grant. Many thanks to Ms. Colleen Clarke and Dr. Dickinson of the International Center at MUN, who administered this scholarship and gave me kind help in everyday life. A computer and conference travel funds were provided by the Coasts Under Stress research project. The Social Sciences and Humanities Research Council of Canada (SSHRC), and the Natural Sciences and Engineering Research Council of Canada (NSERC) provided the major funds for the "Coasts Under Stress" Project through the SSHRC Major collaborative Research Initiatives (MCRI) program.

TABLE OF CONTENTS

LIST OF TABLES

LIST OF FIGURES

LIST OF ABBREVIATIONS AND SYMBOLS

Abbreviations

BRP --- biological reference point
CI --- comparison index
CV --- coefficient of variation
GzLM --- generalized linear model
ICES --- the International Council for the Exploitation of the Sea
NAFO --- Northwest Atlantic Fisheries Organization
p.d.f. --- probability density function
REB --- relative estimation bias
REE --- relative estimate error
RMSE --- root mean square error
SPA --- sequential population analysis
SR --- stock-recruitment
TAC --- total allowable catch
VPA --- virtual population analysis
YPR --- yield-per-recruit

Symbols

B_0 --- stock biomass at the beginning of the fishery

B_{msy} --- Biomass at MSY. Biomass corresponding to Maximum Sustainable Yield from a production model or from an age-based analysis using a stock-recruitment model. Often used as a biological reference point in fisheries management, it is the calculated long-term average biomass value expected if fishing at F_{MSY}.

B_t --- stock biomass in year t

C_t --- catch in year t

$C_{a,y}$ --- is the catch in number of age a and in year y

cdf --- cumulative distribution function

d --- shape parameter in discarding model

$d50$ --- age at which 50% of the individuals are vulnerable to be discarded

F --- fishing mortality

$F_{0.1}$ --- A biological reference point. The fishing mortality rate at which the marginal yield-per-recruit (i.e. the increase in yield-per-recruit in weight for an increase in one unit of fishing mortality) is only 10 percent of the marginal yield-per-recruit on the unexploited stock. The fishing mortality rate at which the slope of the yield-per-recruit curve is only one-tenth the slope of the curve at its origin.

F_{cur} --- current fishing mortality

$F_{\max}$ --- A biological reference point. It is the fishing mortality rate that maximizes equilibrium yield-per-recruit.

F_{msy} --- fishing mortality rate which, if applied constantly, would result in Maximum Sustainable Yield (MSY).

G_t --- surplus production of stock biomass in year t

I_t --- a biomass index observed in the fishery or surveys in year t

$I_{a,y}$ --- research vessel survey index expressed as mean numbers per tow at age a and in year y

k --- Brody growth parameter in length-at-age model and weight-at-age model

K --- carrying capacity or virgin biomass

L --- likelihood function

LL --- the loglikelihood function

L_a --- length-at-age data

L_∞ --- maximum attainable length

m --- shape parameter in the selectivity model

M --- natural mortality

$N(\mu,\sigma^2)$ --- define a normal distribution with the mean of μ and variance σ^2

$N_{a,y}$ --- number alive at age a at the beginning of year y,

ND_t --- number of fishes caught at age t that are discarded at sea

$P(Y > X)$ --- probability of Y larger than X

$P_{a,y}$ --- proportion of catch-at-age

q --- catchability coefficient

r --- parameter describing the stock intrinsic growth rate

R --- recruitment

S --- stock abundance or biomass

s_j --- selectivity coefficient for fish at age j, $s_j = \dfrac{1}{1+e^{-m(j-S50)}}$

$S50$ --- age at which 50% of the individuals are vulnerable to the fishing gear in the selectivity model

$t0$ --- hypothetical age at which the length is 0 in the length-at-age model or the weight is 0 in the weight-at-age model

t_l --- maximum age of fish that could contribute to the fishery

t_r --- age of entry into the fishery

$U(0,1)$ --- uniform distribution between 0 and 1

W_t --- weight-at-age

W_∞ --- maximum attainable weight

Y --- attained yield

α --- parameter in the Cushing, Ricker, and Beverton-Holt models

β --- parameter in the Cushing, Ricker, and Beverton-Holt models

β^*_i --- estimated parameter value in the ith simulation

ε --- error term

ε_n --- error term that follows normal distribution

ε_g --- error term that follows gamma distribution

ε_p --- error term that follows Poisson distribution

$\boldsymbol{\eta}$ --- A linear predictor, which is given by $\boldsymbol{\eta} = \sum_{j=1}^{p} \mathbf{X}_j \beta_j$

μ --- mean of an estimated parameter

σ --- standard deviation of an estimated parameter

LIST OF APPENDICES

CO-AUTHORSHIP STATEMENT

Chapters 2 and 3 in this thesis were written by myself. They have been accepted for publication in the *Canadian Journal of Fisheries and Aquatic Science*. Dr. Schneider, Dr. Chen and Dr. Wroblewski provided advice, and also edited the papers. They are co-authors.

Chapter 4 and Chapter 5 in this thesis were written by myself. The latter one has been submitted to *Canadian Journal of Fisheries and Aquatic Science*. Dr. Chen and Dr. Wroblewski provided advice, and also edited the paper. They are co-authors.

Chapter 6 in this thesis was written by myself. It has been submitted to *Fisheries Research*. Dr. Chen and Dr. Wroblewski provided advice, and also edited the papers. They are co-authors.

CHAPTER 1: INTRODUCTION

Optimal management of fish populations requires full understanding of their population dynamics. Such understanding is obtained through fitting quantitative models to data collected in the fisheries to estimate vital parameters in stock assessment. The quality of stock assessment is thus a central issue in fisheries management. The collapse of the fisheries worldwide has been attributed to gross overestimation of stock size, overfishing, discarding, negative environmental effects on recruitment, changes in distribution and mortality, food competition and predation. Ignoring or mis-estimating and mis-interpreting uncertainty in stock assessment modeling and fisheries management was another important reason leading to mismanagement of many fisheries (Hilborn and Walters, 1992; Ludwig et al., 1993; Walters and Maguire, 1996). Lack of consideration, misuse of uncertainties, and inappropriate incorporation of errors in stock assessment modeling can result in poor parameter estimation, leading to mis-estimation of fish population dynamics. Thus, an understanding of the error structure in stock assessment models and how an assumption of the model error structure may affect the parameter estimation is a critical issue in stock assessment and management. In this study I focused on evaluating and quantifying uncertainties in modeling stock-recruitment data, stock biomass dynamics, age-structured catch data, and growth data. I also evaluated how these uncertainties may influence the estimation of biological reference points and how the uncertainties can be incorporated in determining the status of fish stocks.

1.1 Review of uncertainty types in fisheries population dynamic modeling

Uncertainty is the condition of being uncertain, or doubt, or the incompleteness of knowledge about the states or processes in nature (Houghton Miflin, 1992; FAO, 1995). Uncertainties are often caused by estimating population properties from stochastic, or from inaccurate, deficient, or biased data which results in errors and information loss. This leads to variation, even disparity in statistical properties between population and samples drawn from the population. Classification of the uncertainties in fisheries can be found in Schnute (1989), Hilborn and Walter (1992), Polacheck et al. (1993), FAO (1995, 1996), and Chen and Paloheimo (1998). Uncertainties in fisheries are mainly from the following sources: measurement errors, process errors, model errors, decision errors and implementation errors, etc (FAO 1996).

Measurement error is the error in the observed fishery used for analysis, such as catches, efforts and biological parameters. Process error is the underlying stochasticity in the population dynamics such as the variability in recruitment, and the mis-understanding of the relationships between the different elements of the fishery system and their interaction. Model error is the misspecification of model structure. Estimation error is the error in the estimation of the populations and parameters. It can result from any, or a combination of the above errors. Decision error is the error in decisions that management takes on the basis of gained information. In fisheries, when models are related to fisheries management, control uncertainties or operational uncertainties appear, which refer to human operational factors, such as the inability to exactly achieve a TAC, or fishing mortality, etc.

Uncertainties may be decreased or minimized by increasing data quantity and quality and by using statistical techniques appropriate to the data and model structure.

1.2 Review of stock assessment of Atlantic cod

The Atlantic cod (*Gadus morhua*) used to support one of the most valuable commercial fisheries in Canada. The fishery was critical to Newfoundland's economy and society. For management purposes, the cod fishery is divided into stocks; however, these stocks likely do not represent distinct populations (de Young and Rose, 1993). The Atlantic cod around Newfoundland was divided into several stocks (Figure 1.1). There are six major stocks within Canadian waters: Labrador-NorthEast Newfoundland (NAFO Div. 2J + 3K + 3L), Southern Grand Bank (NAFO Div. 3N + 30), Southern Newfoundland (NAFO Div. 3Ps), Western Newfoundland (NAFO Div. 4R + 4S + 3Pn), Southern Gulf of St. Lawrence (NAFO Div. 4T + 4Vn), and E. Scotian Shelf (NAFO Div. 4Vs + 4W). Tagging data show that there are migrations or dispersal among these populations (Templeman, 1979; Rose, 1993; Campana et al., 1999).

Atlantic cod in Division 2J3KL was used as an example when modeling uncertainties in fish population dynamic models. Canadian fisherman once captured 70-75% of cod caught in the Northwest Atlantic (Scott and Scott 1988). Kurlansky (1997) gave a thorough review of the cod fishery and its historic impact, Garrod and Schumacher (1994) reviewed catches of Atlantic cod, and Hutchings and Myers (1995) reviewed the history of the Atlantic cod fishery along with changes in catches and fishing technology.

The fishery history is shown in Figure 1.2. The total catch peaked up at the late 1960s but declined from the early 1970s until the 1980s. There was a small increase late in the 1980s, but the trend suddenly declined in 1991. By 1992, there was a dramatic decline in the northern cod stocks. Canada had to declare a moratorium on fishing in July 1992 (DFO, 1996).

Total Allowable Catches (TACs) were introduced in 1974, but were set too high to be effective (Lear and Parsons, 1993). In 1976, Canada implemented a 200 mile limit. It did significantly reduce catches because foreign fishing declined. Canada, however, made large investments to expanding their fleet and catches grew again during the late 1970s and 1980s (Taggart et al., 1994; Garrod and Schumacher, 1994; Hutchings and Myers, 1995). Another result of high fishing mortality was the collapse in the age structure of stocks. Older fish, which would have made large contributions during spawning, were being removed (Hutchings and Myers, 1995). By 1993, the age distribution had narrowed and the average age of Atlantic cod in 2J3KL divisions had fallen to 4 years (Taggart et al., 1994). Catch in survey fishery in NAFO Division 2J3KL had almost no fish older than age 9 from 1993 to 1998 (Data from Shelton et al., 1996; Lilly et al., 2001).

Although data from Atlantic cod fishery were used in this study, this study was not designed for identifying the causes of declines in cod stocks. Rather I just used the data to facilitate the development of new methods in modeling uncertainties in stock

assessment. Thus, the interpretations of management implications should be done with caution.

1.3 Overview of the uncertainties in the biological data pertinent to the stock assessment

The quality of stock assessment could be affected by not incorporating important physical processes, such as climate-ocean oscillation, by ignoring some key biological processes, such as predation, and by ignoring natural variation of fish population itself resulted from natural environmental variations. Recent studies have suggested large variations of life-history processes, which in many cases covary with the climate ocean variables, but not all the time. Statistically averaging over a number of events sometimes cannot show the important details.

Marine fisheries ecosystem varies with its environments, such as turbulence, vertical mixing, tidal mixing and run-off on a scale of less than one kilometer, fronts, upwelling and tides, tidal mixing and internal waves on a scale of 1-1000 kilometers, gyres, large currents, global climate oscillations etc (Steele, 1998). The causes for fluctuations of many fish species, such as Atlantic cod, are not well understood in general, but are postulated to be closely related to variations in year-class success with variations related to environmental factors (e.g. Bishop and Shelton, 1997). The production of fish biomass in the oceans is governed by interactions among numerous physical, chemical, and biological processes. With ever increased coastal development,

the impact of human activities on coastal areas cannot be ignored. Fishing influences the dynamics of ecosystems. Climate changes are likely to exacerbate existing stresses on fish stocks. Recent anomalies in periodicities of cod stock fluctuations are likely due to heavy fishing in an unfavorable climate regime.

It is almost impossible to identify or develop a population dynamics model that can incorporate all effects from climate, fishing, and other environmental variables. Model predictions often failed because of lack of understanding of the interactions between natural and human-induced variations (Rigler, 1982). Biological life-history processes of fish, such as growth and recruitment, are heavily impacted by changing environment and human activities (Shelton *et al.*, 1999). It is critical to identify methodological and theoretical gaps in current knowledge and explore the possibilities for resolving them in stock assessment and in fishery management.

Many biological studies have been conducted on Atlantic cod because of its commercial importance. The following biological processes are regarded to be pertinent to stock assessment. They are recruitment, growth, maturity, natural mortality, predation, spatial distribution, stock definition and bycatch, discarding and fishing mortality. I discussed some of them that were included in this thesis. Because I used Atlantic cod data as examples in this study, I will focus the discussions on the cod.

1.3.1 Recruitment

Large variations in recruitment have been observed for many fish species (e.g., Myers et al., 1995; Myers and Barrowman, 1996; Power, 1996; Hinrichsen, 2001). Stock-recruitment (SR) models are mathematical functions that describe relationships between spawning stock abundance and subsequent recruitment. Future recruitment can be estimated from current spawners using SR models, which is essential for fisheries management (Hilborn and Walters, 1992). The lack of model fit of recruitment evokes the controversy of the relationship between stock and recruitment (e.g., Myers and Barrowman, 1996; Gilbert, 1997).

The recruitment of Atlantic cod 2J3KL was significantly correlated with the spawning stock biomass (Myers et al., 1995). The recruitment of Atlantic cod 2J3KL estimated both from survey index (Lilly et al., 2001) and from VPA analysis (Baird et al., 1992) varied greatly. The variation of recruitment may be caused by environmental variation (e.g. Koslow et al., 1987; de Young and Rose, 1993); but the relationship between recruitment and climate-ocean index is not clear (Hutchings and Myers, 1994).

1.3.2 Growth

As variation is observed in recruitment, there are also large variations in length-at-age among years in many fish stocks. For Atlantic cod 2J3KL stock, many hypotheses had been developed to explain the variations including variations in environmental factors such as water temperature (Hutchings and Myers, 1994; Gomes et al., 1995; Shelton et al., 1999), food (Krohn et al., 1997), density-dependant effect (Hanson and Chouinard,

1992; Swain 1993), and population stress as a result of over-exploitation (Beacham, 1983, Trippel, 1995). The following factors were also considered in causing growth variations: size-selective mortality (Myers, 1989; Hanson and Chouinard, 1992), early life history (Otterson and Loeng, 2000), energy allocation (Chen and Mello, 1999), and sampling and stock structure (Lilly, 1996). The temporal variation of growth might also result from the inclusion of cod mixing from other stock or population whose growth patterns differ. This also might lead to observed temporal and spatial variations in growth.

1.3.3 Environmental characteristics and migration

Oceanography plays a large role in the early stages of life. Currents act to disperse fish eggs and larvae, which has a large impact on survival rates. The changes of water temperature, salinity, and other environmental variables greatly impact life-history parameters, such as growth, fecundity, survival. The continental shelf off the Canadian east coast is characterized by a number of shallow regions known as banks, which are favored habitats for the cod. Two major currents dominate this area. The Labrador Current brings fresher, colder water from the north over the banks, where it meets the warmer, saltier Gulf Stream coming from the south (Fisheries and Oceans, 1995; DFO, 1996a). This configuration imparts a general southward drift along most of the bank area (DFO, 1996a). Ice conditions and storms can also impact the survival of eggs and larvae.

Work carried out by DFO in the early 1990s made a number of interesting discoveries about Atlantic cod migration and spawning habits (Rose, 1993). Cod tend to

migrate in large schools along trenches in the continental shelf. These trenches are favored because the water is 2-3°C warmer than the shelf. The cod follow the trenches inshore where they spread out to feed during the summer. By autumn they have moved northward and then back offshore, following a circular route.

Understanding the spatial distributions and migrations has clear economic and ecological benefit to humans and will result in more precise assessments of managed stocks (Giske et al., 1998). A lot of work has been done to collect information on the spatial dynamics of the cod fishery (Rose, 1993; Rose et al., 1994; 2000; Hutching et al., 1993; Hutching, 1996; Brander 1994, 1996; Dalley and Anderson, 1997; Atkinson et al., 1997; Campana et al., 1999; Brattey 2000; Lawson and Rose, 2000).

1.3.4 Bycatch and discarding

Approximately one quarter of the marine commercial catch is discarded at sea in the worldwide fisheries. Bycatch and discarding was considered to play a role in cod's decline (e.g. Myers, 1997). Kulka (1996) estimated the discarded cod at age from 1980 to 1994. The Canadian observer program estimated the averaged discarding rate in 2000 was about 1.33% in biomass (Lilly et al., 2001). Though it is not a large proportion in biomass, its impact on recruitment and number of fish is much larger because the discarding mainly consists of age 1-4 fishes. The uncertainties in the estimation of bycatch and discarding were not quantified, but were thought to be large.

1.3.5 Seal predation

Predation was considered to play a role on cod's decline (e.g. Shelton and Healey, 1999; DFO, 2000). The estimated predation by harp seal was large, and perhaps larger than the estimated population biomass from VPA (Stansbury et al., 1998; DFO, 2000). The estimated consumption by seals has not been incorporated into the current cod SPA model (Lilly et al., 1998). The uncertainty associated with the estimated consumption of cod by seals is large (Lilly et al., 2001).

1.3.6 Fishing mortality (Indicator biological reference point)

Fishing mortality was historically used as the indicator in fisheries management of Atlantic cod 2J3KL. From 1972 to 1992, the biological reference points were all based on constant fishing mortality (F_{max} and $F_{0.1}$ based fishing mortality) (Bishop and Shelton, 1997; Shelton, 1998). The retrospective F estimates were subsequently found to be higher than those estimated at the time of the assessment (Bishop and Shelton, 1997; Shelton and Rice, 2002).

1.4 Risk and total risk

Risk in general is the possibility of suffering harm or loss, danger; a factor, thing, element, or course involving uncertain danger, a hazard (Houghton Milflin, 1992). Risk is conceived as a permanent property of any random phenomenon. If the population distribution of the phenomenon were known, the risk would then be exactly known in any analysis and decision related to the phenomenon. Risk is identified with probabilities of values greater than, or smaller than, a given value. This risk is the basic risk, and is

inherent in the phenomenon itself, and cannot be avoided with a change in the population itself. New types of risks are then associated with the changed populations, e.g., regime shift in ecosystems or climate changes, or introduced species. Total risk is to consider all other uncertainties added to the basic risk.

1.5 Research objectives

Stochasticity and uncertainty estimation methods play a key role in current population models (Lande et al., 2003). When fitting the model, different model error structures call for different objective functions, which will result in different model fit and parameter estimates. Misspecifications of error structure or parameter estimation methods may severely bias model assessments, population forecasting, and estimations of overexploitation risk.

1.5.1 Why consider model error structure in stock-recruitment models?

Information on future recruitments of fish populations is commonly estimated from the corresponding spawning stock biomass, which is critical to fishery management (Hilborn and Walters, 1992). Large variations in recruitment have been observed in many cod stocks (e.g. Myers et al., 1995). The stock-recruitment (SR) relationship of cod stocks has been explored in many studies (e.g. Myers et al., 1995). However, as noted by Hilborn and Walters (1992), the estimation of the SR relationship is perhaps the most difficult task in fisheries stock assessment. For many fish stocks, the SR relationships are not well defined and unclear (Ricker, 1975; Hilborn and Walters, 1992; Iles, 1994;

Gilbert, 1997; Quinn and Deriso, 1999). Often the shape of the recruitment curve is hard to determine because of small sample sizes and because of the high variability in recruitment in a given level of stock. To respond to the uncertainties in stock-recruitment data, an understanding of the model error structure and how the model error structure influences the parameter estimation are essential in improving SR modeling (Francis, 1997).

A combination of the assumed model's deterministic form and error structure determines an objective function, which in turn dictates the parameter estimation (Chen et al., 2003). The lack of fit of an SR model to data does not necessarily establish the independence between the stock and recruitment. It likely results from a highly skewed distribution of recruitment values for a given level of stock (Chen and Paloheimo, 1995). Thus understanding the model error structure is necessary in evaluating and estimating the relation of recruitment to stock size, but it is often ignored in the SR model fit. For example, in fitting a SR model using a nonlinear least-square method, the assumed model error distribution is always normal. A commonly used practice is to linearize SR models by taking an appropriate transformation (e.g., logarithmic for the Cushing, Ricker model; reciprocal for Beverton-Holt model) and then to use a least-square criterion to estimate parameters. Large variations in recruitment have led to the wide adoption of the assumption that recruitment at a given level of spawning biomass follows a log normal distribution (Hilborn and Walters, 1992). This has been used as an alternative to the normal distribution (Hennemuth et al., 1980; Walters, 1986; Lapointe et al., 1992; Quinn

and Deriso, 1999). The intrinsic recruitment distribution has often been ignored for the convenience of parameter estimation, perhaps resulting in estimation errors (Chen and Paloheimo, 1995).

In Chapter 2 and Chapter 3 I used a Generalized Linear Model (GzLM) method to explore and identify appropriate error structures in modeling stock-recruitment data for cod stocks. A Monte Carlo simulation was developed and used to explore the importance of error structure in modeling SR data (Chapter 2), and then empirical data of all the cod stocks for which stock-recruitment data are available were analyzed to determine whether there were consistent patterns among different gadoid stocks in identifying appropriate SR model error distributions (Chapter 3).

1.5.2 Why consider model error structure in production models and sequential age-structured population analysis models?

Both surplus production models and age- or size-structured population dynamics models have been most commonly used in stock assessment of many fisheries worldwide (Shepherd 1988; Megrey 1989; Zhang et al., 1991). Like all other stock assessment models, care in implementation and choice of statistical methods can be as important as the model specification itself (Xiao 1997, 2000). When fitting the model, different model error structures call for different objective functions, which can result in different model fit and parameter estimates.

Parameter estimation for the surplus production model and age-structured population models usually takes the form of an observation-error estimator. Observation-error estimators have been suggested to perform better than other estimators such as process-error estimators, in fitting production models to data (Punt 1988; Hilborn and Walters 1992; Polancheck et al., 1993). These estimators are constructed by assuming that the population dynamics models are deterministic, having no process error, and that errors only occur in the observation model that describes the relationship between stock biomass and the abundance index.

When solving the models to get the parameter estimate, a nonlinear least-square method was often used. Because of the arguments of the normally distributed error in survey indices, lognormal error structure was widely used, i.e., log transformed population abundance follows a normal distribution. Argument on the lognormal assumption arises both from the statistical results, practical data analysis, and simulation study (Firth, 1988; Myers and Pepin, 1990; Cadigan and Myers, 2001). A diagnostic procedure is needed to identify the assumption of normally, or lognormally, or gamma distributed error structure in the survey indices in the population production model and population dynamic models.

In Chapter 4 I incorporated a Generalized Linear Model (GzLM) method to the surplus production model and the sequential population analysis, to identify appropriate error structures in modeling catch, catch-at-age, and abundance index. Atlantic cod in NAFO divisions 2J3KL was used as an example.

1.5.3 Why consider growth variation and why relate it to stock mixing?

Growth, as a key life-history process, greatly influences population dynamics and stock assessment. Large variations have been observed in length-at-age data of cod in Atlantic Canada within and among year classes. Several hypotheses have been developed to explain the growth variation observed in the cod stocks, ranging from influx of individuals from different populations with different life-history parameters to natural response to changes in population density and environmental conditions. Large areas of migration and mixing among stocks of Atlantic Cod have been documented in Atlantic Canada. In Chapter 5, I quantitatively evaluated the mixing hypothesis through a Monte Carlo simulation study. I considered temporal variation in growth resulting from the mixing of cod from another stock with different growth pattern. I demonstrate in the simulation that such a mixing also might lead to observed temporal variation in growth. Impacts of sample size in subsampling catch on the observed growth variations were also evaluated in the simulation study.

1.5.4 Why consider uncertainties in a biological reference point (BRP)? How does it influence the risk assessment in decision making?

A management reference point is an estimated value derived from an agreed scientific procedure and an agreed model to which corresponds a state of the resource and of the fishery and which can be used as a guide for fisheries management (FAO, 1996). The decline in stock size of Atlantic cod, widely discussed environmental effects, and

improved methodology on risk assessment call for close evaluation of BRPs. As stated in the 1.1, 1.2, 1.3 and 1.4, factors such as seal predation, growth variation, bycatch and discarding, and uncertainties in model or parameters used to estimate those processes, need to be incorporated in the BRP analysis, necessary for evaluating the current fishing status. Because the Atlantic cod 2J3KL has been historically managed based on $F_{0.1}$, we used the $F_{0.1}$ BRP to illustrate the method developed in this study. Including uncertainty in stock assessment was believed to be an alternative approach of population dynamic models to environmental changes and observation errors in current scientific level. Sensitivity analysis was used to identify important pathways and parameters where assumptions about distributional form contribute significantly to overall uncertainty. Risk management without risk assessment is nonsense. The current approach used in stock assessment and risk analysis usually only considers the uncertainty associated with indicator reference points, but does not consider the uncertainty associated with management reference points (Fogarty et al., 1996). In Chapter 6 $F_{0.1}$ and F_{max} were explored through a sensitivity analysis. I used an approach to determine the likelihood of overfishing in comparing indicator and management reference points, which considers the fact that both indicator and management target reference points are subject to large uncertainty.

Finally, the work in this dissertation is summarized in Chapter 7 with a brief description of the future directions that I believe are necessary for better understanding and management of marine fish populations.

Figure 1.1 Atlantic cod distribution in the Atlantic Ocean and the stocks around Northwest Atlantic waters.

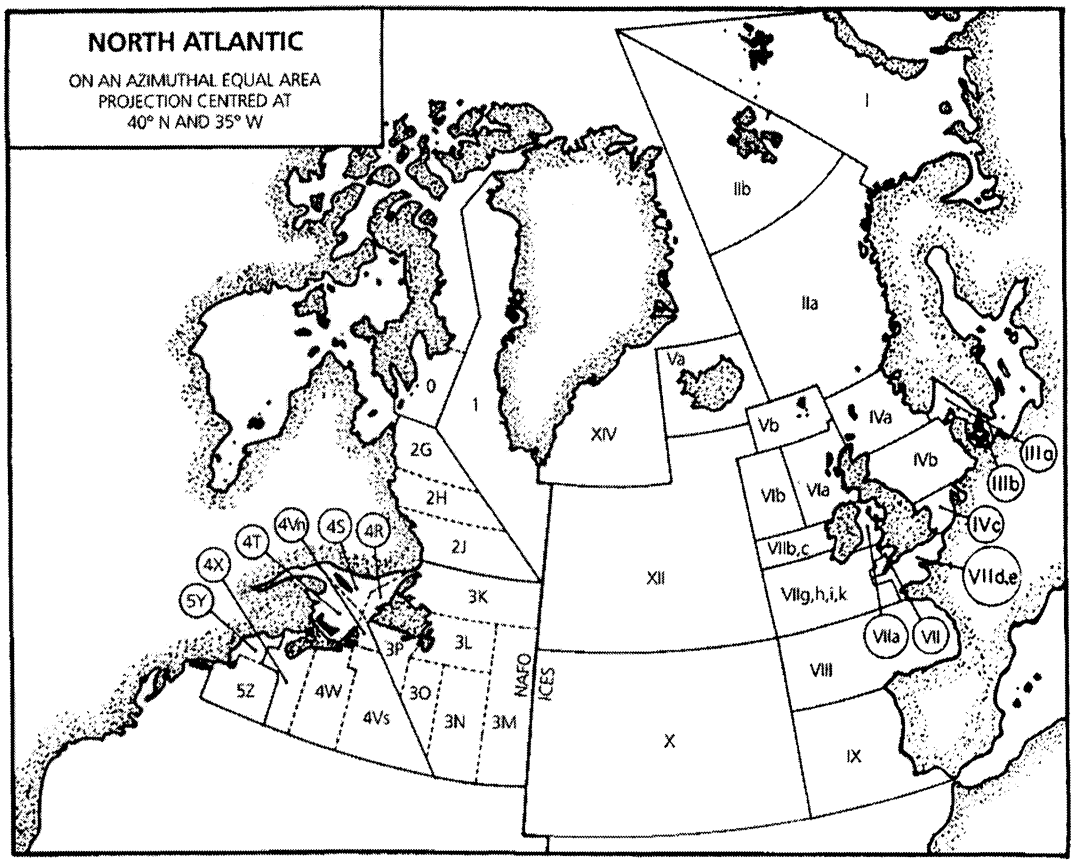

Figure 1.2. Atlantic cod 2J3KL total allowable catch (TAC) and landings from 1959 to 2000 (Lilly et al., 2001). Landing by gear types (top panel); landings by Canadian and non-Canadian (middle panel); landings by divisions (bottom panel).

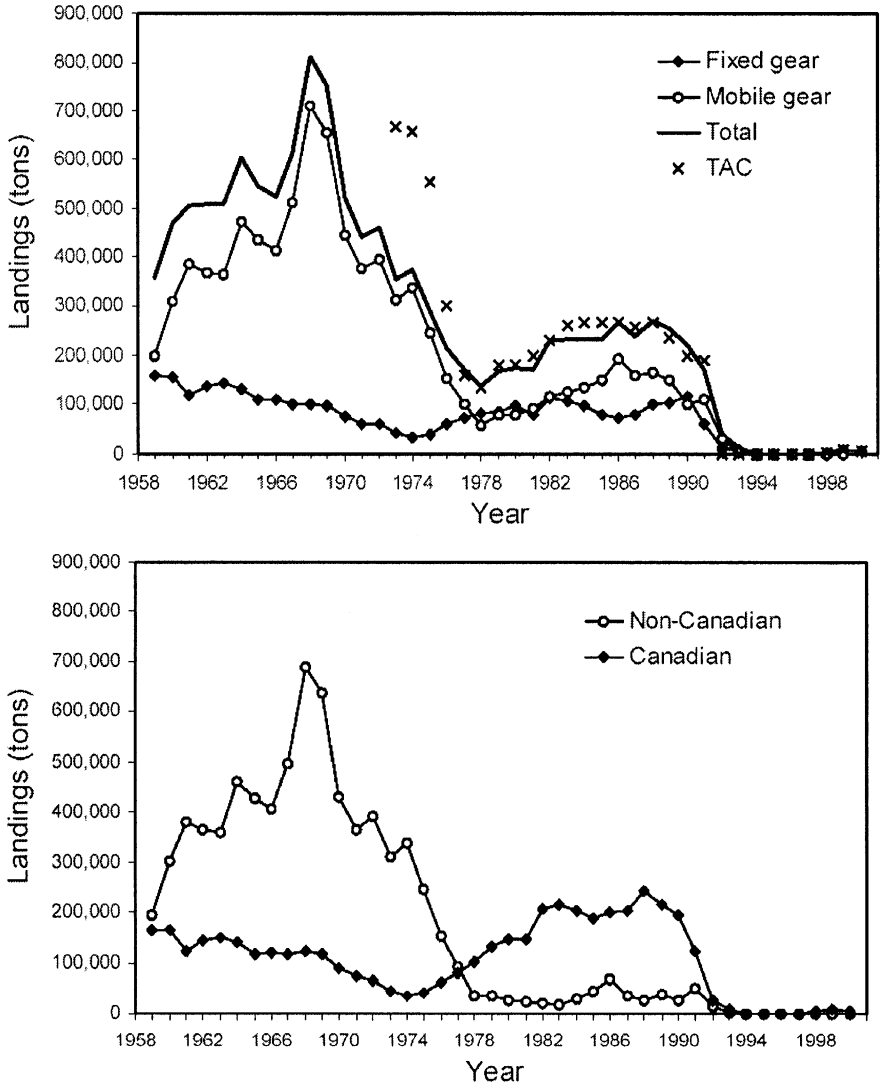

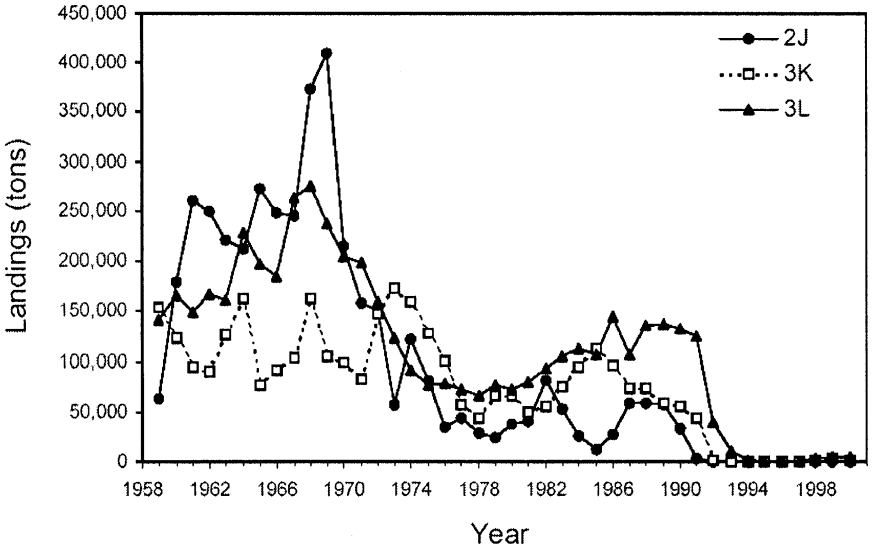
450,000
400,000
350,000
300,000
250,000
200,000
150,000
100,000
50,000
0
Landings (tons)
1958
1962
1966
1970
1974
1978
1982
1986
1990
1994
1998
Year
2J
3K
3L

CHAPTER 2

A SIMULATION STUDY OF IMPACTS OF ERROR STRUCTURE ON MODELING STOCK-RECRUITMENT DATA USING GENERALIZED LINEAR MODELS

Abstract

Stock-recruitment (SR) models are commonly fitted to SR data with a least-square method. Errors in modeling are usually assumed to be normal or log normal, regardless of whether such an assumption is realistic. A Monte Carlo simulation approach was used to evaluate the impact of the assumption of error structure on SR modeling. The generalized linear model, which can readily deal with different error structures, was used in estimating parameters. This study suggests that the quality of SR parameter estimation, measured by estimation errors, can be influenced by the realism of error structure assumed in estimation, the number of SR data points, and the number of outliers in modeling. A small number of SR data points and presence of outliers in SR data could increase the difficulty in identifying an appropriate error structure in modeling, which might lead to large biases in the SR parameter estimation. This study shows that generalized linear model methods can help identify an appropriate error distribution in SR modeling, leading to an improved estimation of parameters even when there are outliers and the number of SR data points is small. I recommend the generalized linear model be used for quantifying stock-recruitment relationships.

2.1 Introduction

Stock-recruitment (SR) models are mathematical functions that describe relationships between spawning stock abundance and subsequent recruitment. Future recruitment can be estimated from current spawners using SR models, which is essential for fisheries management (Hilborn and Walters 1992).

Large variations in recruitment have been observed for many fish species (e.g., Myers and Barrowman 1996; Power 1996; Hinrichsen 2001). The variations tend to increase with spawning stock biomass (Myers et al. 1995). This has led to wide adoption of the assumption that recruitment at a given level of spawning biomass follows a log normal distribution (Hilborn and Walters 1992). This has been used as an alternative to the normal distribution (Hennemuth et al. 1980; Quinn and Deriso 1999; Hinrichsen 2001). The normal error distribution assumption is no longer widely used in SR analyses, although it tends to be more realistic if the survival of individuals during their early life stages is density independent and constant (Shelton 1992).

Error structure is an integral part of modeling (Carroll and Ruppert 1984; Schnute 1991; Chen and Paloheimo 1998). The impact of unrealistic assumptions of model error structure on parameter estimation has been evaluated with various fisheries models (Deriso et al. 1985; Bajdik and Schneider 1991; Cadigan and Myers 2001). Inappropriate error distribution assumptions can cause inaccurate estimates of model parameters, their variability, and the attained significance level of the fitted model. In this study, using a Monte Carlo simulation approach, I evaluated the importance of having a

proper error distribution assumption and the effectiveness of using a generalized linear model in identifying a proper error distribution in modeling SR data.

The generalized linear model (GzLM) is a maximum likelihood-based method, which provides a systematic framework to estimate parameters when the model error structure belongs to the exponential family. I considered several error structures in the exponential family. These error structures included normal, lognormal, gamma, and Poisson distributions. The likelihood of recruitment having normal or lognormal distributions was discussed in Shelton (1992) and Fogarty (1993). Lognormal and gamma distributions were used by Myers et al. (1995). The Poisson distribution is considered appropriate for count data, and nonnegative and highly varied data (Bajdik and Schneider 1991; White and Bennetts 1996), and may be appropriate for recruitment.

Because the number of SR data is often small (Hilborn and Walters 1992) and outliers are likely to be present in the SR data (Chen and Paloheimo 1995; Hinrichsen 2001), the role of sample size and outliers in identifying appropriate error structure in SR modeling was also evaluated in the simulation study.

The theory of GzLM was developed in the 1970s (Nelder and Wedderburn 1972), and later was expanded in theory and application during the 1980s and 1990s (McCullagh and Nelder 1983, 1989; Dobson 1990). The GzLM can be implemented by various software such as GLIM (Numerical Algorithms Group), SAS (SAS institute), and SPLUS (MathSoft). MATLAB (Math Works) was used in this study.

2.2 Materials and Methods

2.2.1 Data simulation

I used the Cushing model, the Ricker model and the Beverton-Holt model (Quinn and Deriso 1999) as examples in modeling SR data. The Cushing model can be written as

(1) $$R = \alpha S^{\beta},$$

the Ricker model as

(2) $$R = \alpha S e^{-\beta S},$$

and the Beverton-Holt model as

(3) $$R = \frac{\alpha S}{1 + \beta S}$$

where α and β are two parameters to be estimated, and S and R are the spawning stock biomass and its subsequent recruitment, respectively. The Ricker and Beverton-Holt models consider a density-dependent effect, but the Cushing model does not. In practice, the choice of these models depends upon the data. In this study, I considered the Cushing model first. Two scenarios were used in simulating SR data with equation (1). One scenario was to randomly sample S data from 1000 to 10 000 using a uniform distribution, and then calculate corresponding R values according to equation (1) and an

assumed error structure which includes normal, lognormal, gamma, and Poisson functions (Table 2.1). The values of 2.012 and 0.857 were used for $Ln(\alpha)$ and β, respectively, in simulating the R data from the S data, which were taken from the pink salmon (*Oncorhynchus gorbuscha*) fishery in the northern southeast Alaska (Quinn and Deriso 1999). For the second scenario, the SR data were simulated using actual S data of pink salmon in northern southeast Alaska using the four types of error distributions listed in Table 2.1 and the two parameters for the pink salmon described above. The data simulated in the first and second scenarios are referred to as the first and second data sets, respectively, in this paper.

I then repeated the above approach for the Ricker and Beverton-Holt models (i.e., equation 2 and 3). The values used for the two parameters in the Ricker model were $Ln(\alpha) = 1.047$, $\beta = 5.52 * 10^{-5}$, in the Beverton-Holt model were $Ln(\alpha) = 1.042$, $\beta = 5.92 * 10^{-5}$, also taken from the pink salmon stock.

2.2.2 Generalized linear model (GzLM)

The generalized linear model is sometimes abbreviated as GLM (McCullagh and Nelder 1989; Lindsey 1997; Myers et al. 2001), GLIM (Software of GLIM distributed by Numerical Algorithms Group), or GLZ (StatSoft). In this paper I write GzLM to differentiate the generalized linear model from the general linear model (GLM) and the software GLIM.

A GzLM has three components (McCullagh and Nelder 1989). One is the random component $\mathbf{Y}$, which is a vector of observations y having n components that are independently distributed with mean vector $\boldsymbol{\mu}$. The second is the systematic component, which is a specification for the vector $\boldsymbol{\mu}$ in terms of a small number of unknown parameters $\beta_1, \beta_2, ..., \beta_p$. A linear predictor $\boldsymbol{\eta}$ is given by $\boldsymbol{\eta} = \sum_{j=1}^{p} \mathbf{X}_j \beta_j$, where $\mathbf{X}$ is the model matrix or the covariates for observation $\mathbf{Y}$. The third component is the link between the random and systematic components. It is often written as $\boldsymbol{\eta} = g(\boldsymbol{\mu})$, where g is the link function (McCullagh and Nelder 1989). In the case of the GLM, $\eta = \mu$ (i.e.identity link). Thus GLM is a special case of GzLM. The likelihood function of Y can be written as

$$L = \prod_{1}^{n} f(y;\theta). \tag{4}$$

Where f is the probability distribution function (pdf.) which depends on the parameter(s) θ. If the pdf is a member of the exponential class, when Y is of a discrete type, then

$$f(y;\theta) = \exp[p(\theta)K(y) + s(y) + q(\theta)], \qquad y = a_1, a_2, a_3, \cdots, \tag{5}$$

$$= 0 \qquad \text{elsewhere,}$$

The log-likelihood function is then

$$(6) \qquad LL = p(\theta)\sum_{1}^{n} K(y_i) + \sum_{1}^{n} S(y_i) + nq(\theta),$$

in which $\sum_{1}^{n} K(y_i)$ is a sufficient statistic for the parameter θ, and $p(\theta)$ is the canonical link for a distribution whose p.d.f. is $f(y;\theta)$. Here, Y is recruitment R, X is spawning stock biomass S, and θ is the parameter vector in the SR models.

The exponential family includes the normal, Poisson, gamma and other distributions. The link function $\eta = g(\mu)$ relates the mean of the response variable Y to the linear combination of the X_i. Common choices of link functions include identity, logarithmic, reciprocal, power, and logit (McCullagh and Nelder 1989; The Math Works Inc. 2002). The GzLM is flexible to incorporate different links and not be limited to the canonical links. The links I used in this paper were based on the SR model structure, because I did not consider changing the SR model form. The choice of the link functions did not affect the assumption about the distribution of Y in GzLM. The distributions, their corresponding canonical links, and links used in this paper are shown in Table 2.1. The GzLM model was used to estimate the parameters given the link function $\eta = g(\mu)$ according to the maximum log-likelihood method (i.e., equation 6). The parameters were then used to calculate the expected value of the response variable (i.e., recruitment), and then the residuals. Homogeneity of residuals was evaluated and used as a criterion to determine if the model error structure was appropriate. When different model error assumptions were used in a GzLM, the one that resulted in homogeneous residuals was

considered as the most appropriate one (McCullagh and Nelder 1989). An example is shown (Fig. 2.1), which resulted from the application of GzLM with the four error distributions to SR data simulated with a normal distributed error. This example suggests that residuals tend to be homogeneous when error distribution is correctly defined in the GzLM.

2.2.3 The GzLM parameter estimations for stock-recruitment models

Cushing model

A log transformation in conjunction with a normal-error assumption is commonly used in fitting the Cushing model to SR data. This is equivalent to assuming that the untransformed recruitment has a lognormal distribution. With the lognormal transformation, the Cushing model (i.e., equation 1) can be rewritten as:

(7) $$Ln(R) = Ln(\alpha) + \beta Ln(S) + \varepsilon$$

where ε has a normal distribution defined as $N(0,\sigma^2)$. Ln(R) is the dependent variable, and Ln(S) is the independent variable in the GzLM. The identity link is used, and the error is normal. The parameter estimates are the same as those from the GLM model after the Cushing model is log transformed (i.e., equation 7).

For error distributions that are normal, gamma and Poisson, one can rewrite the Cushing model as:

(8) $$E(R) = E(\alpha S^{\beta}) = E(e^{Ln(\alpha)+\beta Ln(S)}),$$

model parameters are estimated based on the assumption of the distribution of R. For a normal distributed error, I assume R follow $N(\hat{R},\sigma^2)$. For a gamma distributed error, one assumes R follow $G(\hat{R}/k,k)$. k is a scale parameter of gamma distribution. I used k = 6 in the simulation study. For a Poisson distributed error, one assumes R follow $P(\hat{R})$. Here, $\hat{R} = \alpha S^{\beta}$. In the GzLM analysis, R is the dependent variable, and Ln(S) is the independent variable. The log link is used, and the error choice is normal, gamma, and Poisson respectively. The parameter estimates using a normal error distribution are the same as those estimated using a nonlinear least squares method.

Ricker model

When the lognormal distribution is assumed for the error distribution of the Ricker model, equation 2 can be re-written as:

(9) $$Ln(R) = Ln(\alpha) - \beta S + Ln(S) + \varepsilon \ ,$$

which is equivalent to:

(10) $$R = Se^{\ln(\alpha)-\beta S}e^{\varepsilon} \ ,$$

where ε follows $N(0,\sigma^2)$. $Ln(R)$ is the dependent variable, negative S is the independent variable, and Ln(S) is an offset in the GzLM. The identity link ($\eta = \mu$) is used, and the choice of error is normal. The parameter estimates are the same as those from the GLM model after linearizing the Ricker model. The commonly used linearization method, which can be expressed as:

(11) $$R/S = e^{\alpha - \beta S} + \varepsilon ,$$

is likely to introduce estimation errors since variable S appears in both sides of the equation (Quinn and Deriso 1999).

For error distributions that are normal, gamma, and Poisson, the Ricker model can be written as:

(12) $$E(R) = E(e^{\ln(\alpha) - \beta S + \ln(S)}) .$$

Model parameters are estimated based on the assumption of the distribution of R (see *Cushing model*). Here, $\hat{R} = \alpha S e^{-\beta S}$. R is the dependent variable, negative S is the independent variable, and Ln(S) is an offset in the GzLM. The log link, $\eta = \log(\mu)$, is used, and the choice of error is normal, gamma, and Poisson respectively.

Beverton-Holt model

When the normal, gamma or Poisson distribution is assumed for the error distribution of the Beverton-Holt model, equation 3 can be re-written as

(13) $$E(R) = E(\frac{1}{\frac{1}{\alpha}\frac{1}{S} + \frac{\beta}{\alpha}}) ,$$

model parameters are estimated based on the assumption of the distribution of R (see *Cushing model*). Here, $\hat{R} = \frac{\alpha S}{1 + \beta S}$. R is the dependent variable; 1/S is the independent variable in the GzLM. The reciprocal link ($\eta = 1/\mu$) is used, and the choice of error is normal, gamma, and Poisson respectively.

For error distributions that are lognormal, the Beverton-Holt model can be written as:

$$Ln(R) = Ln\frac{\alpha S}{1+\beta S} + \varepsilon \quad = Ln(\alpha) + Ln(S) - Ln(1+\beta S) + \varepsilon \quad , \tag{14}$$

where ε is the error term following $N(0,\sigma^2)$. Because of the non-linear parameters in the above equation, the code and method used to get the parameter estimate are complicated and approximated when using GzLM. Equation 14 can be regarded as a nonlinear equation with normal distributed error structure, where $Ln(R)$ is the response variable; S is the independent variable. Considering the fact that the parameter estimate using GzLM in equation 14, equals that using the nonlinear least-square estimate, a nonlinear least-square method was used in solving this equation instead of GzLM.

2.2.4 Simulation design

The following procedure was used in the simulation:(1) simulate SR data sets using the Cushing model for error scenarios listed in Table 2.2 with the total number of observations being 10, 20 and 40; (2) simulate SR data sets with outliers by adding atypical errors to 10%, 20% and 40% of the data with the number of observations being 40. Both the SR data sets discussed previously in the **Data Simulation** section were used in simulating data with and without outliers. The same approach was then applied to the Ricker model. The combination of three models (Cushing, Ricker and Beverton-Holt), two data sets (randomly drawn S data and true S data for the pink salmon), four error

distributions used in simulating the SR data (normal, lognormal, gamma, and Poisson), four error distributions assumed in the GzLM for parameter estimation (normal, lognormal, gamma, and Poisson), three sample sizes (10, 20 and 40 SR observations), and three different levels of outlier contaminations (10%, 20%, and 40%) at a sample size of 40, resulting in 480 simulation scenarios in total being evaluated in this study. When adding outliers in the simulation study, if 10% of outliers were added, 90% of SR data with the supposed model error structure were first simulated; then another 10% of the outliers with another model error structure were simulated. Finally the 90% common data and 10% outliers were added together before the generalized linear model was used to estimate the parameters. For each simulation scenario 1000 simulations were run to obtain the stable results.

Departure of the estimated parameters from the true values was measured by the relative estimation bias (REB), relative estimate error (REE) and root mean square error (RMSE). REB is calculated as:

$$REB(\%) = \frac{\left| \left(\sum_{n} \beta_i^*\right)/N - \beta \right|}{\beta} 100 \tag{15}$$

the REE is calculated as:

$$\text{REE}\ (\%) = \frac{\sum_{n} \left|\beta_i^* - \beta\right|}{N\beta} 100 \tag{16}$$

and the RMSE can be expressed as:

$$RMSE = \sqrt{\frac{\sum_{i=1}^{N} (\beta^*_i - \beta)^2}{N}} \quad (17)$$

where β^*_i is the estimated parameter value in the ith simulation; N is the number of simulations; β is the true parameter value. The smaller the REB, REE and RMSE values, the better the estimation approach performs.

2.2.5 Quantification of residuals' homogeneity

Pearson residuals of the model fitting were calculated for each simulation scenario. Pearson residuals are the differences between observed and predicted values, standardized (divided by the estimated standard deviation of the fitted value) to make their variance (theoretically) constant. If the error distribution assumed in the estimation was consistent with the error distribution used in simulating the SR data, a plot of resultant Pearson residuals should show constant variances. Thus in order to determine if the residuals are homogeneous, one can look at the residual diagnostic plot. A visual inspection of residual diagnostic plots is commonly used in evaluating the residual homogeneity, although the approach may be subjective, in particular when sample sizes are small. In this study, because 1000 simulations were run for each scenario to derive stable results, direct observation was laborious. Thus, I used the following quantitative method to evaluate the homogeneity of the residuals: (1) regress the Pearson residual value (r) and the model predicted value ($\hat{R}$), i.e.,:

(18) $$r = a_1 + b_1 * \hat{R}$$

Estimate the p value for b_1 to determine if it was significantly different from zero, $\alpha = 10\%$ was used; (2) regress the absolute Pearson residual value (r_2) and the model predicted value ($\hat{R}$), i.e.,:

(19) $$r_2 = a_2 + b_2 * \hat{R}$$

Estimate the p value for b_2 to determine if it was significantly different from zero, $\alpha = 10\%$ was used; (3) if both the estimated p values were larger than $\alpha = 10\%$, I regarded the residuals as homogeneous, else I regarded the residuals as not homogeneous. Many of the residuals show a right or left triangular shaped pattern symmetric about the x axis, when an inappropriate model error structure were used. That is why I double checked this situation by using both residuals and absolute value of residuals in the regression. This proposed method, referred hereafter as the regression method, was compared with the commonly used method, which involves visual examination of residual homogeneity, in 100 simulations to determine if both methods derived consistent conclusions in evaluating the residual homogeneity.

In this chapter, regression method is used to diagnose the residuals (Anscome and Tukey, 1963). This regression method may not be able to measure all the nonhomogeneity patterns, such as a nonlinear pattern etc. The efficiency of the regression

method in identifying the residual homogeneity is analyzed by comparing the regression method with the commonly used visual-checking method for the residual homogeneity.

2.3 Results

The efficiency of the regression method in identifying the residual homogeneity was influenced by sample size (Table 2.2). When the sample size was 10, the percentage of the simulations with homogeneous residuals was 81% on average. This increased slightly with an increase in sample size (averaged 84% and 89% for sample sizes of 20 and 40, respectively; Table 2.2). A comparison of the regression method with the commonly used visual-checking method for the residual homogeneity suggests that the proposed regression method effectively identified the simulations that had homogeneous residuals.

When the error distributions used in the GzLM analysis were the same as those used in simulating SR data, percentages of the simulations that had homogeneous residuals increased with an increase in sample size (Table 2.3). The REEs and RMSEs for α and β tended to decrease with sample size increasing (Fig. 2.2, Table 2.3). Because the REB is the difference between the mean parameter estimate in total simulation runs and the true value divide by the true value, the variance among the simulation runs was hidden. The REB estimate is not consistent comparing with the REE and RMSE estimates, which accumulate error in every simulation run. I did not show the REE estimates in the tables, I only show it in Figure 2.2 as an example.

When the error distributions used in the GzLM analysis differed from those used in simulating SR data, percentages of the simulations that had homogeneous residuals became smaller with an increase in sample size (Table 2.4). This was different from the observations made when model error distributions used in the GzLM analysis were the same as those used in simulating SR data. The REBs of α and β increased with an increase in sample sizes when normal errors were used in simulating SR data. For other errors used in simulating data, they decreased as the sample size increased (Table 2.4). The RMSEs of α and β decreased with increasing sample size.

A comparison of Table 2.3 and Table 2.4 indicates that percentages of the simulations with homogeneous residuals were always higher and REBs and RMSEs of α and β were always lower when the error assumptions used in the GzLM were the same as those used in simulating SR data, compared with those derived in the simulations when the model error distributions in the GzLM were not the same as the ones used in simulating data (Tables 2.3 and 2.4).

Different error assumptions in the GzLM yielded different estimates for the model parameters. Parameters estimated using lognormal and gamma distributions were similar, but parameters estimated using normal distribution in the GzLM were different from those estimated using lognormal and gamma distributions in the GzLM. Parameters estimated using a Poisson distribution tended to have values between those estimated using the normal error distribution versus lognormal and gamma distributions. Because this is a simulation study I did not show the parameter estimates in every simulation. The

trend of the mean error in total simulations can be observed from the REE and RMSE estimates (Fig. 2.2, Tables 2.3 and 2.4).

When the second SR data (see **Data Simulation** section) were used for the Cushing model, percentages of the simulations with homogeneous residuals were higher when the error distributions used in the GzLM were the same as those used in simulating SR data (Table 2.5). Parameters estimated using the lognormal and gamma distributions were similar. Parameters estimated using the normal distribution in the GzLM differed from those estimated using the lognormal and Gamma distributions. Parameters estimated using the Poisson distribution in the GzLM had values between those estimated using normal error and lognormal and gamma distributions in the GzLM. When the error distribution used in the GzLM was the same as that used in simulating SR data, the percentages of the simulations with homogeneous residuals were higher and the REBs and RMSEs of α and β were smaller, and vice versa. This was consistent with the results derived for the first set of data which had S values randomly drawn from 1000 to 10 000.

For the first set of data (randomly drawn S data) with outliers, when the error distributions used in the GzLM was the same as those used in simulating SR data, the percentages of the simulations with homogeneous residuals decreased and the REBs and RMSEs of α and β increased with an increase in the number of outliers (Table 2.6). When the error distributions used in the GzLM were not the same as those used in simulating SR data, the percentages of the simulations with homogeneous residuals

increased with an increase in the number of outliers, if error distributions used in simulating SR data were normal and error distributions used in the GzLM were lognormal and gamma. The same result could also be observed when the error distributions used in simulating SR data were the lognormal, gamma and Poisson and the model errors used in the GzLM were normal. For other combinations of the distributions in simulating data and GzLM analyses, the percentages of the simulations with homogeneous residuals decreased with an increasing number of outliers (Table 2.6). The REBs and RMSEs of α and β increased with an increase in the number of outliers in most cases (Table 2.7). Similar conclusions could be obtained when outliers were present in the second set of data simulated based on pink salmon S data (Tables 2.8 and 2.9).

When the Ricker model and Beverton-Holt model were applied to data simulated under different scenarios, the results derived were consistent with those described above for the Cushing model. The results for those two models are shown in the appendix in this thesis.

2.4 Discussion

The regression method proposed for checking the residual homogeneity was effective in identifying homogeneous distributions of residuals. However, the effectiveness decreased with sample size. This was consistent with the fact that visual observation for residual homogeneity was difficult when sample sizes were small. This suggests that the regression method I used in checking residual homogeneity of a large

number of simulations was effective. However, I would suggest using the visual observation method in SR modeling where there is only one set of residuals output.

The simulation results show that GzLM can help identify an appropriate model error distribution for parameter estimation through a residual homogeneity analysis. In most cases of the simulation the true model error distribution used in the GzLM provided the highest percentage of simulation runs with homogeneous residuals. According to the simulation, this (i.e., the use of an appropriate error distributions in the GzLM) can improve the parameter estimation.

This study suggests that the number of SR data can greatly influence the effectiveness of identifying correct error distributions in the GzLM analyses and estimation errors. A small number of SR data is likely to lead to low effectiveness in identifying homogeneous residuals and large estimation errors in SR modeling. Thus, one should be cautious in using the GzLM when analyzing a small number of SR data.

The presence of outliers can also impact a GzLM analysis in identifying a correct error distribution. When outliers composed 10% of the data, the percentage of simulation runs with homogeneous residuals was the highest for the case where the correct error distributions were used in the GzLM analysis. When the number of outliers increased to 40% , the percentages of homogeneous residuals was no longer the highest for the case where the correct error distributions were used in the GzLM analysis. The normal error distribution tended to be more sensitive to outliers compared with the lognormal and

gamma distributions. This study shows that even when the GzLM is less effective in identifying the correct error distribution with an increase in the number of outliers, the model error distribution used in the GzLM that shows the highest percentage of simulation runs with homogeneous residuals usually provides better parameter estimates with smaller REB and RMSE. An example could be found in Figure 2.3 which illustrated the changes in estimation errors for $Ln(\alpha)$ and β when different percentages of data were outliers This suggest that the appropriate model error distribution may not be the underlying true error distribution because of the existence of outliers.

This study suggests that if the model error distribution used in simulating SR data follows the Poisson, the parameters estimated using different error distributions in the GzLM have smaller differences. Thus, a Poisson distributed error in SR data is less sensitive to sample size, outliers, and choice of error distributions in the GzLM. The use of the Poisson distribution in the parameter estimation also showed robustness with respect to Misspecification of error structure, small sample size, and outliers. For example, when the error distribution used in simulating SR data was normal and the data were contaminated with lognormal distributed outliers, the Poisson error distribution used in the GzLM analysis provided the highest percentage of simulation runs with homogeneous residuals and better parameter estimates. Thus, I recommend using the Poisson distribution in a GzLM analysis of SR data.

The simulated results did not show obvious difference when different SR models were used. Because this is a simulation study, the data sets are based on "true" parameters with random errors, the performances of the models are difficult to compare.

I suggest the GzLM method be used to quantify SR data relationships. The GzLM provides a convenient and effective way to evaluate and identify the appropriate model error distributions for a given set of data and models, leading to improved parameter estimation.

Table 2.1: The distributions, their corresponding canonical links, and links used in this chapter.

Distribution	Canonical link	Links used in this paper	
		Cushing and Ricker models	Beverton-Holt model
Normal	$\eta = \mu$	$\eta = \log(\mu)$	$\eta = 1/\mu$
Lognormal (log transformed data)	$\eta = \mu$	$\eta = \mu$	
Gamma	$\eta = 1/\mu$	$\eta = \log(\mu)$	$\eta = 1/\mu$
Poisson	$\eta = \log(\mu)$	$\eta = \log(\mu)$	$\eta = 1/\mu$

Table 2.2: Comparison of the regression method proposed in this paper with the commonly used visual checking method in identifying the residual homogeneity for the 100 simulations. In this study the Cushing model was used. The results derived for different sample sizes (10, 20 and 40) are compared.

Model error distribution		Sample size = 10		Sample size=20		Sample size=40	
		% of simulations with homogeneous residuals					
In simulating SR data	In GzLM estimation	Regression method	Visual checking	Regression method	Visual checking	Regression method	Visual checking
Normal	Normal	87	88	93	88	92	87
	Lognormal	70	68	40	48	10	16
	Gamma	72	70	43	47	10	13
	Poisson	83	77	80	80	40	40
Lognormal	Normal	82	57	65	40	20	18
	Lognormal	97	75	85	75	82	87
	Gamma	88	72	82	77	85	93
	Poisson	87	63	75	58	57	50
Gamma	Normal	82	47	57	43	33	27
	Lognormal	80	72	87	77	70	70
	Gamma	83	78	87	83	70	70
	Poisson	83	60	78	62	73	58
Poisson	Normal	83	62	70	62	43	40
	Lognormal	87	60	72	52	53	58
	Gamma	85	63	75	47	53	58
	Poisson	88	67	80	77	93	87

Table 2.3: Summary of the simulations when the model error distributions used in the generalized linear model analyses were the same as those used in simulating stock-recruitment (SR) data. The Cushing model and the first set of data which had S values randomly drawn from 1000 to 10 000 were used in the simulation. Relative estimate bias (REB) and root mean square error (RMSE) for parameters are shown.

Model error distribution in simulating SR data	Number of observations	% of simulations with homogeneous residuals	REB for $\ln(\alpha)$ (%)	REB for β (%)	RMSE for $\ln(\alpha)$	RMSE for β
Normal	10	71.9	0.15	0.04	0.4398	0.0518
	20	79.1	0.02	0.01	0.2989	0.0351
	40	80.4	0.02	0.05	0.2106	0.0248
Lognormal	10	74.3	6.9	1.93	2.9511	0.3585
	20	79.4	0.01	0.19	1.9812	0.2413
	40	80.8	2.21	0.60	1.3260	0.1618
Gamma	10	71.3	0.61	0.15	0.4516	0.0542
	20	73.5	0.73	0.21	0.2915	0.0351
	40	79.1	0.37	0.10	0.1860	0.0224
Poisson	10	73.6	0.026	0.008	0.0724	0.0086
	20	78.5	0.026	0.008	0.0491	0.0059
	40	80.6	0.008	0.002	0.0342	0.0041

Table 2.4: Summary of the simulations when the model error distributions used in the generalized linear model analyses were not the same as those used in simulating stock-recruitment data. The Cushing model and the first set of data which had S values randomly drawn from 1000 to 10 000 were used in the simulation. Relative estimate bias (REB) and root mean square error (RMSE) for parameters are shown.

Model error distribution		Number of SR observations	% of simulations with homogeneous residuals	REB for $\ln(\alpha)$ (%)	REB for β (%)	RMSE for $\ln(\alpha)$	RMSE for β
In simulating SR data	In GzLM						
Normal	Lognormal	20	26.3	2.57	0.7	0.4096	0.0486
		40	5.0	2.94	0.8	0.3033	0.0360
	Gamma	20	24.7	0.91	0.26	0.3999	0.0474
		40	4.6	0.84	0.23	0.2916	0.0346
	Poisson	20	55.5	0.31	0.09	0.3216	0.0378
		40	34.9	0.47	0.13	0.2315	0.0273
Lognormal	Normal	20	37.4	24.6	8.2	11.2407	1.2923
		40	13.1	5.25	3.02	2.2124	0.2666
	Gamma	20	81.8	4.39	0.45	2.0394	0.2480
		40	85.8	2.43	0.94	1.4105	0.1724
	Poisson	20	63.2	7.89	0.55	2.2546	0.2733
		40	43.9	2.72	0.85	1.5502	0.1890
Gamma	Normal	20	44.1	1.13	0.32	0.3392	0.0406
		40	17.8	0.2	0.05	0.2302	0.0277
	Lognormal	20	73.7	1.09	0.28	0.2924	0.0352

		40	64.2	0.09	0.01	0.1861	0.0224
	Poisson	20	72.6	0.85	0.24	0.2935	0.0353
		40	67.7	0.38	0.1	0.1915	0.0231
Poisson	Normal	20	58.6	0.041	0.012	0.0539	0.0064
		40	36.6	0.027	0.008	0.0367	0.0044
	Lognormal	20	58.5	0.046	0.013	0.0525	0.0063
		40	39.4	0.009	0.002	0.0371	0.0044
	Gamma	20	59.1	0.026	0.008	0.0525	0.0063
		40	37.9	0.016	0.005	0.0371	0.0044

Table 2.5: Summary of the simulations when the Cushing model and the second set of data which had true S values of pink salmon were used in the simulation. Relative estimate bias (REB) and Root mean square error (RMSE) for parameters were shown.

Model error distribution		% of simulations with homogeneous residuals	REB for ln(α) (%)	REB for β (%)	RMSE for ln(α)	RMSE for β
In simulating SR data	In GzLM					
Normal	Normal	82.25	0.01	0.01	0.2144	0.0258
	Lognormal	26.91	2.18	0.59	0.3486	0.0425
	Gamma	31.05	0.37	0.10	0.3408	0.0415
	Poisson	59.60	0.01	0.01	0.2451	0.0296
Lognormal	Normal	37.12	7.86	0.80	2.8999	0.3556
	Lognormal	80.84	0.64	0.21	1.8501	0.2309
	Gamma	86.05	6.58	0.27	1.9416	0.2418
	Poisson	77.01	12.22	1.93	2.1647	0.2682
Gamma	Normal	32.78	0.43	0.12	0.3286	0.0405
	Lognormal	73.83	0.67	0.16	0.2644	0.0328
	Gamma	75.59	0.22	0.06	0.2636	0.0327
	Poisson	82.47	0.19	0.05	0.2639	0.0327
Poisson	Normal	53.04	0.011	0.003	0.0470	0.0058
	Lognormal	39.87	0.002	0.002	0.0472	0.0058
	Gamma	42.55	0.03	0.007	0.0472	0.0058
	Poisson	83.28	0.02	0.006	0.0417	0.0051

Table 2.6: Summary of the simulation when the model error distributions used in the generalized linear model analyses were the same as those used in simulating stock-recruitment (SR) data. The Cushing model and the first set of data which had S values randomly drawn from 1000 to 10 000 were used in the simulation. Outliers were added and the sample size was 40. Relative estimate bias (REB) and root mean square error (RMSE) for parameters are shown.

Model error distribution in simulating SR data	Distribution that outliers follow	% of data being outliers	% of simulations with homogeneous residuals	REB for $\ln(\alpha)$ (%)	REB for β (%)	RMSE for $\ln(\alpha)$	RMSE for β
Normal	Lognormal	10	66.8	1.77	0.67	0.7189	0.0866
		20	58.4	2.28	0.97	1.1859	0.1477
		40	43.4	5.83	2.29	1.5351	0.1852
Lognormal	Normal	10	80.0	4.08	1.17	1.2193	0.1485
		20	81.6	0.36	0.09	1.1835	0.1444
		40	79.5	0.52	0.16	0.9844	0.1203
Gamma	Normal	10	55.2	0.14	0.03	0.2030	0.0244
		20	47.9	1.37	0.38	0.2273	0.0273
		40	29.0	0.16	0.04	0.2332	0.0278
Poisson	Normal	10	68.4	0.12	0.03	0.0780	0.0092
		20	69.5	0.13	0.04	0.1044	0.0123
		40	59.5	0.14	0.04	0.1499	0.0177

Table 2.7: Summary of the simulation when the model error distributions used in the generalized linear model analyses were not the same as those used in simulating stock-recruitment (SR) data. The Cushing model and the first set of data which had S values randomly drawn from 1000 to 10 000 were used in the simulation. Outliers were added and the sample size was 40. Relative estimate bias (REB) and Root mean square error (RMSE) for parameters are shown.

Model error distribution		% of data being outliers	% of simulations withhomogeneous residuals	REB for $\ln(\alpha)$ (%)	REB for β (%)	RMSE for $\ln(\alpha)$	RMSE for β
In simulating SR data	In GzLM						
Normal	Lognormal	10	56.6	1.21	0.31	0.4658	0.0563
		20	69.8	1.69	0.46	0.6479	0.0788
	Gamma	10	56.0	1.03	0.12	0.5111	0.0619
		20	68.8	0.15	0.31	0.7147	0.0870
	Poisson	10	70.4	0.25	0.10	0.5843	0.0664
		20	68.3	0.38	0.24	0.7996	0.0972
Lognormal	Normal	10	18.9	3.21	0.51	1.9861	0.2385
		20	22.0	1.38	1.66	1.9122	0.2305
	Gamma	10	83.2	7.83	0.72	1.2994	0.1572
		20	83.0	4.04	0.20	1.2773	0.1557
	Poisson	10	49.1	9.25	1.13	1.4226	0.1724
		20	54.6	4.76	0.01	1.4020	0.1704

Gamma	Normal	10	23.3	0.19	0.05	0.2329	0.0279
		20	30.6	1.20	0.33	0.2283	0.0273
	Lognormal	10	56.4	0.78	0.19	0.2042	0.0245
		20	47.0	2.17	0.58	0.2325	0.0278
	Poisson	10	75.5	0.17	0.04	0.2001	0.0241
		20	78.1	1.15	0.32	0.2100	0.0252
Poisson	Normal	10	64.5	0.16	0.04	0.0730	0.0086
		20	71.2	0.13	0.04	0.0952	0.0112
	Lognormal	10	50.3	0.33	0.09	0.1017	0.0121
		20	42.4	0.34	0.09	0.1347	0.0160
	Gamma	10	47.6	0.08	0.02	0.0983	0.0117
		20	42.4	0.11	0.03	0.1317	0.0157

Table 2.8: Summary of the simulation when the model error distributions used in the generalized linear model analyses were the same as those used in simulating stock-recruitment (SR) data. The Cushing model and the second set of data which had true S values of pink salmon were used in the simulation. Outliers were added in simulating the data. Relative estimate bias (REB) and root mean square error (RMSE) for parameters are shown.

Model error distribution in simulating SR data	Distribution that outliers follow	% of data being outliers	% of simulations homogeneous residuals	REB for $\ln(\alpha)$ (%)	REB for β (%)	RMSE for $\ln(\alpha)$	RMSE for β
Normal	Lognormal	10	64.3	0.02	0.18	0.3168	0.0395
		20	40.2	18.44	11.32	3.1441	0.3871
		40	21.8	27.32	8.55	2.9112	0.3597
Lognormal	Normal	10	77.4	0.60	0.18	1.8214	0.2266
		20	67.3	4.57	1.29	1.5377	0.1895
		40	26.7	1.99	0.57	1.3729	0.1690
Gamma	Normal	10	76.2	0.22	0.06	0.2616	0.0323
		20	70.5	0.10	0.02	0.2411	0.0297
		40	61.0	0.63	0.18	0.2321	0.0286
Poisson	Normal	10	80.2	0.07	0.02	0.0590	0.0074
		20	69.1	0.08	0.02	0.1134	0.0142
		40	48.2	0.08	0.03	0.1209	0.0152

Table 2.9: Summary of the simulation when the model error distributions used in the generalized linear model analyses were not the same as those used in simulating stock-recruitment (SR) data. The Cushing model and the second set of data which had true S values of pink salmon were used in the simulation. Outliers were added when simulating the data. Relative estimate bias (REB) and root mean square error (RMSE) for parameters are shown.

Model error distribution		% of data being outliers	% of simulations with homogeneous residuals	REB for $\ln(\alpha)$ (%)	REB for β (%)	RMSE for $\ln(\alpha)$	RMSE for β
in simulating SR data	in GzLM						
Normal	Lognormal	10	83.2	1.71	0.43	0.5946	0.0760
		20	53.1	5.36	1.57	1.1047	0.1408
	Gamma	10	84.3	7.05	2.21	0.6534	0.0840
		20	53.5	18.04	5.66	1.2074	0.1549
	Poisson	10	73.8	4.05	1.33	0.4979	0.0641
		20	40.1	25.31	7.74	2.0522	0.2580
Lognormal	Normal	10	80.0	11.95	2.16	2.9611	0.3629
		20	86.1	41.40	10.64	1.3247	0.1527
	Gamma	10	82.1	14.52	2.72	1.9505	0.2412
		20	73.4	26.27	6.28	1.7398	0.2113
	Poisson	10	81.1	19.76	4.27	2.1775	0.2689

		20	85.7	35.73	9.03	1.4945	0.1772
Gamma	Normal	10	78.4	0.27	0.08	0.3213	0.0395
		20	83.0	0.07	0.03	0.1981	0.0241
	Lognormal	10	74.4	0.72	0.18	0.2617	0.0323
		20	69.3	0.67	0.16	0.2416	0.0297
	Poisson	10	84.2	0.09	0.03	0.2575	0.0318
		20	85.7	0.06	0.02	0.2004	0.0245
Poisson	Normal	10	65.7	0.14	0.04	0.0560	0.0068
		20	59.4	0.11	0.03	0.1596	0.0197
	Lognormal	10	87.7	0.05	0.02	0.0673	0.0085
		20	82.7	0.11	0.04	0.0870	0.0111
	Gamma	10	89.6	0.01	0.01	0.0671	0.0085
		20	82.5	0.03	0.01	0.0866	0.0110

Figure 2.1. An example for showing the homogeneity and heterogeneity of residual distributions. Pearson residuals were used. The model error distribution used in simulating the stock-recruitment data was normal; the model error distribution used in the generalized linear model for the parameter estimation are normal (a), lognormal (b), gamma (c), and Poisson (d).

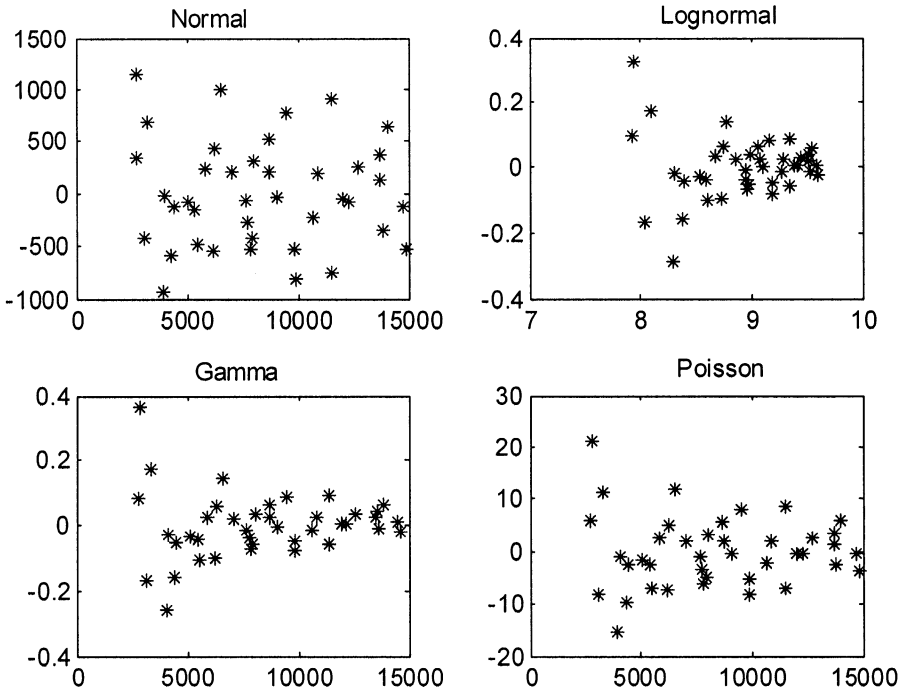

Figure 2.2. Relative estimation error (REE) for the two parameters, $Ln(\alpha)$ (a) and β (b), in the Cushing model in 1000 runs of simulation when different sample sizes are used in the simulation study. The simulated model error distribution is normal, the model error distributions used in the parameter estimates are normal (solid line), lognormal (dash-dot line), gamma (dashed line) and Poisson (dotted line).

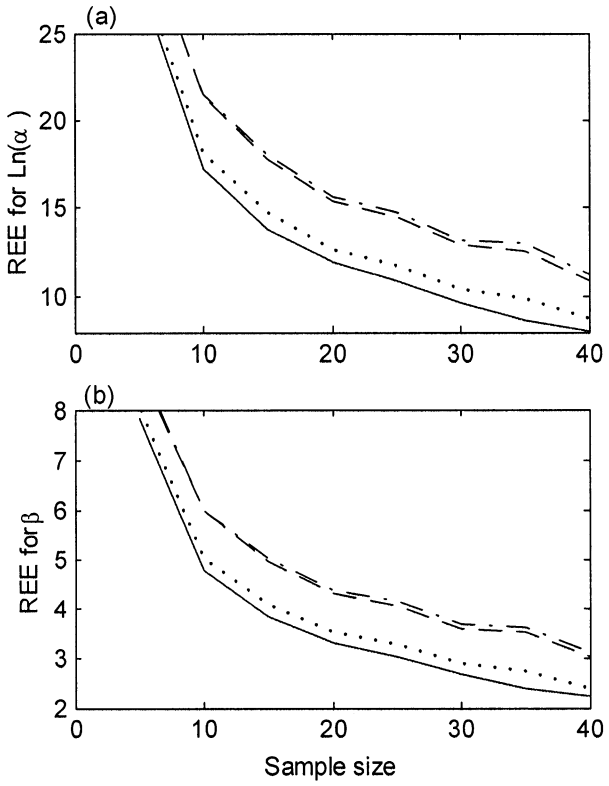

Figure 2.3. Relative estimation error (REE) for the two parameters, $Ln(\alpha)$ (a) and β (b), in the Cushing model in 1000 runs of simulation when different percentages of outliers were added in the stock-recruitment data. The number of stock-recruitment observations used in the simulation is 40. The model error distribution used in simulating stock-recruitment data is normal, the model error distributions used in the generalized linear model for the parameter estimation are normal (solid line), lognormal (dash-dot line), gamma (dashed line) and Poisson (dotted line).

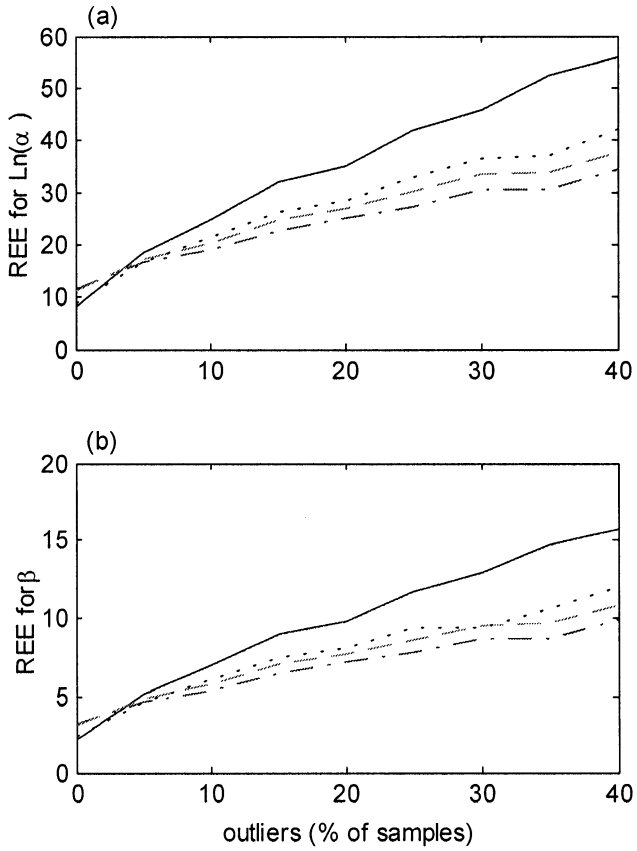

CHAPTER 3

AN ANALYSIS OF ERROR STRUCTURE IN MODELING THE STOCK-RECRUITMENT DATA OF GADOID STOCKS USING GENERALIZED LINEAR MODEL

Abstract

When modeling the stock-recruitment (SR) relationship, the Cushing, Ricker, and other SR models, are fitted to the observed SR data by estimating parameters with assumptions made concerning the model error structure. Using a generalized linear model approach, I explored and identified the appropriate model error structure in modeling SR data for gadoid stocks. The SR parameter estimation was found to be influenced by the choice of error distributions assumed in the analysis. This study suggests that the acceptable SR model error structure can be normal and/or lognormal, which is widely assumed in SR modeling, but it can be gamma and/or Poisson also. In modeling SR data for gadoid stocks, the Beverton-Holt model was found to be more sensitive to the assumption of model error distribution than the Cushing and Ricker models. The lognormal and gamma distribution had a higher probability to be an acceptable model error distribution. Cluster analyses and summary statistics of error distributions in SR modeling did not show a consistent pattern in the identification of an acceptable model error structure among species, geographic distributions and sample sizes. A better understanding of the factors and mechanisms resulting in differences in the choice of appropriate model error distributions for different populations is needed in

future research. I recommend that the generalized linear model be used to identify acceptable model error structures in quantifying SR relationships.

3.1 Introduction

Many species in the family Gadidae have high economic values, such as Atlantic cod (*Gadus morhua*) in the North Atlantic and walleye Pollock (*Theraga chalcogramma*) in the North Pacific. Information on their future recruitments, which is commonly estimated from the corresponding spawning stock biomass, is critical for their management (Hilborn and Walters 1992). Large variations of recruitment have been observed in many cod stocks (e.g., Myers et al. 1995; Myers and Barrowman 1996; Hinrichsen 2001). The dynamics of the recruitment requires full understanding of the dynamics of the spawning stock biomass (Ricker 1975). Knowledge of the stock-recruitment (SR) relationship is commonly obtained through quantitative modeling. The SR relationship of cod stocks has been explored in many studies (e.g., Myers et al. 1995; Myers and Barrowman 1996; Power 1996). However, as noted by Hilborn and Walters (1992), the estimation of the SR relationship is perhaps the most difficult work in fisheries stock assessment. For many fish stocks, the SR relationships are not clear (Ricker 1975; Hilborn and Walters 1992; Iles 1994). Often the shape of the recruitment curve is hard to determine because of small sample size and because of the high variability in recruitment.

A combination of the assumed model form and error structure determines an objective function, which in turn dictates the parameter estimation (Chen et al. 2003). The lack of fit of data to an SR model does not necessarily establish the independence

between the stock and recruitment. It likely results from a highly skewed distribution of recruitment values for a given level of stock (Chen and Paloheimo 1995). Thus understanding the model error structure is necessary in evaluating and estimating the relation of recruitment to stock size.

Modeling errors result from inappropriate model form or inappropriate error structure (Carroll and Ruppert 1984; Schnute 1991; Schnute and Richards 2001). Different mathematical functions have been developed for the SR models based on ecological and mathematical theories (Hilborn and Walters 1992). The model error structure is often ignored in the SR model fit. For example, in fitting a SR model using a nonlinear least-square method, the assumed model error distribution is always normal. A commonly used practice is to linearize SR models by taking an appropriate transformation (e.g., logarithmic for the Cushing, Ricker model; reciprocal for the Beverton-Holt model) and then to use a least-square criterion to estimate parameters. The intrinsic recruitment distribution has often been ignored for the convenience of parameter estimation, perhaps resulting in estimation errors (Chen and Paloheimo 1995).

The necessity of having a realistic error structure or applying an estimation method that is robust to the error structure assumption in modeling the dynamics of fish populations has been discussed in various studies (Bajdik and Schneider 1991; Chen and Paloheimo 1998; Shertzer and Prager 2002). In this chapter I used a generalized linear model method to explore and identify acceptable error structures in modeling SR data for cod stocks. The generalized linear model method is a maximum likelihood-based

method, which provides a convenient and effective way to evaluate and identify the acceptable model error distribution for given data and models. The choice of the link function, which is an essential component in the generalized linear model method, does not affect the assumptions concerning the distribution of the independent variable, unlike the case of transformations used in least-square methods (Bajdik and Schneider 1991; Quinn and Deriso 1999). In an extensive Monte Carlo simulation study, Jiao et al. (2003) found that the quality of SR parameter estimates, measured by estimation errors, could be influenced by the realism of error structure assumed in an estimation, the number of SR data points, and the number of outliers in modeling. A small number of SR data points and presence of outliers in SR data could increase the difficulty of identifying the appropriate error structure in modeling, which might lead to large biases in SR parameter estimation. They also found that the generalized linear model could help identify the acceptable error distribution in SR modeling, leading to an improved estimation of parameters even when there were outliers and the number of SR data points was small (Jiao et al. 2003).

In this study, using the generalized linear model method, I explore and identify acceptable model error structures for commonly used Cushing, Ricker and Beverton-Holt models in fitting the SR data of gadoid stocks. Four model error distributions (normal, lognormal, gamma and Poisson), were used in this study. The normal distribution is widely used for biological and fishery variables in fisheries modeling, which results from an assumption that environmental variations are random. Because of large environmental

changes or other reasons, the variations of those variables might be skewed. Even when both recruitment and stock size follow normal distributions, the model error might not be normal (Chen and Paloheimo 1995). So, I included the skewed distributions of lognormal and gamma in this study. I also included the Poisson distribution because the recruitment is non-negative count data. The use of the Poisson distribution in the parameter estimation also showed robustness with respect to Misspecification of error structure, small sample size, and outliers in our simulation study (Jiao et al. 2003). For example, when the error distribution used in simulating SR data was normal and the data were contaminated with lognormally distributed outliers, the Poisson error distribution used in the generalized linear model analysis provided the highest percentage of simulation runs with homogeneous residuals and better parameter estimates (Jiao et al. 2003).

I evaluated all the cod stocks for which SR data are available, to determine whether there were consistent patterns among different gadoid stocks in identifying acceptable SR model error distributions.

3.2 Materials and Methods

The SR data used in this study are cod stocks in the family Gadidae obtained from Dr. R.A. Myers's website at http://www.mscs.dal.ca/~myers/welcome.html. The fishery divisions and the data sources are shown in Dr. Myers's website and in Myers et al. (1995). The stocks in the North Atlantic generally follow the divisions of the Northwest Atlantic Fisheries Organization (NAFO) or the International Council for the Exploitation

of the Sea (ICES) (Fig. 3.1). Some of the stocks are called the location name if they are commonly applied to the stocks in practice, or if the NAFO or ICES regions do not adequately describe the presently used stock boundaries (Myers et al. 1995). For the Atlantic cod (*Gadus morhua*) stock in NAFO division 2J3KL I updated the SR data to the year 1997 using catch data (Lilly et al. 2001) and sequential population analysis. NAFO division 3Ps updated SR data were estimated based on the data from Brattey et al. (2001).

In this study I analyzed the SR relationship based on the Cushing, Ricker model and Beverton-Holt model (Quinn and Deriso 1999) to explore the identification of acceptable SR model error distributions in cod stocks. The Cushing model can be written as

(1) $$R = \alpha S^{\beta},$$

and the Ricker model can be written as

(2) $$R = \alpha S e^{-\beta S},$$

and the Beverton-Holt model can be written as

(3) $$R = \frac{\alpha S}{1 + \beta S}$$

where α and β are two parameters to be estimated, and S and R are the spawning stock biomass and its subsequent recruitment, respectively.

The generalized linear model was used to explore the model error distributions. The generalized linear model is sometimes abbreviated as GLM (McCullagh and Nelder 1989; Lindsey 1997; Myers et al. 2001), GLIM (Software of GLIM distributed by Numerical Algorithms Group), or GLZ (StatSoft). In this paper I write GzLM to differentiate the generalized linear model from the general linear model (GLM) and the software GLIM.

The procedure of GzLM parameter estimation for the Cushing, Ricker and Beverton-Holt models was detailed in Jiao et al. (2003). Following that study, I used the following procedure to determine whether an assumed error structure was acceptable for a given set of SR data and SR model. A SR model is fitted to a SR data set by assuming an initial error distribution to estimate the model parameters. Pearson residuals (McCullagh and Nelder 1989) from the model fitting were calculated. Pearson residuals are the differences between observed and predicted values, standardized (divide by the estimated standard deviation of the fitted value) to make their variance (theoretically) constant. The Pearson residuals were first used to check for the homogeneity of model error distributions. Visual checking was used by looking at the plot of the Pearson residuals against fitted values. For a given SR model and set of data, I selected acceptable model error distributions according to variance diagnostic analyses (See Fig. 2.1 in Jiao et al. 2003). An assumed model error distribution in SR modeling resulting in homoscedastic residuals was regarded as an acceptable model error distribution, and vice versa (McCullagh and Nelder 1989). Because the SR data points are not evenly distributed in many of the data sets and some of the SR data sets have small sample size, it is

subjectively biased when visual checking is used based on the Pearson residuals against fitted values. This is the main criteria to diagnose the residuals. Normal probability plot is used as the second step to diagnose the residuals. A disadvantage of the Pearson residual is that the distribution of Pearson residuals for non-normal distribution is often markedly skewed, and so it may fail to have properties similar to those of a normal-theory residual. Anscombe residuals (McCullagh and Nelder 1989) improved the normal theory characteristics to a degree. They normalize the probability functions and stabilize the variance through transformations (McCullagh and Nelder 1989). In this study, Anscombe residuals were used to diagnose the model error also. When an acceptable model error distribution is used in the generalized linear model, the normal probability plot of the Anscombe residuals will show normal probability characteristics, i.e., the normal probability plot of the Anscombe residuals will be linear. As an example, the SR data for NAFO divisions 2J3KL cod (*Gadus morhua*) from Dr. Myers' website were analyzed using the three SR models with four types of model error distributions assumed in estimating parameters in the SR models (Table 3.1).

I used a cluster analysis to identify the similarities, grouping patterns among species/stocks based on their error distributions observed in SR modeling using the GzLM. I used a sequential, agglomerative, hierarchical algorithm based on the Manhatten distance in the cluster analysis (Everitt et al. 2001). It means that in the hierarchical clustering, the agglomerative method was used. Here I used the average linkage (UPGMA) to do the agglomerative hierarchical clustering. The distance used in the clustering analysis is the Manhatten distance. Species and stocks listed in Table 3.2

and 3.3 are clustered according to their acceptable SR Cushing, Ricker and Beverton-Holt model error distributions identified in the GzLM.

3.3 Results

The parameter estimates varied with the error distribution assumed in the GzLM estimation for NAFO 2J3KL cod, which was used as an example in this study (Table 3.1). The residual diagnostic plots for the Cushing model did not clearly show which error distribution yielded homogeneous residuals, but the residuals diagnostic plots when normal and Poisson distribution were used looked better than when lognormal and gamma distribution were used (Fig. 3.2). The normal probability plot of Anscombe residuals clearly showed that the normal error distribution yielded normal residuals, while the Poisson distribution assumptions were less acceptable (Fig. 3.3). Combining the above diagnosis the normal distribution was regarded as the acceptable model error structure. When the four model error distributions were assumed in the GzLM for the Cushing model, the parameter estimates and model fits differed greatly (Table 3.1 and Fig. 3.4). I showed parameter estimates when the four model error distributions were assumed in the GzLM for the Ricker and Beverton-Holt models but I did not show residual diagnostic plots and normal probability plots because of too many figures (Table 3.1). The estimation procedure and the residual diagnostic procedure are the same when determining an acceptable model error distribution.

When the SR data for the 17 Gadidae species (86 stocks) were analyzed based on the Cushing, Ricker and Beverton-Holt models using the GzLM, the acceptable model error distributions were found to depend on the stocks and choice of the models (Tables 3.2 and 3.3). A comparison of the acceptable model error distributions in using data from Dr. Myers' website with the updated SR data for NAFO division 2J3KL and 3Ps cod stocks (Table 3.2) suggested that the identification of acceptable model error distributions in GzLM was also related to sample size, or the years that were included in the analysis. There were stocks for which several model error distributions were acceptable for the SR models (e.g., GM20, MM47). There were also stocks for which none of the four error distributions included in this study was acceptable for a SR model (e.g., GMP2, MG60).

The proportion of the *Gadus morhua* stocks for which an acceptable model error distribution could be identified (Table 3.2) was similar to that for all the stocks analyzed (Table 3.3). The lognormal distribution was acceptable in 52% of the cases when the Cushing model was used, in 57% of the cases when the Ricker models were used and in 48% of the cases when the Beverton-Holt model was used for the 86 gadoid stocks (Table 3.3). They were 50%, 62% and 47%, correspondingly, for the 34 *Gadus morhua* stocks (Table 3.2). The gamma distribution was ranked second by the number and percentage for being identified as acceptable model error distributions in the analyses. The gamma distribution was acceptable in 36% of the cases when the Cushing model was used and 33% of the cases when the Ricker model was used, and 37% of the cases when the Beverton-Holt model was used for all the gadoid stocks. They were 35%, 32% and 41%,

correspondingly, for 34 *Gadus morhua* stocks. The number of acceptable model error distributions for the Cushing model was slightly more than that for the Ricker and Beverton-holt models. The numbers of the normal, lognormal, gamma and Poisson distributions being identified as acceptable model error distributions were similar for all the Cushing, Ricker and Beverton-Holt models (Tables 3.2 and 3.3).

The 34 *Gadus morhua* stocks could be divided into two groups according to the cluster analysis of the error distributions observed in SR modeling using the GzLM (Fig. 3.5). Group 1 included stocks that had only lognormal and/or gamma model error distributions identified acceptable in the GzLM analysis of SR data for a given SR model. Among these stocks, in group 1A only the lognormal and/or gamma distribution were identified as acceptable error distributions in the GzLM analysis of the three SR models except in stock GM32, where the Poisson distribution was identified as an acceptable error distribution in the Cushing model. For stocks in group 1B, only the lognormal distribution was identified as an acceptable error distribution in the GzLM analysis of the three SR models, except in GM24 where none of the distributions were identified as an acceptable error distribution in all three SR models, and in stock GM27, where none of the distributions were identified as an acceptable error distribution in the Ricker and Beverton-Holt models. For stocks in group 2B, the normal and/or Poisson were identified as the acceptable model error distributions in the GzLM analysis of SR data, except in stock GM7, where the gamma distribution was identified as an acceptable error distribution in the Ricker and Beverton-Holt models. Stocks in group 2A differed from

those in groups 1 and 2B in that multiple error distributions were identified as acceptable in the GzLM analysis of SR data for the SR models.

All the gadoid stocks could be divided into three groups according to the cluster analysis of the SR modeling errors in the GzLM (Fig. 3.6). The group 1 and 3 were composed of stocks for which all three SR models had one or two error distributions that could be defined as acceptable in the GzLM. Group 2 was mainly composed of stocks for which the SR models had multiple error distributions that could be defined as acceptable in the GzLM. For group 1A1, the acceptable SR modeling error distributions were none or only one in one of the SR models. In stocks GM27 and TC80 only lognormal distribution was acceptable in the Cushing model in the GzLM analysis. In stocks MA39, MG61 and TC76 only the lognormal distribution was acceptable in the Ricker model. In stocks MA53 and TC77 only the Poisson distribution was acceptable in the Beverton-Holt model and the Ricker model separately. Subgroup 1A2 was composed of the stocks for which only the lognormal error distribution was acceptable in most of the cases. In subgroup 1A2A the the acceptable SR model error distribution was only lognormal in all the three SR models. For all stocks in group 1C the lognormal and/or gamma error distributions were the acceptable model error distributions. Subgroup 1C2 was composed of the stocks for which only gamma error distribution was acceptable in most of the cases. In group 3A the Poisson and/or gamma error distributions were acceptable. In group 3B, the stocks had normal and/or Poisson distributions as the acceptable SR model error distribution. In other subgroups, the SR models of the stocks had multiple acceptable

model error distributions or no common features in the acceptable model error distributions.

The grouping based on the cluster analyses of SR modeling errors (i.e., residuals) did not show a clear pattern among species/stocks, geographic distributions and sample sizes (Figs. 3.5 and 3.6). For stocks with sample sizes ≤ 15, the lognormal distribution had the highest probability to be defined as an acceptable model error structure for the Cushing and Ricker models, but in the Beverton-Holt model the gamma distribution had the same proportion as the lognormal distribution. As the sample size increased to > 15, the lognormal distribution had the highest probability to be defined as an acceptable model error distribution in all the three SR models, but the proportion of the stocks for which lognormal or gamma was identified as acceptable in the GzLM decreased when the sample size increased to > 30 (Table 3.4). From the total value of the proportion of the stocks for which a particular model error distribution was identified as acceptable in the GzLM analysis, the number of acceptable model error distributions have no obvious relationship with the sample size.

The proportion of the stocks for which the four distributions were identified as the acceptable model error structure in the GzLM differed somewhat between the stocks in the Northwest Atlantic area and the stocks in the Northeast Atlantic area (Table 3.5). The lognormal distribution still has the highest probability to be defined as an acceptable model error structure in the SR data of the stocks in the Northeast Atlantic. In the Northwest Atlantic the gamma distribution has the highest probability to be defined as an

acceptable model error structure in the stocks. For the stocks in the Northwest Atlantic, the proportion of the four distributions identified as the acceptable SR model error distribution differed not as much as for the stocks in the Northeast Atlantic. For stocks from the North Pacific areas, the lognormal distribution also had the highest probability to be defined as an acceptable model error structure. For stocks from the Southeast Atlantic, each of the four error distributions defined as an acceptable model error structure did not differ greatly (Table 3.5). Because this study only included eight stocks from the North Pacific and six stocks from the Southeast Atlantic, and the sample sizes in those stocks are small, this result might not be conclusive. This study also included two stocks MMH65 and MA67 from Southwest Atlantic and Southwest Pacific ocean areas. However, because of their small number of stocks I would not try to make a conclusion about their possible error distributions in modeling SR data.

3.4 Discussion

An inappropriate model error assumption in SR modeling was likely to yield an inappropriate estimation of SR model parameters (Jiao et al. 2003). It is thus important to evaluate if the error structure assumed in the modeling is acceptable for a given SR model and data set and to identify the most appropriate model error assumption for the SR modeling. The normal error distribution tends to be sensitive to outliers in SR models (Jiao et al. 2003). Large variations in environment conditions may lead to skewed distributions of the recruitment, and even when both stock and recruitment follow a normal distribution, errors in modeling SR data may not be normal. Thus the GzLM can

improve the parameter estimation in the SR modeling compared with the General Linear Model, which is limited to the normal error distribution only.

This study suggests that the acceptable model error structures differ among data sets. It could differ among SR models also, though 57% of the SR data sets had the same acceptable model error structure in the three SR models in this study. Error distributions assumed in the SR modeling acceptable to one data set or model were not necessarily acceptable to other data sets (with the same model) or to other SR models (with the same data set). Thus, the choice of error distributions should be fisheries-specific and model-specific. This study indicates that there are situations where several distributions are acceptable and where the GzLM could not determine which one is the most appropriate. This study also suggests that, normal error distribution, although not usually used in SR modeling now, may be an acceptable error structure in many cases.

The possibility of having several acceptable model error distributions or no acceptable model error distributions demonstrates the difficulty of selecting the best model error assumption for the parameter estimation in the SR modeling. A quantitative goodness-of-fit criterion needs to be developed for identifying the most appropriate model error distribution when estimating parameters using the maximum likelihood method. The commonly used quantitative goodness-of-fit criteria, such as the maximum likelihood value and scaled variance, are only used for comparing the differences when the same model error distribution is used because the maximum likelihood function differs for different error structures assumed in SR modeling.

The proportion of the stocks for which the particular model error distributions were identified as acceptable model error distributions in the GzLM analysis of SR data in gadoid stocks implies that in modeling gadoid SR data the Beverton-Holt model is more sensitive to the model error distribution assumption than the Cushing and Ricker models. The lognormal and gamma distributions have a higher probability to be defined as an acceptable model error distribution while the normal and Poisson distributions have a relatively lower probability to be defined as an acceptable model error distribution. The results presented in Tables 3.2 and 3.3 and Figures 3.5 and 3.6 might help select an acceptable model for stocks included in this study. But I recommend re-analyzing the SR data using the GzLM approach proposed in this study if more recent years of data are included in future studies, because the identification of acceptable error distributions tends to be data-specific.

The cluster analysis of SR modeling error distributions suggests that there were no clear patterns in the identification of the acceptable model error distributions for stocks from different geographic areas and for different species. This variation in modeling error distribution is likely to result from intrinsic as well as extrinsic biological and physical processes (Armstrong and Shelton 1988; Fogarty 1993; Iles and Beverton 1998). Species or stocks in a local ecosystem can be influenced by large scale climate changes, but the magnitude of the impacts might be different in ocean basins because of their distinctive oceanographic characteristics. That might explain the stock-specific SR patterns and model error structures.

Four model error distributions were considered in this study. There are, however, other distributions such as the Weibull distribution. GzLM can do parameter estimates only when model error distributions belong to the exponential family. For distributions that do not belong to the exponential family, the maximum likelihood method may be used to find parameter estimates and to perform model error distribution diagnostics. To identify acceptable model error structure, we recommend exploring other possible model error structures when the model error distribution is not in the exponential family, not only limited investigations to the four distributions shown in this study.

The choice of acceptable model error distributions can also be influenced by the choice of SR models. Thus for stocks where I could not identify an acceptable error distribution, the lack of an acceptable model error distribution might result from an inappropriate choice of SR functions. Although I did not consider the choice of SR functions in this study, I recommend the multiple choices of SR functions be considered when no apparently acceptable or multiple acceptable error distributions can be defined, or when a certain SR model does not fit the data well. For example, for cod (*Gadus morhua*) in NAFO 3Ps stock, the residual diagnostic plot showed that all four error distributions were acceptable when all three SR models were used. Recruitment obviously could not be explained well by the stock biomass. A new SR function needs to be developed considering biological and physical processes of recruitment in this case (Koster et al. 2001). Incorporation of vital environmental variables in SR modeling may be necessary (Hilborn and Walters 1992).

Table 3.1. Stock-recruitment parameter estimates for the Atlantic cod (*Gadus morhua*) in NAFO Divisions 2J3KL stock when the four different model error distributions were used in the GzLM.

Model	Error distribution	Parameter estimate from GzLM		R^2
		α	β	
Cushing	Normal	430.8880	1.0592	0.7374
	Lognormal	4918.7063	0.6600	0.6757
	Gamma	9632.7740	0.5832	0.6598
	Poisson	2500.9341	0.7978	0.7008
Ricker	Normal	649.2384	1.000×10^{-7}	0.7304
	Lognormal	719.5640	2.5091×10^{-4}	0.6808
	Gamma	1072.9489	5.2325×10^{-4}	0.5880
	Poisson	730.4731	1.0673×10^{-4}	0.7127
Beverton -Holt	Normal	649.2401	2.5423×10^{-5}	0.7304
	Lognormal	800.3312	8.0680×10^{-6}	0.6565
	Gamma	1353.1077	7.7507×10^{-6}	0.5665
	Poisson	2849.6326	1.6283×10^{-5}	0.3899

Table 3.2. *Gadus morhua* stocks and their acceptable stock-recruitment model error distributions identified in the GzLM for the Cushing, Ricker and Beverton-Holt models. The stocks generally follow the Northwest Atlantic Fisheries Organization (NAFO) or the International Council for the Exploitation of the Sea (ICES) divisions or the commonly used name based on their distribution. N, L, G, and P represent normal, lognormal, gamma and Poisson distribution, respectively. 0 indicates an unacceptable model error distribution and 1 indicates an acceptable model error distribution. The fishery distribution areas are classified as Northeast Atlantic (NEA), Northwest Atlantic (NWA).

Gadus morhua (cod)		Code	Fishery Distribution	Sample size	Cushing model				Ricker model				Beverton-Holt model			
					N	L	G	P	N	L	G	P	N	L	G	P
Baltic Areas 22 and 24		GM3	NEA	22	1	0	1	0	1	0	1	0	1	0	1	0
Baltic Areas 25-32		GM4	NEA	24	0	1	1	0	0	1	1	0	0	1	1	0
Celtic Sea		GM5	NEA	22	0	1	0	0	0	1	0	0	0	1	0	0
Faroe Plateau		GM6	NEA	33	0	0	1	0	0	1	0	0	0	0	1	0
Flemish Cap (NAFO Div. 3M)	1	GM7	NWA	9	0	0	0	1	0	0	1	1	0	0	1	1
Flemish Cap (NAFO Div. 3M)	2	GM8	NWA	27	0	0	1	0	0	0	1	0	0	0	1	0
Greenland offshore component		GM9	NEA	35	0	1	0	0	0	1	0	0	0	1	0	0
ICES VIId		GM10	NEA	18	0	1	0	0	0	1	0	0	0	1	0	0
ICES VIa		GM11	NEA	27	0	1	1	0	0	1	1	0	0	1	1	0
Iceland		GM12	NEA	68	0	1	0	0	0	1	0	0	0	1	0	0
Irish Sea		GM13	NEA	27	0	0	1	0	0	1	0	0	0	0	1	0
Kattegat		GM14	NEA	21	1	0	0	0	1	0	0	0	0	0	0	1
NAFO 2J3KL		GM15	NWA	28	1	0	0	0	1	0	0	0	0	0	0	1

NAFO 2J3KL updated	N_2J	NWA	36	1	0	0	1	1	0	0	1	0	0	0	1
NAFO 3M	GM16	NWA	10	0	0	0	0	0	1	1	0	0	0	1	0
NAFO 3NO	GM17	NWA	31	0	0	1	0	0	0	1	0	0	0	1	0
NAFO 3Pn4RS 1	GM18	NWA	17	0	0	0	0	0	1	1	0	0	0	0	0
NAFO 3Pn4RS 2	GM19	NWA	21	0	1	1	0	0	1	1	0	0	1	1	0
NAFO 3Ps	GM20	NWA	31	1	1	1	1	1	1	1	1	1	1	1	1
NAFO 3Ps updated	N_3Ps	NWA	41	1	0	0	1	1	0	0	1	1	0	0	1
NAFO 4TVn	GM21	NWA	41	1	0	1	1	1	1	0	0	1	0	1	1
NAFO 4VsW	GM22	NWA	33	1	0	0	1	1	0	0	1	1	0	0	1
NAFO 4X	GM23	NWA	45	0	0	1	0	0	0	0	0	0	0	1	0
NAFO 5Y 1	GM24	NWA	7	0	0	0	0	0	0	0	0	0	0	0	0
NAFO 5Y 2	GM25	NWA	34	0	1	0	0	0	1	0	0	0	1	0	0
NAFO 5Z 1	GM26	NWA	20	0	1	0	0	0	1	0	0	0	1	0	0
NAFO 5Z 2	GM27	NWA	34	0	1	0	0	0	0	0	0	0	0	0	0
North East Arctic 1	GM28	NEA	43	0	1	0	0	0	1	0	0	0	1	0	0
North East Arctic 2	GM29	NEA	45	0	1	0	0	0	1	0	0	0	1	0	0
North East Arctic 3	GM30	NEA	59	0	1	0	0	0	1	0	0	0	1	0	0
North East Arctic 4	GM31	NEA	59	1	0	0	0	1	0	0	1	1	0	0	1
North Sea	GM32	NEA	30	0	1	1	1	0	1	1	0	0	1	1	0
Skagerrak	GM33	NEA	13	0	1	0	0	0	1	0	0	0	1	0	0
West Greenland (NAFO 1)	GM34	NWA	35	0	1	0	0	0	1	0	0	0	1	0	0
Total				9	17	12	7	9	21	11	6	6	16	14	9
Proportion				0.26	0.50	0.35	0.21	0.26	0.62	0.32	0.18	0.18	0.47	0.41	0.26

Table 3.3. Gadidae species and stocks (except for *Gadus morhua*) and their acceptable stock-recruitment model error distributions identified in the GzLM. The stocks generally follow the Northwest Atlantic Fisheries Organization (NAFO) or the International Council for the Exploitation of the Sea (ICES) or the commonly used name based on their distribution. N, L, G, and P represent normal, lognormal, gamma and Poisson distribution, respectively. 0 and 1 indicate unacceptable and acceptable model error distributions, respectively. The fishery distribution areas are classified as Northeast Atlantic (NEA), Northwest Atlantic (NWA), Northeast Pacific (NEP), Northwest Pacific (NWP), Southeast Atlantic (SEA), Southwest Atlantic (SWA), and Southwest Pacific (SWP) according to their geographic distribution.

Species and stocks	Code	Fishery Distribution	Sample size	Cushing model				Ricker model				Beverton-Holt model			
				N	L	G	P	N	L	G	P	N	L	G	P
Gadus macrocephalus (Pacific cod)															
Eastern Bering Sea	GMP1	NEP	10	0	1	1	0	0	0	1	1	0	1	1	0
Hecate Strait	GMP2	NEP	14	0	0	0	0	0	0	0	0	0	0	0	0
Melanogrammus aeglefinus (Haddock)															
Faroe Plateau	MA35	NEA	33	0	0	0	1	0	0	0	1	0	0	0	1
ICES VIa	MA36	NEA	29	0	1	0	0	0	1	0	0	0	1	0	0
Iceland	MA37	NEA	28	0	0	1	0	0	0	1	0	0	0	1	0
NAFO 4TVW	MA38	NWA	38	0	1	0	0	0	1	0	0	0	0	0	0
NAFO 4X 1	MA39	NWA	24	0	0	0	0	0	1	0	0	0	0	0	0
NAFO 4X 2	MA40	NWA	26	1	0	0	0	1	0	0	1	1	0	0	0
NAFO 5Z	MA41	NWA	68	0	0	1	0	0	0	1	0	0	0	1	0
North East Arctic	MA42	NEA	44	0	0	1	0	0	0	1	0	0	0	1	0
North Sea 1	MA43	NEA	32	0	0	1	0	0	0	0	0	0	0	1	0

North Sea 2	MA44	NEA	66	0	1	0	0	0	1	0	0	0	1	0	0
Rockall Bank	MA45	NEA	9	1	0	0	0	0	1	0	0	0	0	1	1
Merlangius merlangus (Black Sea whiting)															
Eastern Black Sea	MM46	NEA	24	0	1	0	0	0	1	0	0	0	1	0	0
Western Black Sea	MM47	NEA	23	1	1	1	1	1	1	1	1	1	1	1	1
Merlangius merlangus (Whiting)															
Celtic Sea	MM48	NEA	9	0	1	0	0	0	1	0	0	0	1	0	0
ICES VIId	MM49	NEA	14	1	0	0	1	1	0	0	0	1	0	0	1
ICES VIa	MM50	NEA	27	0	1	0	0	0	1	0	0	0	1	0	0
Irish Sea	MM51	NEA	13	0	0	0	0	1	1	1	1	0	0	0	0
North Sea 1	MM52	NEA	27	0	1	1	0	0	1	1	0	0	1	0	0
North Sea 2	MM53	NEA	74	0	0	0	0	0	0	0	0	0	0	0	1
Merluccius bilinearis (Silver hake)															
Mid Atlantic Bight	MB54	NEA	33	0	1	0	0	0	1	0	0	0	1	0	0
NAFO 4VWX	MB55	NWA	13	0	1	1	0	0	1	1	0	0	1	1	0
NAFO 5Ze	MB56	NWA	33	0	0	0	1	0	0	0	1	0	0	0	1
Merluccius capensis (S.A. Hake)															
South Africa 1.6	MC57	SEA	20	0	1	0	0	0	0	0	0	0	1	0	0
South Africa South Coast	MC58	SEA	12	0	0	0	0	0	0	0	0	0	0	0	0
Merluccius gayi (Peruvian hake)															
Chile - South Central zone	MG59	SEA	14	1	0	0	1	1	0	0	1	0	0	0	0
Chile- Northern zone	MG60	SEA	14	0	0	0	0	0	0	0	0	0	0	0	0
Peru documentation	MG61	SEA	8	0	0	0	0	0	1	0	0	0	0	0	0
Merluccius merluccius (Hake)															
ICES VIIIa,b, d, VIIb-k	MMH62	NEA	20	1	1	1	1	1	1	1	1	1	1	1	1
ICES VIIIc and IXa	MMH63	NEA	16	1	1	1	1	1	1	1	1	1	1	1	1
Jabuka Pit, Adriatic Sea	MMH64	NEA	26	0	0	0	1	1	0	0	1	1	0	0	1
Southwest Atlantic Ocean	MMH65	SWA	9	1	1	1	1	1	1	1	1	1	1	1	1
Merluccius productus (Pacific hake)															
W. US. +Canada	MP66	NEP	23	0	1	0	0	0	1	0	0	0	1	0	0

Micromesistius australis (Southern blue whiting)															
Campbell Island, NZ	MA67	SWP	14	0	1	0	0	0	1	0	0	0	1	0	0
Micromesistius poutassou (Blue whiting)															
Northern ICES	MPB68	NEA	20	0	1	0	0	0	1	0	0	0	1	0	0
Southern ICES	MPB69	SEA	10	1	1	1	1	1	1	1	1	1	1	1	1
Pollachius virens (Pollock or saithe)															
Faroe	PV70	NEA	32	0	1	0	0	0	1	0	0	0	1	0	0
ICES VI	PV71	NEA	30	1	1	1	1	0	0	0	0	1	1	1	1
Iceland	PV72	NEA	32	1	1	1	1	0	0	0	0	0	0	1	0
NAFO 4VWX5	PV73	NWA	10	0	0	1	1	0	0	1	1	0	0	1	1
North East Arctic	PV74	NEA	32	1	0	0	0	0	1	1	0	1	0	0	0
North Sea	PV75	NEA	33	0	1	1	0	0	1	1	0	0	1	1	0
Theragra chalcogramma (Walleye pollock)															
E. Bering Sea	TC76	NEP	24	0	0	0	0	0	1	0	0	0	0	0	0
East Kamchatka	TC77	NWP	12	0	0	0	0	0	0	0	1	0	0	0	0
Gulf of Alaska, Alaska	TC78	NEP	25	0	1	0	0	0	0	1	0	0	1	0	0
Japan-Pacific coast of Hokkaido	TC79	NWP	15	0	1	0	0	0	1	0	0	0	1	0	0
West Bering Sea	TC80	NWP	21	0	1	0	0	0	0	0	0	0	0	0	0
Trisopterus esmarkii (Norway pout)															
North Sea	TE81	NEA	20	1	1	1	1	1	1	1	1	0	1	1	1
Urophycis chuss (Red hake)															
NAFO Gulf of Maine, N. Georges Bank	UC82	NWA	13	1	0	1	1	1	0	0	0	1	0	0	1
NAFO S. New England	UC83	NWA	15	0	0	0	0	0	0	0	0	0	0	0	0
Urophycis tenuis (White hake)															
NAFO 4T	UT84	NWA	14	0	0	0	0	0	0	0	0	0	0	0	0
Total (including *Gadus morhua*)				23	44	30	22	21	48	28	21	17	40	31	24
Proportion				0.27	0.52	0.36	0.26	0.25	0.57	0.33	0.25	0.20	0.48	0.37	0.29

Table 3.4. Proportion of the stocks for which a particular model error distribution was identified as acceptable in the GzLM. The calculation was done for different groups of stocks with different numbers of stock-recruitment observations (n). For a given stock, because multiple error distributions could be defined as acceptable, the sum of the proportions within a group of stocks may be larger than 1.

Sample size	Cushing model				Ricker model				Beverton-Holt model				Total
	N	L	G	P	N	L	G	P	N	L	G	P	
$n \leq 15$	0.25	0.33	0.25	0.29	0.25	0.46	0.33	0.33	0.17	0.33	0.33	0.29	3.63
$15 < n \leq 30$	0.28	0.66	0.44	0.22	0.28	0.66	0.44	0.19	0.22	0.63	0.41	0.25	4.66
$n > 30$	0.27	0.50	0.33	0.27	0.20	0.53	0.20	0.23	0.20	0.40	0.33	0.30	3.77

Table 3.5. Proportion of the stocks for which a particular model error distribution was identified as acceptable in the GzLM. The calculation was done for different groups of stocks distributed at different geographic ocean areas. For a given stock, because multiple error distributions could be defined as acceptable, the sum of the proportions within a group of stocks may be larger than 1.

Geographic area	Number of stocks	Cushing model				Ricker model				Beverton-Holt model				Total
		N	L	G	P	N	L	G	P	N	L	G	P	
Northwest Atlantic	28	0.29	0.29	0.36	0.32	0.29	0.39	0.36	0.29	0.21	0.21	0.39	0.36	3.75
Northeast Atlantic	42	0.29	0.64	0.40	0.24	0.24	0.71	0.33	0.19	0.21	0.62	0.41	0.29	4.57
North Pacific	8	0.00	0.63	0.13	0.00	0.00	0.38	0.25	0.25	0.00	0.50	0.13	0.00	2.25
Southeast Atlantic	6	0.33	0.33	0.17	0.33	0.33	0.33	0.17	0.33	0.17	0.33	0.17	0.17	3.17

Figure 3.1. A map showing the North Atlantic Fisheries Organization (NAFO) areas off the east coast of North America and International Council for the Exploration of the Sea (ICES) areas (modified from Charles 2001; originally produced by Ransom Myers at Dalhousie University).

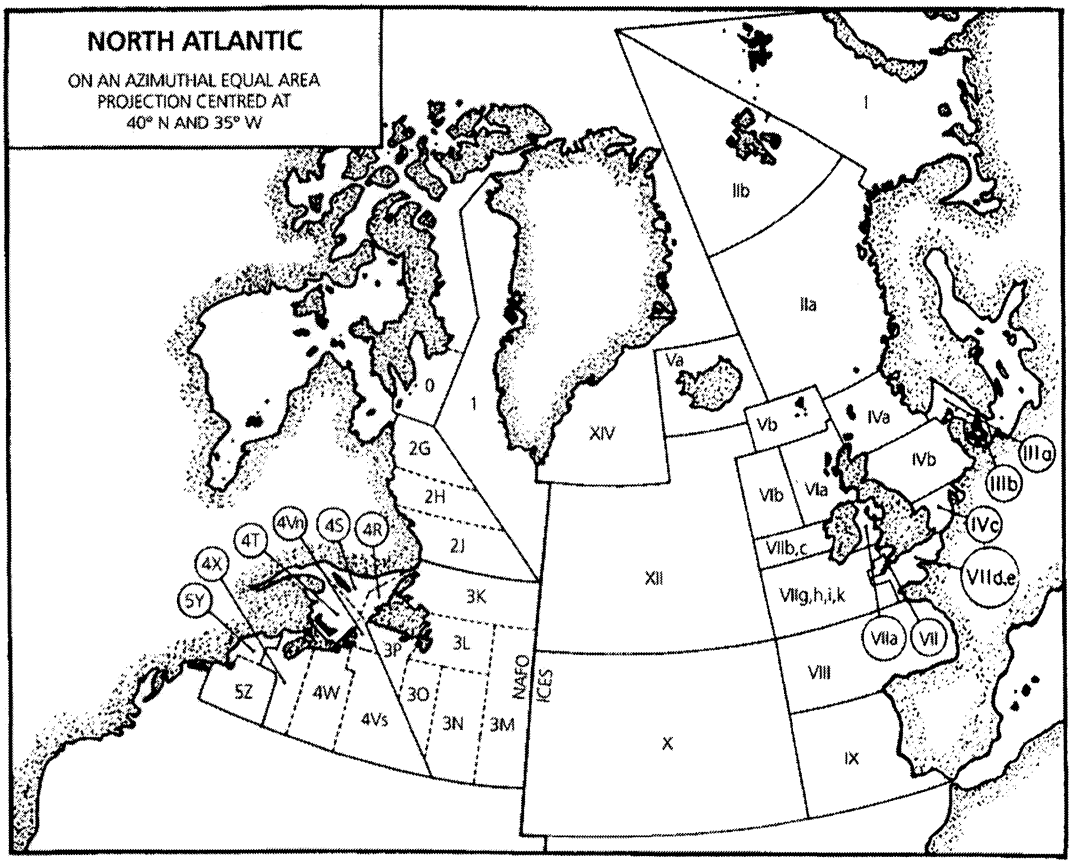

Figure 3.2. Residuals diagnostic plots when the four types of model error distributions were used in the GzLM to estimate the parameters in the Cushing model for Atlantic cod (*Gadus morhua*) NAFO divisions 2J3KL stock. The four model error distributions are: (a) normal distribution, (b) lognormal distribution, (c) gamma distribution and (d) Poisson distribution.

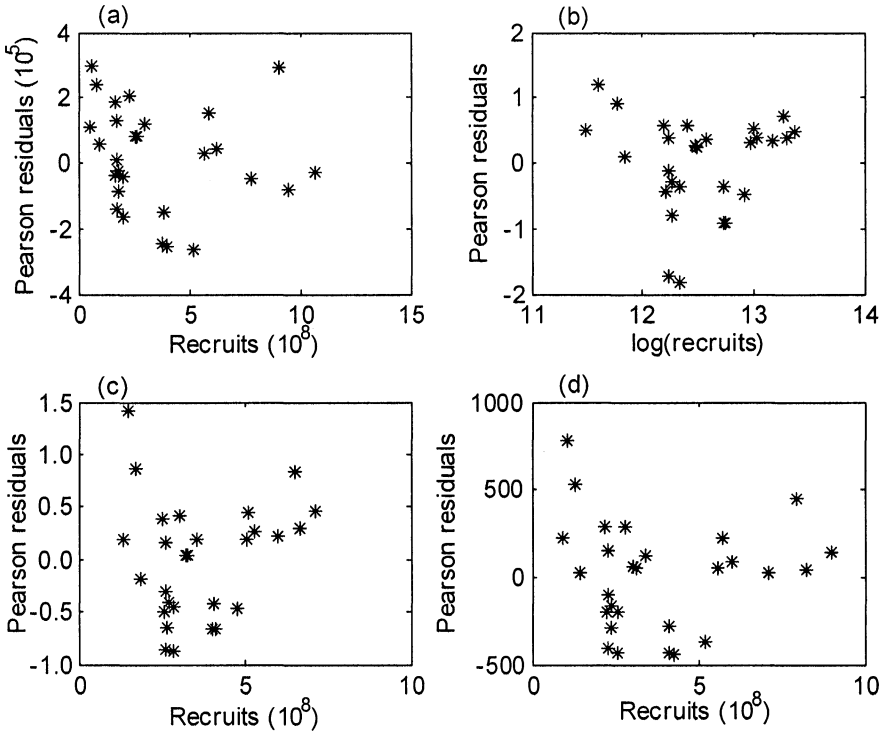

Figure 3.3. Normal probability plot used to diagnose the four types of model error distributions used in the GzLM to estimate the parameters in the Cushing model for Atlantic cod (*Gadus morhua*) NAFO divisions 2J3KL stock. The four model error distributions are: (a) normal distribution, (b) lognormal distribution, (c) gamma distribution and (d) Poisson distribution.

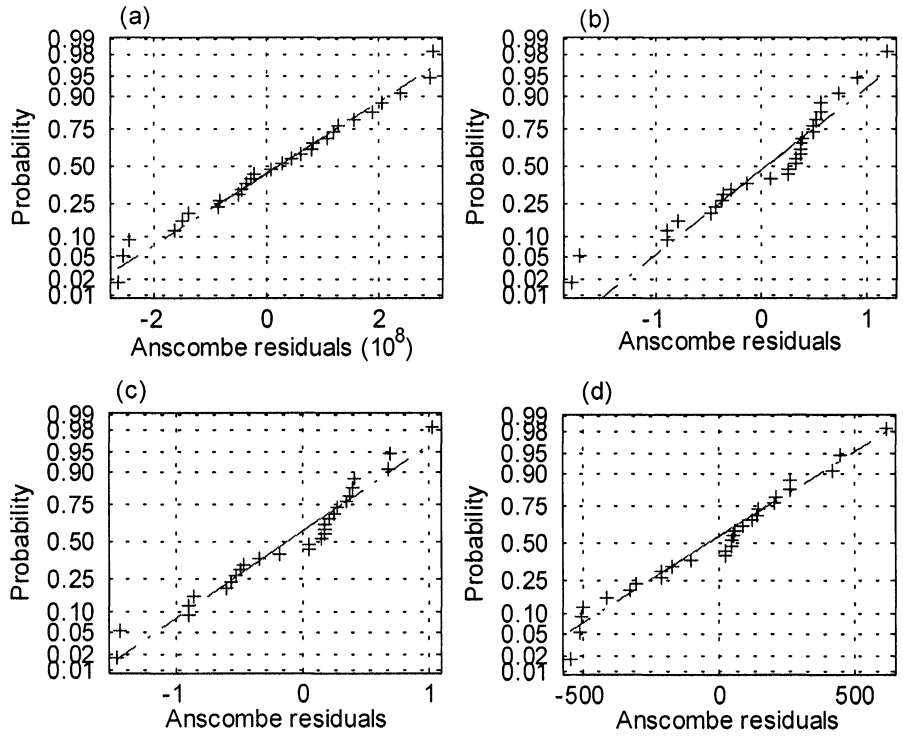

Figure 3.4. Regression analyses when the four types of model error distributions were used in the GzLM to estimate the parameters in the Cushing model for Atlantic cod (*Gadus morhua*) NAFO division 2J3KL stock. Normal (solid line), lognormal (dash-dot line), gamma (dashed line) and Poisson (dotted line).

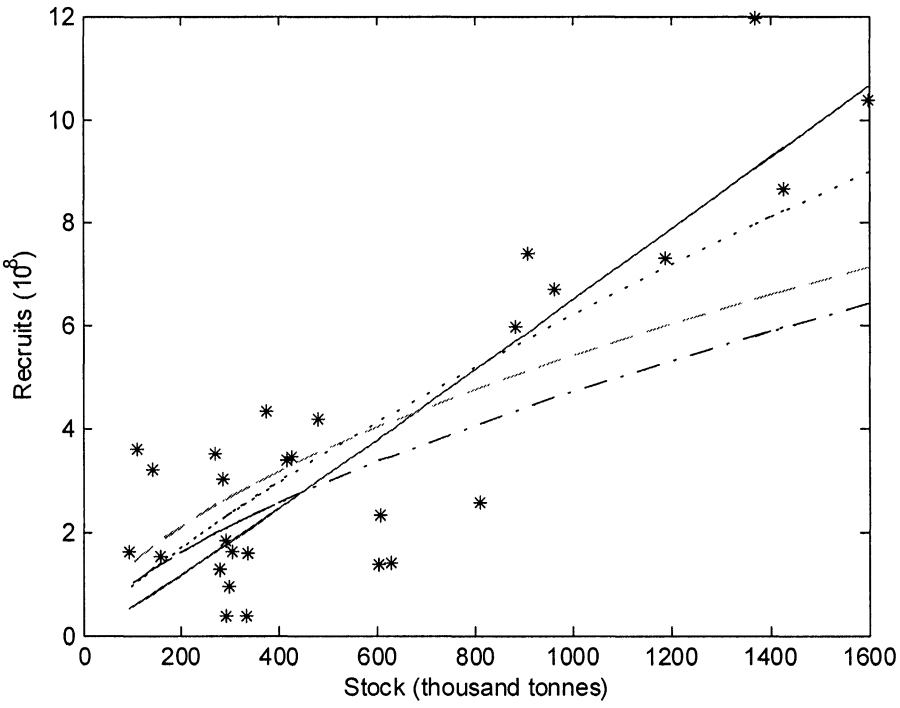

Figure 3.5. A cluster analysis of distributions in stock-recruitment modeling for the *Gadus morhua* stocks.

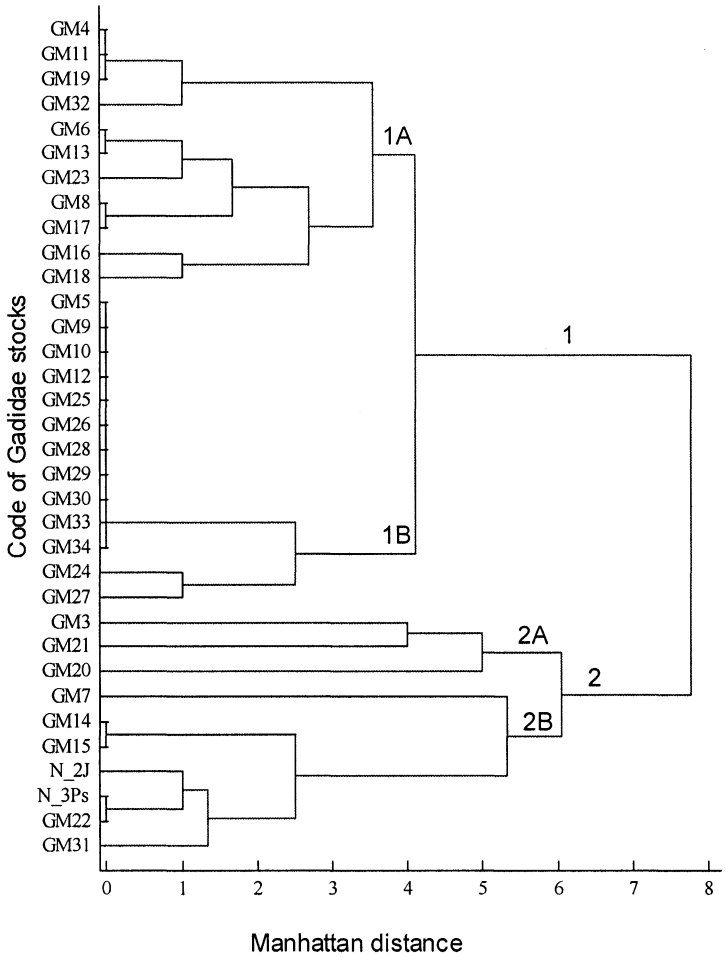

Figure 3.6. A cluster analysis of distributions in stock-recruitment modeling for the Gadidae species and stocks.

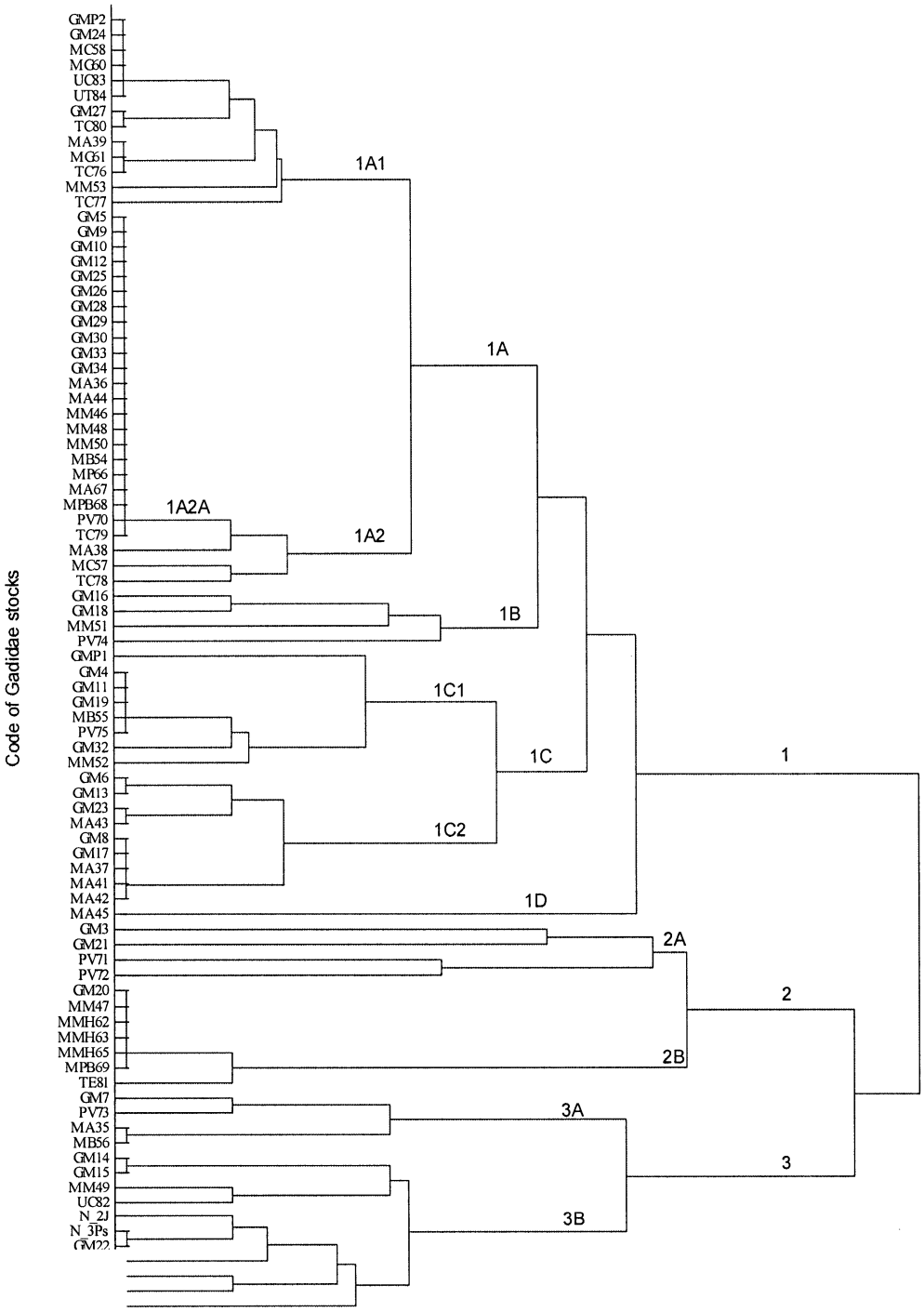

CHAPTER 4

AN APPLICATION OF GENERALIZED LINEAR MODEL IN PRODUCTION MODEL AND SEQUENTIAL POPULATION ANALYSIS

Abstract

Errors in fitting production models and age-structured models are usually assumed to follow a lognormal or normal distribution without an error diagnostic analysis evaluating the assumption made on the error structure of the models. The generalized linear model, which can readily deal with different error structures, was applied to assessing the Atlantic cod (*Gadus morhua*) 2J3KL using a production model and a sequential population model. A framework was developed which combines the production model/or sequential population model and the generalized linear model. This study suggests that the quality of the parameter estimation in both the models can be influenced by the realism of error structure assumed in the estimation. This study identified lognormal and gamma distributions as appropriate model error structures for the production model and gamma and Poisson distributions for the sequential population model in assessing the Atlantic cod 2J3KL stock. I recommend that the generalized linear model be used to identify the appropriate model error structures in quantifying fisheries population dynamics using production models and sequential population models.

4.1 Introduction

Production models and age or size structured population models are widely used in the assessment of many fisheries stocks worldwide (Shepherd 1988; Megrey 1989). Parameter estimation is often done using a nonlinear least squares method. Lognormal error structure was widely assumed in fitting production models and age-structured models to fisheries data.

Firth (1988) showed through asymptotic efficiency that gamma-distribution-based estimators performed better than the lognormal-based estimators. Lognormal-distribution-based estimators were also found to be sensitive to violations in model assumptions in estimating abundance (Myers and Pepin 1990). Gamma-based estimators were found to perform better than the lognormal-distribution-based estimators in sequential population analyses (Cadigan and Myers 2001). A diagnostic procedure is needed to identify the assumption of normally or lognormally distributed error structure in the survey indices in production model and age-structured models.

In this study, I applied generalized linear models, which can deal with different error structures (McCullagh and Nelder 1989), to a production model and an age-structured model. Different distributional assumptions on model error structure were evaluated. I considered normal, lognormal, gamma, and Poisson distributions in this study. The appropriateness of model error structure was diagnosed through residual diagnostic analyses. Both homogeneity and normality of residuals (Pierce and Schafer 1986; McCullagh and Nelder 1989) were diagnosed. The Atlantic cod fishery in NAFO

(Northwest Atlantic Fisheries Organization) 2J3KL was used as an example. Both a production model and an age-structured sequential population analysis model (SPA) were used to model the cod population dynamics (Shepherd 1988; Mohn and Cook 1993; Shelton and Lilly 2000) with the generalized linear models.

4.2 Material and Methods

4.2.1 Generalized linear model (GzLM)

The generalized linear model is sometimes abbreviated as GLM (McCullagh and Nelder 1989; Lindsey 1997; Myers et al 2001), GLIM (Software of GLIM distributed by Numerical Algorithms Group), or GLZ (StatSoft). In this paper I write GzLM to differentiate the generalized linear model from the general linear model (GLM) and the software GLIM.

A GzLM has three components (McCullagh and Nelder 1989). One is the random component $\mathbf{Y}$, which is a vector of observations y having n components that are independently distributed with means $\boldsymbol{\mu}$. The second is the systematic component, which is a specification for the vector $\boldsymbol{\mu}$ in terms of a small number of unknown parameters $\beta_1, \beta_2, ..., \beta_p$. A linear predictor $\boldsymbol{\eta}$ is given by $\boldsymbol{\eta} = \sum_{j=1}^{p} \mathbf{X}_j \beta_j$, where $\mathbf{X}$ is the model matrix or the covariates for observation $\mathbf{Y}$. The third component is the link between the random and systematic components. It is often written as $\boldsymbol{\eta} = g(\boldsymbol{\mu})$, where g is the link function (McCullagh and Nelder 1989). In the case of the GLM, $\eta = \mu$ (i.e. identity link). Thus GLM is a special case of GzLM.

The likelihood function of Y can be written as

(1) $$L = \prod_{1}^{n} f(y;\theta).$$

If the probability density function (p.d.f.) is a member of the exponential class, when X is of discrete type, then I could have

(2) $$f(y;\theta) = \exp[p(\theta)K(y) + s(y) + q(\theta)], \qquad y = a_1, a_2, a_3, \cdots,$$

$$= 0 \qquad \text{elsewhere,}$$

The log-likelihood function is then

(3) $$LL = p(\theta)\sum_{1}^{n} K(y_i) + \sum_{1}^{n} S(y_i) + nq(\theta),$$

in which $\sum_{1}^{n} K(y_i)$ is a sufficient statistic for the parameter θ, $p(\theta)$ is the canonical link for a distribution whose p.d.f. is $f(y;\theta)$. Here, Y is the population abundance index I, X is the population biomass B in the surplus production model or abundance N in population dynamic models, and θ is the parameters in the production and age-structured models (i.e., q).

The exponential family includes the normal, Poisson, gamma and other distributions. The link function $\eta = g(\mu)$ relates the mean of the response variable Y to the linear combination of the X_i. Common choices of link functions include identity, logarithmic, reciprocal, power, and logit (McCullagh and Nelder 1989). The GzLM is flexible to

incorporate different links and is not limited to the canonical links. The links I used in the paper were based on the structures of production models and population models, because I did not consider changing the production and population model forms. The observation-error estimator was used when fitting the surplus production and SPA models (See **Fish production model** section). The choice of the link functions did not affect the assumption about the distribution of Y in GzLM. The GzLM was used to estimate the parameters given the link function $\eta = g(\mu)$ according to the maximum log likelihood method (i.e., equation 3). The parameters were then used to calculate the expected value of the response variable (i.e., population abundance index), and then the residuals. Homogeneity of residuals was evaluated and used as a criterion to determine if the model error structure was appropriate. When different model error assumptions were used in a GzLM, the one that resulted in homogeneous residuals was considered as the most appropriate one (McCullagh and Nelder 1989).

4.2.2 Fish production model

A production model described in Hilborn and Walters (1992) was used to describe the dynamics of stock biomass. The model is written as

(4a) $$B_{t+1} = B_t + G_t - C_t,$$

where B_t is stock biomass, G_t is the surplus production of stock biomass, and C_t is catch, all in year t. The surplus production of stock biomass in year t is often calculated as

(4b) $$G_t = rB_t(1 - \frac{B_t}{K}),$$

where r and K are two parameters describing the stock intrinsic growth rate and carrying capacity or virgin biomass, respectively (Hilborn and Walters 1992). Because stock biomass B cannot be observed directly, an observational model is needed to relate stock biomass B to a variable that is directly related to stock biomass and can be observed in the fishery or in scientific surveys (Hilborn and Walters 1992). A commonly used observational model can be written as

(4c) $$I_t = qB_t,$$

where I_t is an biomass index observed in the fishery or surveys, and q is the catchability coefficient (Hilborn and Walters 1992).

Observation-error estimators have been suggested to perform better than other estimators such as process-error estimators, in fitting production models to data (Punt 1988; Hilborn and Walters 1992; Polacheck et al. 1993). These estimators are constructed by assuming that the SPA model equations (i.e. Equations 4a and 4b) are deterministic, and therefore, have no process error, and that errors only occur in the observation model that describes the relationship between stock biomass and the abundance index (i.e. equation 4c). With this assumption, one can rewrite observation model equation (4c) as

(5) $$E(I_t) = E(qB_t)$$

where I_t is an abundance index in year t, q is catchability coefficient, B_t is stock biomass in year t. Model parameters are estimated based on the assumption of the distribution of

I. For a normal distributed error, one assumes I_t follows $N(\hat{I}_t,\sigma^2)$. For a gamma distributed error, one assumes I_t follows $G(\hat{I}_t/k,k)$. k is a scale parameter of gamma distribution. For a Poisson distributed error, one assumes I_t follows $P(\hat{I}_t)$. Here, $\hat{I}_t = q\hat{B}_t$. With the assumption that I follows a certain distribution, such as the normal, the estimates of the model parameters can be obtained by optimizing an objective function based on the distribution of the I. Lognormal error structure was widely used, thus I can rewrite equation (5) as

(6) $$\log(I_t) = \log(qB_t) + \varepsilon'_t$$

where ε'_t is an independent and usually assumed to be normally distributed error term.

In this study, I explored normal, lognormal, gamma, and Poisson distributions for ε_t in equation (5). The residuals resulting from different model error distributions were diagnosed to identify the most appropriate model error structure in equation 5.

The time series of stock biomass is estimated by projecting the biomass at the start of the catch series forward with the historical annual catches, an estimated stock biomass in the beginning of the fishery (B_0), and parameters r and K (Hilborn and Walters 1992).

For the Atlantic cod 2J3KL fishery, the catch data were available from 1962 to 2000. Population abundance index data were available from 1979 to 2000. Because population abundance index data from 1983 to 2000 were weighted and renewed (Shelton et al., 1996; Lilly et al., 2001), only the data in this period was used in this study. The biomass

index data used in the production model were calculated based on the number-at-age per tow and weight-at-age data in the surveys (Lilly et al. 2001), i.e., $I_t = \sum_{age}$ number-at-age in year t $\times$ mean weight-at-age in year t. The biomass of 3 million tonnes in 1962 was used as the carrying capacity K (Haedrich and Hamilton 2000). Parameters q, r, B_{1983} (B_0) were estimated. To further examine the results from different model error distributions, the predicted and observed abundance indices were compared. Under the assumption of logistic population growth, $B_{msy} = rK/4$ and $F_{msy} = r/2$. The estimated fishing mortality F relative to F_{msy} (F/F_{msy}), and stock biomass relative to B_{msy} (B/B_{msy}) were also compared among different assumptions on model error structures.

4.2.3 Fishery population dynamic model

A sequential population analysis was used to model the population dynamics. The underlying population dynamic model for the SPA is:

(7a) $$N_{a+1,y+1} = N_{a,y}e^{(-M)} - C_{a,y}e^{(-M/2)},$$

where $N_{a,y}$ is the number of fish in age a in the beginning of year y, $C_{a,y}$ is the catch in number at age a and year y, assumed taken in the middle of the year, M is the annual instantaneous rate of natural mortality, assumed to be 0.2. As stated in the production model, the stock numbers at age $N_{a,y}$ cannot be observed directly, the research vessel survey indices expressed as mean numbers per tow at age, $I_{a,y}$, from the fall groundfish bottom trawl survey were used to "calibrate" the model ,

(7b) $$I_{a,y} = q_a N_{a,y} + \varepsilon_{a,y}$$

where q_a is the catchability coefficient at age a. Model parameters are estimated based on the assumption of the distribution of I (see Fish Production Model section). As stated in the production model, when the log transformed population abundance was assumed to follow a normal distribution, equation 7b would be rewritten as:

(7c) $$\log(I_{a,y}) = \log(q_a N_{a,y}) + \varepsilon'_{a,y}$$

where $\varepsilon'_{a,y}$ is also an independently and normally distributed error term.

Like the production model, I explored normal, lognormal, gamma, and Poisson distributions for ε_t in equation (7b). The residuals resulting from different model error distributions were diagnosed to identify the most appropriate model error structure in equation 7b.

Parameters q_a and $N_{a,2000}$ were estimated. The focus of this study is to explore the impacts of error structure on the GzLM estimation of fisheries parameters. Other issues such as management implications and quality of survey and fisheries data are beyond the scope of the study.

4.2.4 GzLM for the production model

A framework was developed, which applied the GzLM into the production model to estimate the parameters in the production model (Figure 4.1). For the assumption of error distributions that are normal, gamma and Poisson, the error term ε_t in equation 5 follows

a normal, gamma, and Poisson distributions, respectively. In the GzLM analysis for the production model, abundance index I is the dependent variable, and stock biomass B is the independent variable. The identity link was used, and the error choice was normal, gamma, and Poisson, respectively. The constant term was set to be zero. The GzLM estimated parameters based on a normal error distribution assumption are the same as those estimated using a linear least squares method for any given B.

A log transformation in conjunction with a normal-error assumption is commonly used in fitting equation 5. This is equivalent to assuming that the untransformed recruitment has a lognormal distribution (equation 6). When using the GzLM, $\log(I)$ is the dependent variable, and $\log(B)$ in the production model is an offset term. A matrix which has the same length as B in the production model and all the values in the matrix equal to one is used as the independent variable in the GzLM. The identity link is used, and the error is normal.

4.2.5 GzLM for the SPA population model

A similar framework as in the production model was developed. The input in this framework is the current population number-at-age. I do not show it here because of the similarity with the Figure 4.1. For the assumption on error distributions that are normal, gamma and Poisson, the error term $\varepsilon_{a,y}$ in equation 7b follows a normal, gamma, and Poisson distribution, respectively. In the GzLM analysis for the SPA model, $I_{a,y}$ is the dependent variable, and $N_{a,y}$ is the independent variable. The identity link was used, and the error choice was normal, gamma, and Poisson, respectively. The constant term was

set to be zero. The GzLM-estimated parameters based on a normal error distribution assumption are the same as those estimated using a linear least squares method.

A log transformation in conjunction with a normal-error assumption is commonly used in fitting equation 7b. This is equivalent to assuming that the untransformed abundance index has a lognormal distribution (equation 7c). When using the GzLM, $\log(I_{a,y})$ is the dependent variable, and $\log(N_{a,y})$ in the SPA model is an offset term. A matrix which has the same length as N_y in the SPA model and all the values in the matrix equal to one is used as the independent variable in the GzLM. The identity link is used, and the error is normal.

4.2.6 Homogeneous residuals and its quantification

Pearson residuals are widely used to diagnose if the model errors are homogeneous. They are calculated as differences between observed and predicted values, standardized (divide by the estimated standard deviation of the fitted value) to make their variance (theoretically) constant (McCullagh and Nelder 1989). When using the Pearson residuals to diagnose the residuals of the production model, because the sample is small (i.e., 18 years) the residuals can be diagnosed visually through the residuals plotted against the fitted population size. When the Pearson residuals are used to diagnose the residuals of the age-structured SPA model, the sample size is much larger (18 years*20 ages = 360). Because the samples are not distributed randomly between the fitted values of the population size, it is difficult to diagnose the residuals through visual inspection for such a large size of samples.

A random sampling method was used to diagnose the Pearson residuals of the SPA model. This method consists of the following procedure: 1) 40 pairs of residuals and fitted abundance indices are selected randomly from the total pairs of residuals and fits; 2) the residuals and fitted abundance indices are diagnosed through visual checking. 3) repeat step 1 and step 2 for 100 times; and 4) count the number of times that yielded homogeneous residuals in the 100 times of random sampling. The model error structure that gave higher percentage of homogeneous residuals in this 100 times of sampling was regarded as the better model error structure.

4.2.7 Normal theory residual and its quantification

A disadvantage of the Pearson residual is that the distribution of Pearson residuals for non-normal distribution is often markedly skewed, and so it may fail to have properties similar to those for normal distributions. Anscombe residuals improved the normal distributed characteristics to a degree (Pierce and Schafer 1986). They normalize the probability functions through variance function cube-root transformations and then stabilize the variance , i.e., $A(.) = \int \frac{du}{V^{1/3}(u)}$; $r_A = \frac{A(Y) - A(u)}{\sqrt{V(u)}}$ (McCullagh and Nelder 1989). Here, A(.) is the transformation function. V is the variance function of u. In this study, Anscombe residuals were also used to diagnose the normality of the residuals.

4.3 Results

4.3.1 GzLM for the production model

When the lognormal and gamma distributions were used, the residuals were homogeneous in the plot of Pearson residuals against the fitted abundance indices (Fig. 4.2). When the normal and Poisson distributions were used, the residuals were heterogeneous in the diagnostic of the Pearson residuals (Fig. 4.2). The normal probability plot of the Anscombe residuals showed that the assumption of normal and Poisson error distributions were not acceptable (Fig. 4.3). When lognormal and gamma distributions were assumed for the model errors in equation 5, the normal probability plot of the Anscombe residuals showed that these assumptions were acceptable though not very good (Fig. 4.3).

The parameter estimates of r, q, and initial biomass B_{1983} were different for different choices of model error distributions (Table 4.1). The r and q estimates were higher for the normal and Poisson distributions compared with the estimates for the lognormal and gamma distributions. The initial biomass B_{1983} and the current biomass B_{2000} were higher when the lognormal and gamma distributions were used, compared with the estimates for the normal and Poisson distributions. The R^2 values were also different for different choices of error assumptions. Although the normal and Poisson distributions were not acceptable for the Atlantic cod production model, they yielded relatively higher R^2 values.

The abundance index in 1986 had been questioned for its quality and has been treated as an outlier in some stock analyses (Shelton and Lilly 2000). In this analysis, when the normal and Poisson distributions were used, the I_{1986} value might be an outlier,

but when the lognormal and gamma distributions were used, it was not an outlier (Fig. 4.2).

The estimated F/F_{msy} and B/B_{msy} were different when different model error distributions were assumed (Fig. 4.4). The estimates of F/F_{msy} and B/B_{msy} were similar for the lognormal and gamma error distributions, and the normal and Poisson model error distributions yielded similar estimates of F/F_{msy} and B/B_{msy}.

The fitted population abundance indices were smaller using the normal and Poisson distributions than those using the lognormal and gamma distributions before the collapse of the cod fisheries (Fig. 4.5).

4.3.2 GzLM for the SPA population model

The residuals homogeneneity diagnostic of plotting the Pearson residuals against the fitted value showed that none of the four distributions was obviously homogeneous (Fig. 4.6). They all showed systematic patterns in the residuals. I concluded that the lognormal distribution was not acceptable based on the Pearson residuals. The points of the residuals in the figures were not evenly distributed, which made it difficult to diagnose the residuals (Figs. 4.6a, 4.6c, and 4.6d). When the random sampling method described earlier was used, only 23% of the random samples resulted in homogeneous residuals for the normal error distribution assumption. When the lognormal distribution was used, there was not even one set of the random sample that could result in homogeneous residuals. When the gamma and Poisson distributions were used, there were 73% and 80% of the random samples that could result in homogeneous residuals. The normal

probability plot of the Anscombe residuals showed that the assumption of normal error distributions were not acceptable (Fig. 4.7a). The normal probability plots of the Anscombe residuals suggested that the lognormal and gamma distribution assumptions were acceptable (Fig. 4.7b, 4.7c). The Poisson distribution was not as good as the lognormal and gamma distribution, but it seemed still acceptable because most points in the normal probability plot were on a straight line (Fig. 4.7d).

The estimates of q and the current abundance N_{2000} were different for different model error distributions (Table 4.3 and Figs. 4.8 and 4.9). The N_{2000} value estimated using the normal error distribution was more than twice of that estimated using the lognormal, gamma and Poisson distributions. The retrospective estimates of N_{1983} did not differ greatly (Table 4.3). The q estimates differed greatly for different model error structure assumptions in GzLM (Fig. 4.9). The q values estimated using the Poisson and gamma distributions were higher than those estimated using the normal and lognormal distributions. The R^2 values were also different for different error distributions. Although the normal distribution was not acceptable, it yielded relatively higher R^2 values.

The estimated q_a for cod of age older than 12 increased greatly when the gamma error distribution was used in the GzLM. For cod older than 18, the results were similar for the normal, lognormal and Poisson distributions. This might result from the large number of zero values in the population abundance index for older age classes in recent

years. The surveyed abundance index can not really show the abundance or biomass of fish in old age classes.

4.4 Discussion

The goal of this study was to illustrate the potential problems associated with the use of a lognormal distribution as the default model error structure in the production model and SPA model. This study suggests that for Atlantic cod 2J3KL, the lognormal assumption is not appropriate for the SPA model, although it is appropriate for the production model.

Different model error assumptions are likely to yield different parameter estimates and model fits. This is clearly shown in this study by different parameter estimates for different model error structures for the production model and SPA model. It is thus important to diagnose if the error structure assumed in the modeling is appropriate for a given fishery and/or a given fisheries model.

The random sampling method proposed in this study for assessing the residual homogeneity in the age structure SPA model helps identify the homogeneous distributions of residuals. This method can be more effective when the fishery has more age classes and long time series. I would suggest using this method for the stock assessment models when the number of data is large.

Further studies should be focused on analyzing the accuracy and precision of parameter estimation resulting from different choices of model error assumptions (Cadigan and Myers 2001). An extensive simulation study on the use of the Poisson

distribution in the SPA model may be needed. The Poisson distribution has shown robustness to violations in model assumptions (Jiao et al. 2003).

I suggest that the GzLM method be used to fit the production model and SPA model. The GzLM provides a convenient and effective way to evaluate and identify a suitable model error distribution for stock assessment models.

Table 4.1: Parameter estimation of production model for Atlantic cod 2J3KL when different model error structures were used in the generalized linear model (see equation 5 and 6).

Model error structure	Parameter estimates				R^2
	q (10^{-4})	r	B_{1983} (10^5 T)	B_{2000} (10^3 T)	
normal	5.2948	1.0799	2.3675	4.5606	0.8332
lognormal	3.7568	0.7257	3.6719	6.3895	0.8302
gamma	3.9542	0.7276	3.6612	6.3728	0.8302
Poisson	6.1149	1.2433	2.0244	4.2525	0.8328

Table 4.2: Summary of the Pearson residuals diagnostic of Atlantic cod 2J3KL SPA model using the random sampling method. 100 sets of random sampling were done. For each random sampling, a sample size of 40 was used. Numbers in the parentheses are the percentage of random samples that had homogeneous residuals.

Model error structure	Frequency of random samples that had homogeneous residuals
normal	23%
lognormal	0%
gamma	73%
Poisson	80%

Table 4.3: Parameter estimation for the Atlantic cod 2J3KL SPA model when different model error structures were used in the generalized linear model.

Model error structure	N2000 (10^7)	N1983 (10^9)	R^2
normal	1.8298	1.7018	0.8717
lognormal	0.7760	1.5414	0.6011
gamma	0.8566	1.5414	0.6026
Poisson	0.7303	1.5414	0.7055

Figure 4.1. A framework to estimate parameters in fish production model by applying generalized linear model into fish production model.

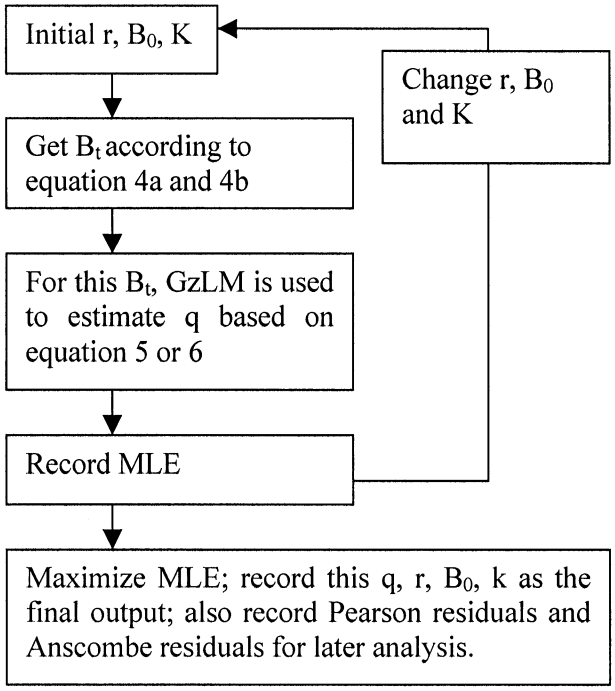

Figure 4.2. Pearson residuals diagnostic plot for different model error structures in the Atlantic cod 2J3KL production model: a) normal distribution; b) lognormal; c) gamma; and d) Poisson. The circled point in the plot is for year 1986.

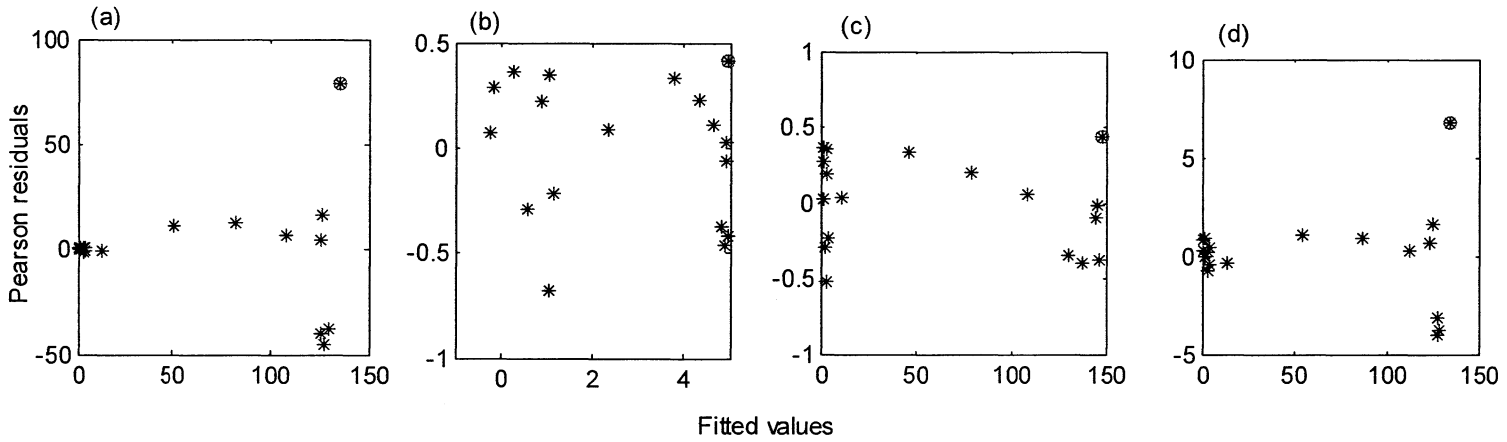

Figure 4.3. Anscombe residuals normality diagnostic for different model error structures in the Atlantic cod 2J3KL production model: a) normal distribution; b) lognormal; c) gamma; and d) Poisson.

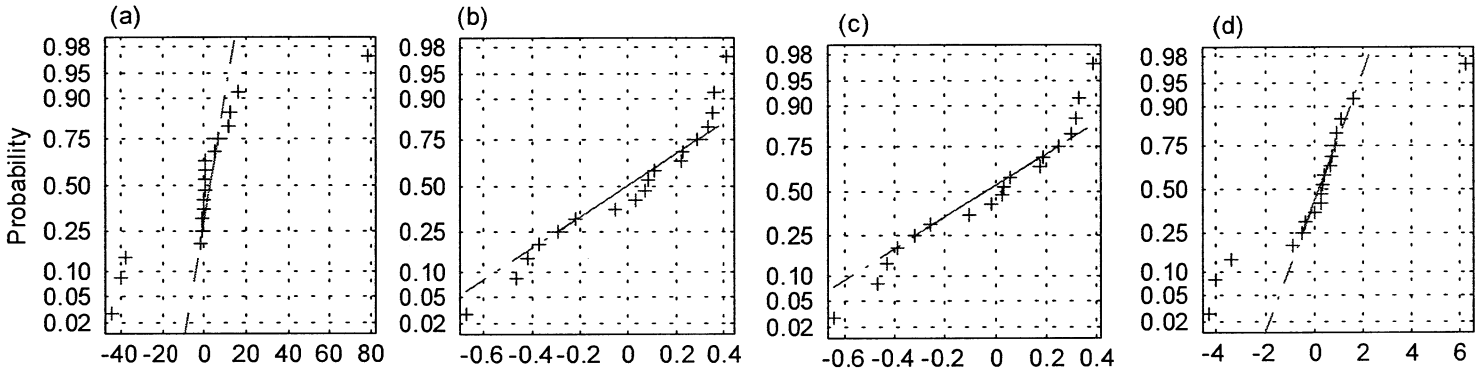

Figure 4.4. F/F_{msy} and B/B_{msy} estimates for different model error distributions in the Atlantic cod 2J3KL production model. N = normal, L = lognormal, G = gamma, and P = Poisson.

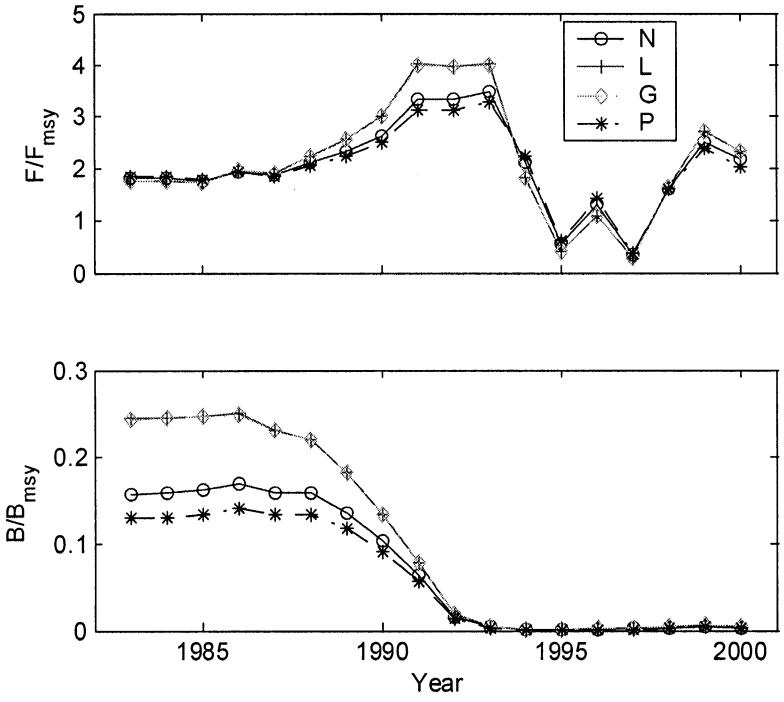

Figure 4.5. Production model fitting under different assumptions of model error structures. Normal = solid line, lognormal = dash-dot line, gamma = dashed line, and Poisson = dotted line.

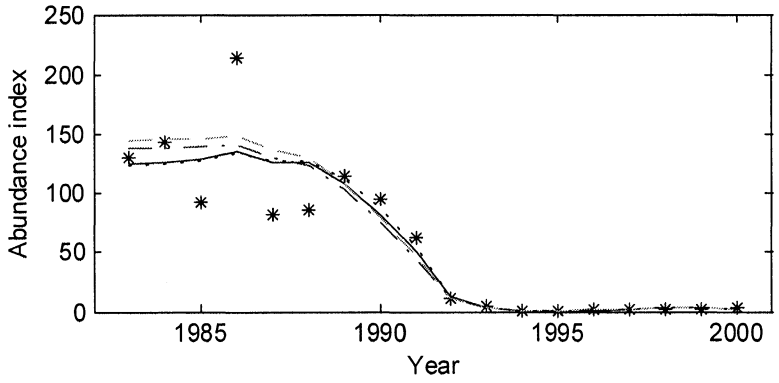

Figure 4.6. Pearson residuals diagnostic plot for different model error structures in the Atlantic cod 2J3KL SPA model: a) normal distribution; b) lognormal; c) gamma; and d) Poisson.

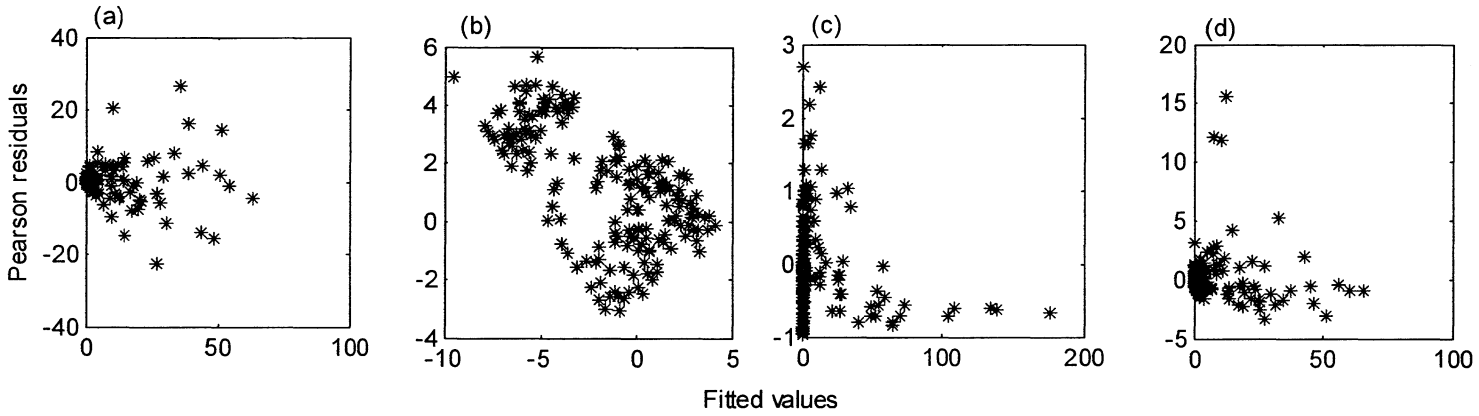

Figure 4.7. Anscombe residuals normality diagnostic for different model error structures in the Atlantic cod 2J3KL SPA model: a) normal distribution; b) lognormal; c) gamma; and d) Poisson.

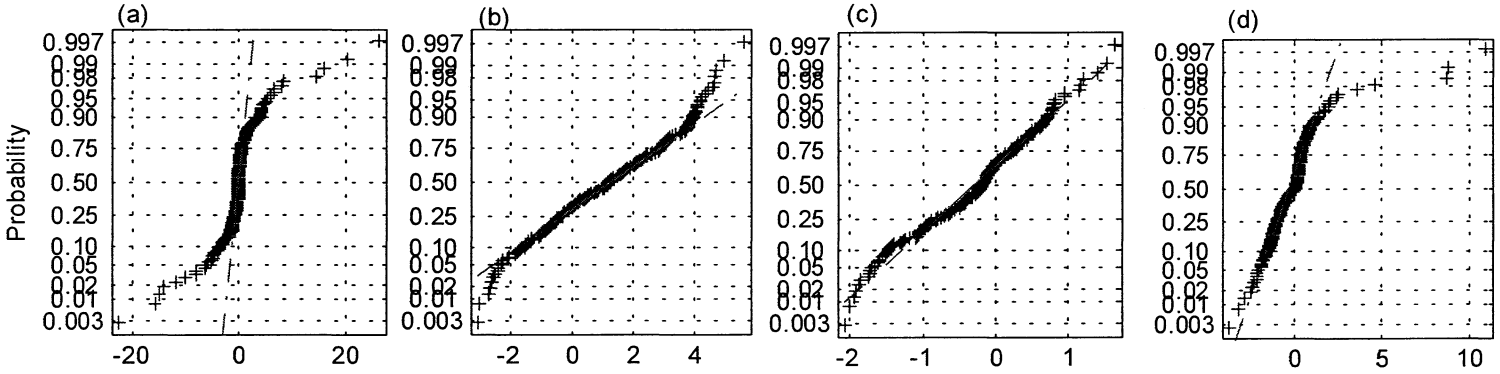

Figure 4.8. Comparisons of the estimated population abundances among different model error structures. Normal = dotted line, lognormal = solid line, gamma = dash-dot line, and Poisson = dashed line.

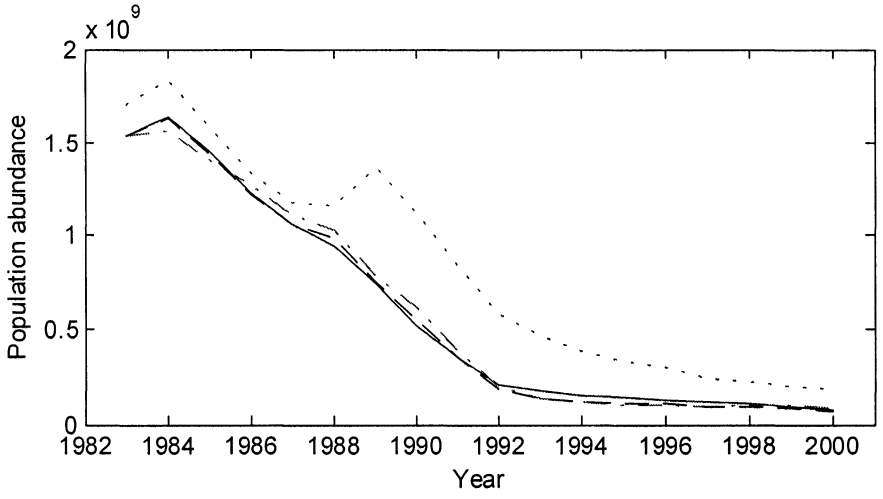

Figure 4.9. Comparisons of the estimated survey catchability for different model error structures. Normal = dotted line, lognormal = solid line, gamma = dash-dot line, and Poisson = dashed line.

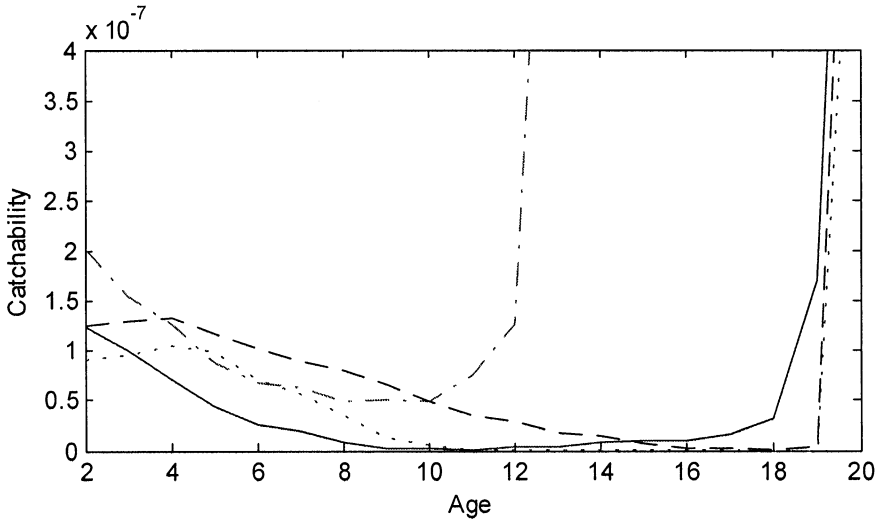

CHAPTER 5

A SIMULATION STUDY OF THE IMPACTS OF POPULATION MIXING ON THE ESTIMATION OF GROWTH PARAMETERS

Abstract

Large variations are often observed in length-at-age data of many fish populations within and among year classes. These can have great impacts on the estimation of various size-dependent life-history processes, thus influencing population dynamics of the fish. Several hypotheses have been developed to explain large variations in length-at-age data, ranging from influx of individuals from different populations with different life-history parameters to natural responses to changes in population density and the ecosystem. Large areas of migration and mixing among populations have been documented, e.g., Atlantic Cod (*Gadus morhua*) in Atlantic Canada. Few studies have been done to quantitatively evaluate the impacts of possible population mixing on stock assessment and management. Using a Monte Carlo simulation approach, I demonstrated how observed variations in length-at-age could be influenced by mixing of individuals from a different population, and how a change in mixing rates might influence the analyses of growth data. The simulation study suggests that population mixing can have great impacts on growth analyses and stock assessment, and a large sample size is needed in subsampling catch in order to identify growth variations resulting from population mixing. I suggest that population mixing be considered as a possible hypothesis for explaining observed

variations in growth and that population mixing be incorporated into stock assessment models to improve the estimation of key fisheries parameters in stock assessment.

5.1 Introduction

Temperature, food availability, and population density are often considered to be main factors influencing growth rates of fishes. These factors are regarded as the dominant factors that result in large variations in growth rates among populations of a fish species. Many studies show that large variations also exist in length-at-age within and among year classes in a population (e.g., *Gadus morhua*; Beacham 1983; Lilly et al. 2001). The large variation in growth among different year classes for Atlantic cod were hypothesized as a result of variations in environmental variables such as water temperature (Hutchings and Myers 1994; Gomes et al. 1995; Shelton et al. 1999), food availability (Krohn et al. 1997), density-dependant effects (Hanson and Chouinard 1992; Swain 1993), and population stress as a result of over-exploitation (Beacham 1983; Trippel 1995). Other factors that may result in large variations in growth for cod include size selective mortality (Myers 1989; Hanson and Chouinard 1992), early life history (Otterson and Loeng 2000), energy allocation (Chen and Mello 1999), sampling design, and population structure (Lilly 1996).

The spatial dynamics of the fishery can have large impacts on fish stock assessment and management. Understanding of spatial distributions and migrations can improve assessments of managed populations (Giske et al. 1998). For example, extensive efforts have been allocated for collecting information on fish spatial dynamics (Rose 1993;

Brattey 2000; Lawson and Rose 2000). These studies have suggested that there are large changes in cod spatial distributions after the decline in cod stock abundance, raising the possibility of overlapped distributions of different populations. Such overlaps are likely to influence data collection and subsequently complicate the estimation of some key life-history parameters (e.g., increased uncertainty in parameter estimation).

Using a simulation approach in this study, I quantitatively evaluated the impacts of potential mixing scenarios on stock assessment. More specifically, I evaluated how observed variations in growth could be influenced by the inclusion of individuals from another stock or population that has different growth patterns.

Length-at-age data were used to describe growth. Changes in length-at-age data in the same stock resulting from changes in temperature and food supply tend to be smaller than changes in weight. One cannot exclude or isolate the influence of the temperature, food availability, size selectivity, density-dependent effect, and other environmental factors; but to simplify the simulation study of mixing on growth variation, one assumed that changes in length-at-age resulting from variations in temperature and other environmental variables were random within the population. I simulated how the mixing of individuals from different populations might affect the length-at-age estimates and subsequently influence the growth parameter estimation. I also evaluated the impacts of different sample sizes in subsampling catch on the estimation of length-at-age values and growth parameters.

5.2 Materials and methods

Mixing was assumed to occur between two populations in the simulation study. Unidirectional mixing was assumed, i.e., mixing always occurred in population A by individuals moving from population B to population A, but not the other way around. This assumption allows us to focus the study on one population. The simulated populations A and B were envisioned to represent the 2J3KL and 3Ps cod (*Gadus morhua*) stocks with similar parameters. The highest set of mean length-at-age values for the 2J3KL cod collected during autumn bottom-trawl surveys in 1978-2000 was used as the default (i.e., "true") mean length-at-age data for population A. The smallest set of mean length-at-age data for the 3Ps cod stock collected during the bottom-trawl surveys in winter-spring 1972-2001 was used as the default mean length-at-age for population B.

5.2.1 Population and mixing pattern simulation

Three pairs of populations were simulated (Table 5.1). They were: 1) the relative population size, defined as $\frac{N_A}{N_B}$, is constant; 2) the relative population size is decreasing; and 3) the relative population size is increasing. In this simulation study, other parameters except recruitment, such as fishing mortality, natural mortality and selectivity in the two populations were regarded as equal. Recruitment size was used to control the population size. If I assumed that the population size was relatively constant, I implied that the recruitment was relatively constant. If I assumed that population size was relatively decreasing, I implied that the recruitment was relatively decreasing, and vice versa.

For every pair of populations, four mixing patterns were considered (Table 5.1), they include: (1) constant mixing rate m_1 over time (i.e., 20%) with a lognormally distributed random variant ε_{mm},

(1) $$m_1(t) = 20\% e^{\varepsilon_{mm}}, \qquad t = 1, 2, \ldots, 50$$

where $\varepsilon_{mm} \in N(0, \sigma_{mm}^2)$, $\sigma_{mm} = 0.01$ was used in the simulation study. t is the year starting from year 0, and $m_1(t = 0) = 0$, thus there is no migration before year 1; (2) linearly decreasing rate with a lognormally distributed random variant defined by the following equation,

(2) $$m_2(t) = (20\% - 0.3\% \times t) e^{\varepsilon_{mm}}, \qquad t = 1, 2, \ldots, 50$$

where $m_2(t = 0) = 0$; (3) linearly increasing rate with a lognormally distributed random variant defined by the following equation,

(3) $$m_3(t) = (20\% + 0.3\% \times t) e^{\varepsilon_{mm}}, \qquad t = 1, 2, \ldots, 50$$

where $m_3(t = 0) = 0$; (4) mixing rate being a function of yearly averaged temperature with a normally distributed random variant defined by the following equation,

(4) $$m_4(t) = (a + b \times T) e^{\varepsilon_{mm}}$$

where m_4 was the immigration rate from population B to population A, T was the yearly averaged temperature in the year of t. The yearly averaged temperature near St. John's

harbor was used in the simulation study. $m_4(t=0)=0$. Climate-related indices such were found to be correlated with the Atlantic cod growth variations in some previous studies (Shelton et al. 1999; Drinkwater 2002), and temperature-driven migrations were also reported (Rose et al. 2000), making the fourth mixing pattern a plausible scenario. The values of a and b in equation (4) were set, rather arbitrarily, at 20% and 3.5%.

The mixing from population B to population A was assumed to begin from year one (Figure 5.1). According to this assumption for a population with 20 age groups, 20 years were needed to allow the mixing procedure to be completed in a simulation. I used length-at-age 5 to explore the mixing effect on changes in length-at-age. The growth parameters were estimated by using the Bertalanffy growth model:

(5) $$L_a = L_\infty(1-e^{-k(a-t0)}),$$

where L_∞ is the maximum attainable length, k is the Brody growth parameter, and t_0 is an hypothetical age at which the length is 0 (Ricker 1975).

5.2.2 Estimating growth parameters for population A for different simulation scenarios

The length-at-age data were generated according to the simulated catch-at-age data, sample size in subsampling catch, and growth characteristics of the populations using the procedure defined below (Figure 5.2).

The number of fish at the beginning of age a, N_a, is calculated from recruitment R as

(6) $$N_a = \mathrm{Re}^{-\sum_{j=1}^{a-1}(s_j F+M)},$$

where R is the number of fish at age 1 (defined as recruitment), s_j is the selectivity coefficient for fish at age j and defined as

(7) $$s_j = \frac{1}{1+e^{-m(j-t50)}}.$$

The recruitment was assumed to follow a normal distribution, $N(\overline{R},\sigma_R{}^2)$. The population composition in the first year was generated according to equation 6. I used the Atlantic cod selectivity curve for both the populations, where $m = 1.5$; $t50 = 3.4$ (Fu et al. 2001). A lognormally distributed error was assumed for S, thus the log transformed S follows the normal distribution with an error term of ε_s, where $\varepsilon_s \in N(0,\sigma_s{}^2)$. I used the value of 0.01 for σ_s in the simulation study. The S values used in the simulation were randomly sampled from the truncated (upper limit to 1) lognormal distribution. Fishing mortality F was assumed to be 0.3. The variation of F was assumed to follow a lognormal distribution, $F = 0.3e^{\varepsilon_F}$, where $\varepsilon_F \in N(0,\sigma_F{}^2)$. The mean natural mortality M was assumed to be 0.2. The variation of M was also assumed to follow a lognormal distribution $M = 0.2e^{\varepsilon_M}$, where $\varepsilon_M \in N(0,\sigma_M{}^2)$. I used 0.05 for both σ_F and σ_M.

The catch-at-age data $C_{a,y}$ were calculated using the standard catch equation and exponential survival equation (Ricker 1975),

(8) $$C_{a,y} = N_{a,y} \frac{s_a F}{s_a F + M}(1 - e^{-s_a F - M}).$$

The total catch numbers in year y was calculated as $TC_y = \sum_a C_{a,y}$. The proportion of catch-at-age was calculated as

(9) $$P_{a,y} = C_{a,y} / C_y.$$

Hereafter, the $P_{a,y}$ were referred to as the proportion of catch at age without subsampling errors.

The subsampling of the total catch was conducted with probabilities $P_{a,y}$. The P follows the multinomial distribution; and the sampling method was described in Chen (1996). It includes the following procedure: (1) generating a random number R_n from the uniform distribution $U(0,1)$; (2) using the $P_{a,y}$ value as the "true" value, $P_{1,y}, P_{2,y}, ..., P_{a,y}, ...$, where $\sum_a P_{a,y} = 1$; (3) if $\sum_{a=1}^{k-1} P_{a,y} < R_n < \sum_{a=1}^{k} P_{a,y}$, assigning one "observation" to group k; (4) repeating (1) to (3) n times (i.e. n is the size of subsamples) and denoting "observation" in each group as $n_{1,y}, \ldots, n_{k,y}, \ldots$; and (5) calculating $P_{1,y}' = n_{1,y} / n_y, \ldots, P_{k,y}' = n_{k,y} / n_y, \ldots$, and these $P_{1,y}', \ldots, P_{k,y}', \ldots$ values were the "observed" proportional data. The variation associated with "observed" proportional data was controlled by sample size n (Chen 1996) as

(10) $$SD = \sqrt{\frac{P(1-P)}{n}},$$

where SD is standard deviation, and P is the original proportional value. The subsampling of length-at-age data was conducted based on the "true" P to derive $P_{a,y}^{S'}$, the "observed" age composition data. Superscript S represents population A or B. The following procedure was used: (1) determining the number in each age group and each population, $P_{a,y}^{S} n_y^S = n_{a,y}^S$; (2) generating $n_{a,y}^S$ length-at-age data; If n is the sample size, then simulated numbers of length-at-age is

(11) $$n_{a,y} = n \times P_{a,y},$$

then I generate $n_{a,y}$ length-at-age data, the log transformed length-at-age data was assumed to follow a normal distribution, which is equivalent to the length-at-age data having a lognormally distributed error defined as

(12) $$L_a^{'} = L_a e^{\varepsilon_L},$$

where L_a is the "true" mean length-at-age data, $L_a^{'}$ is the simulated length-at-age data, ε_L is a normally distributed term with $\varepsilon_L \in N(0,\sigma_L^2)$ (I use $\sigma_L = 0.1$ in the $L_a^{'}$ simulation), and the boundary of $L_a^{'}$ was defined as $L_a(1 \pm 20\%)$ to limit the atypical and biologically unrealistic sampling in the simulation; and (3) add the length-at-age data

simulated from the two populations, and then re-estimate the growth parameters in the von Bertalanffy growth model.

The determination of the number in each group and each population is related to the mixing patterns (Table 5.1 and Figure 5.2). To simplify the simulation, I assumed that the fishes immigrating from population B into population A would not move back if they were still alive and the movement from population B to population A occurred before the fishing season in each year. The population numbers-at-age and catch-at-age in populations A and B in Division A (see Figure 5.1) can be calculated based on the population pattern, mixing rate scenarios and the catch equation. The following equations were then used to determine the number of fish in the subsampling from populations A and B in a given year,

(13) $$n_y^A + n_y^B = n$$

(14) $$n_y^A / n_y^B = \frac{TC_y^A}{TC_y^B}$$

where n is the total sample size for estimating growth parameter of population A , n_y^A and n_y^B are the sample numbers in the total samples in the Division A (see Figure 5.1), but are fish from population A and population B, respectively in year y, and TC_y^A and TC_y^B are the total possible catch of fish of populations A and B in the Division A in this year (Figure 5.1). The above equations were formulated according to the mixing

assumption. For simplification, my analysis was focused on the population A only. The above procedure was repeated 1000 times.

Boxplot was used to show the estimates of the mean length-at-age 5 in the simulation. It produced a box and whisker plot for the mean length-at-age 5 estimates out of the 1000 simulation runs in each year. The box has lines at the lower 25 quartile, median, and 75 upper quartile values. The distance between the top and bottom of the box is the interquartile range. The whiskers are lines extending from each end of the box to show the extent of the rest of the data. The plus sign at the top of the plot is an indication of an outlier in the data. An outlier is a value that is more than 1.5 times the interquartile range away from the top or bottom of the box in this plot. If there are no data outside the whisker, a dot is placed at the bottom whisker.

5.2.3 Effects of sample size in subsampling catch on estimation of growth parameters

Growth parameters derived from catch-at-age data without subsampling errors were compared with growth parameters derived from catch-at-age data with different levels of subsampling errors. I used the first year's data. The CV (coefficient of variation) of an estimated parameter over N (N=1000 here) runs of simulation can be calculated as

(15) $$CV = \sigma / \hat{\mu}$$

where $\hat{\mu}$ is the mean of the estimated parameter over the 1000 runs, σ is the standard error of the estimated parameter.

Relative estimate error (REE) is estimated as

$$REE(\%) = \frac{(\sum_{N} |\beta_i^* - \beta|)/N}{\beta} 100 \tag{16}$$

Where β^* is the estimated parameter value in a simulation run; and β is the "true" parameter value. The "true" parameters including the "true" mean length-at-age, "true" growth parameter L_∞, k and t_0.

Departure of the estimated parameter from the true value was also measured by the root mean square error (RMSE), which combines both estimation bias and lack of precision. The RMSE for the estimate of a "true" parameter β can be expressed as

$$RMSE = \sqrt{\frac{\sum_{i=1}^{N} (\beta_i^* - \beta)^2}{N}}. \tag{17}$$

The RMSE for the proportion of catch-at-age was also estimated. In this case, β is the estimated proportion-at-age, that is, $P'_{a,y}$. The RMSE can be expressed as

$$RMSE = \sqrt{\frac{\sum_{i=1}^{N} \left(\sum_{a} (P'_{a,y,i} - P_{a,y})^2 \right)}{N}} \tag{18}$$

Growth parameters derived from catch-at-age data with and without subsampling errors were compared based on their ability to replicate the true population parameters. RMSEs were calculated for each estimated growth parameter using catch-at-age data with and without subsampling errors. A comparison index (CI) was calculated as

$$(19) \qquad CI = \frac{\text{RMSE calculated using catch-at-age data with random sampling error}}{\text{RMSE calculated using catch-at-age data without random sampling error}}$$

Thus, a CI value greater than 1 indicates a parameter estimated using catch-at-age data subject to random subsampling errors has larger errors than that estimated using catch-at-age data without subsampling errors.

5.3 Results

The growth curves for populations A and B show that fish in population B are smaller in length (Figure 5.3). The estimated growth parameters indicate that for population A, the L_∞ is 171.8, k is 0.067, and t_0 is -0.93, and that for population B, the L_∞ is 98.3, k is 0.116, t_0 is 0.17. Because I assumed that the population had 20 age groups in the simulation study, the age-composition of population A tended to be relatively stable from the mixing of individuals from population B after 20 years with the assumed fishing patterns. When the relative population size was constant, (i.e., NA/NB= 5), the L_∞, k and t_0 estimates of population A randomly varied without an obvious trend when the mixing fraction from populations B to A was constant (20%) (Figure 5.4). When the mixing was linearly decreasing, the L_∞ of population A increased slowly over time, k decreased slowly, and t_0 also decreased slowly though not obviously. When the mixing was linearly

increasing, the L_∞ of population A continued decreasing, k and t_0 increased. When the mixing was a function of yearly average temperature, the L_∞, k and t_0 values had no obvious temporal trends, but there were small variations among years. The mean length-at-age 5 became relatively stable. When the mixing fraction was constant over years, the average length-at-age 5 values of 1000 simulations tended to be stable (Figure 5.5a). When the mixing fraction was linearly decreasing with years, the average length-at-age 5 tended to be increasing (Figure 5.5b). When the mixing fraction was linearly increasing, the length-at-age 5 tended to decrease (Figure 5.5c). When the mixing over years was a function of temperature, no obvious trend could be detected in the average length-at-age 5 (Figure 5.5d).

When the size of population A was constant with random variations, while population B was linearly increasing with random variations, the L_∞ value of population A continued to decrease, k and t_0 increased with random variations when the mixing fraction from population B to population A was constant (20%). When the mixing was linearly decreasing, there were no obvious trends for L_∞, k and t_0 values of population A. When the mixing was linearly increasing and when the mixing was a function of yearly averaged temperature, the L_∞ value of population A continued to decrease, k and t_0 were increasing (Figure 5.6). When the mixing fraction was constant, the length-at-age 5 values averaged over the 1000 simulations after the first 5 years of mixing continued to decrease (Figure 5.7a). When the mixing fraction was linearly decreasing, the average length-at-age 5 tended to be stable (Figure 5.7b). When the mixing fraction was linearly increasing,

the length-at-age 5 decreased (Figure 5.7c). When the mixing over years was a function of temperature, the average length-at-age 5 tended to decrease (Figure 5.7d).

When population A was constant, population B linearly decreased, and mixing rate from populations B to A was constant, the estimated L_∞ of population A increased slowly after the first 20 years of mixing, k decreased slowly, and t_0 varied randomly without an obvious trend. When the mixing rate linearly decreased, the L_∞ value of population A increased over the time, k decreased, and t_0 also slightly decreased in the last ten years. When the mixing rate decreased linearly, the L_∞, k, and t_0 values had no obvious temporal trends. When the mixing rate was a function of yearly average temperature, the L_∞, k, and t_0 values had no obvious trends until the last five years. The L_∞ value increased slightly and the k value decreased slightly in the last five years (Figure 5.8). When the mixing rate was constant, the average length-at-age 5 values over the 1000 simulations increased after the 5^{th} year (Figure 5.9a). For all the three mixing scenarios (i.e., the mixing rate decreased linearly over time, increased linearly and was a function of temperature), the average length-at-age 5 tended to increase over the time (Figures 5.9b, 5.9c, and 5.9d). When the mixing fraction was linearly increasing, the average length-at-age 5 increased slower (Figure 5.9c).

For all the simulation scenarios the averages of L_∞, k, and t_0 over the 1000 simulation runs varied over years. The range represented as the interquantile range and whisker lines in the boxplot of the length-at-age 5 changed because of the mixing process. When the

mixing began, the range of the length-at-age 5 increased, there were more outliers. After the 5th year the range continued increasing when the mixing fraction increased, or when the relative population size was decreasing (Figures 5.5 and 5.7). The range could decrease because of changes in the mixing fraction and the relative population size. (Figures 5.5 and 5.9).

When the subsample size was small (<1000), CV and REE for parameters L_∞, k, and t_0 were large, indicating that the estimation errors for the parameters were larger compared with those estimated based on large subsample sizes. With increased sizes of subsamples, the differences in estimation errors decreased quickly, the CV values approached 0, the REE values became smaller (Figure 5.10). When the sample size approached 2000 the CV and REE values tended to be stable.

When the subsample size increased the CV and REE for length-at-ages 5 and 10 decreased, but the CV and REE values for length-at-age 10 were much higher than those for length-at-age 5 (Figure 5.11). The subsample size used in the simulation was the total sample size for all age groups. The sample size at age was determined by age composition of the catch. The proportion of fish in age 5 was much higher than that for fish in age 10, which led to a higher subsmaple size for fish in age 5 and subsequently smaller errors for the estimated length at age 5.

The CI values for L_∞, k and t_0 were large when sample size was small. However, CI values would approach 1 if sample size increased. This implied that the influence from

random sampling decreased when the sample size increased. The observed proportion of catch-at-age in subsampling was also influenced by the total sample size. The CI value for catch-composition was large at small sample sizes, but approached 1 with increased subsample sizes (Figure 5.12).

5.4 Discussion

The simulation study suggested that the mixing of individuals from another population with different growth rates could influence the growth parameter estimation. When mixing occurred, the changes in the relative population size could also influence the growth parameter estimation and length-at-age estimates. It is thus important to evaluate impacts of possible spatial overlaps between different populations on data collection and stock assessment. Misinterpreting large variations in length-at-age data resulting from spatial overlaps of different populations as a result of variations of other environmental variables may lead to errors in stock assessment.

In this simulation study I assumed fish underwent a unidirectional movement between two populations. The results can, however, be extended to the situations where there are two or more substocks in one stock and there are movements among the substocks.

The growth data were unbiasedly simulated according to the catch-at-age and length-at-age. In practical sampling, however, because the samples were taken yearly or seasonally from different fishing ports and fishing boats, the sampled catch-at-age might

not accurately represent the true catch-at-age data. The model was based on an assumption that the distribution of fish is random within its distribution ranges. This may not be true for many fish species. For example, some fish species exhibit size-dependent distribution patterns (e.g., Chen et al. 1997). The impacts of such non-random and, in particular, size-dependent distribution patterns on subsampling catch for the collection of growth data need to be evaluated. Subsample size was shown to have large impacts on the estimation of growth parameters. This study suggests that large sample sizes are needed for reliable estimation of growth parameters. In practice sizes of subsampling for estimating length-at-age data are often small. For example, for the 2J3KL Atlantic cod the length-at-age values for fish older than 5 were often estimated from small sample sizes. For many age groups, the length-at-age data were estimated from samples smaller than 5. This may lead to inaccurate estimates of growth parameters (Lilly 1998). Sample size needs to increase greatly in order to improve the accuracy of the estimates.

The simulation study suggest that the length-at-age estimation can be influenced by the population mixing, and the effect can be seen in the trend of the mean length-at-age changes, variations of length-at-age, and the number of the outliers. This implies a possibility of using the length-at-age data as an indicator of population mixing, or even using the growth data to predict population mixing. However, this can only be done if I can exclude the possibilities that changes in length at age are the responses of fish to changes in its ecosystems (e.g., changes in inter- and intra-species competitions).

In this study the impact from other factors, such as temperature, food availability, were regarded as random. An analysis on population mixing would be more practical by excluding the influence from other factors. Combining this study with the knowledge from tagging experiments would give more implications on population mixing and growth variations.

Temporal and spatial changes in size at age have been observed for many fish stocks (e.g., Chen and Mello 1999). So far we have largely attributed such changes to changes in the ecosystems and/or fishes' responses to human exploitations. Limited studies have been done to explore possibility of changes in spatial distributions of fish and subsequent overlapping of fish of different stocks. This study suggests that such a mixing can result in temporal changes in size-at-age data for a fish population. I suggest that influence of potential mixing on the estimation of growth parameters be considered in fisheries stock assessment.

Table 5.1: Population scenarios and mixing patterns in the simulation study. t is the year distance from the beginning year in the simulation; T is the temperature in the simulation year.

Populations scenarios	Mixing patterns	Migration fraction from population B to population A
A/B = 5 A —— B ——	Constant mixing	20%
	Linearly decreasing	20%-0.3%*t
	Linearly increasing	20%+0.3%*t
	Function of the temperature	20%+3.5*T
A/B ↓ A —— B ／	Constant mixing	20%
	Linearly decreasing	20%-0.3%*t
	Linearly increasing	20%+0.3%*t
	Function of the temperature	20%+3.5*T
A/B ↑ A —— B ＼	Constant mixing	20%
	Linearly decreasing	20%-0.3%*t
	Linearly increasing	20%+0.3%*t
	Function of the temperature	20%+3.5*T

Figure 5.1. A diagram showing the movement from population B to population A and the population composition in Division A in the simulation study.

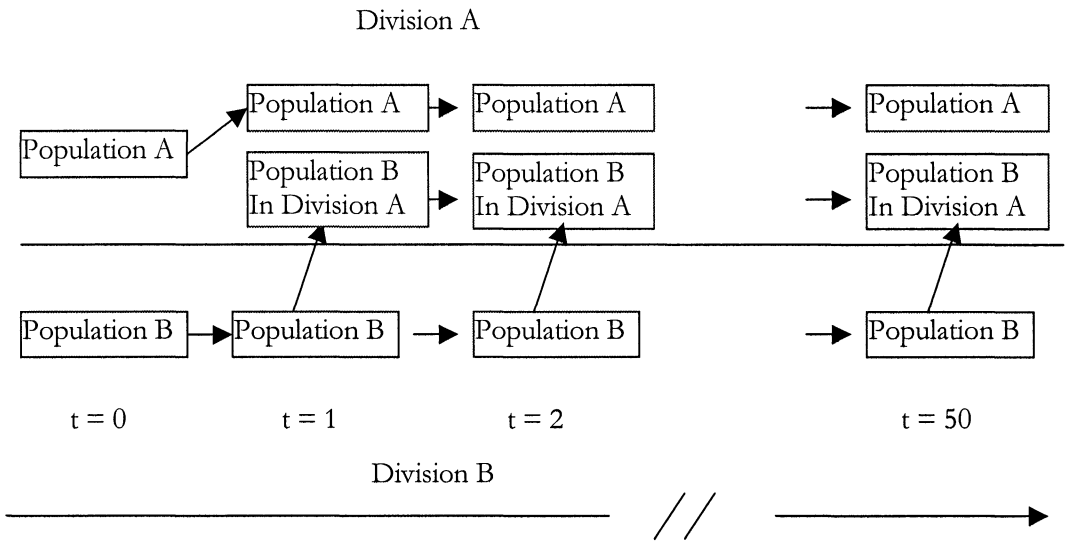

Figure 5.2. The simulation procedure of population mixing between populations A and B.

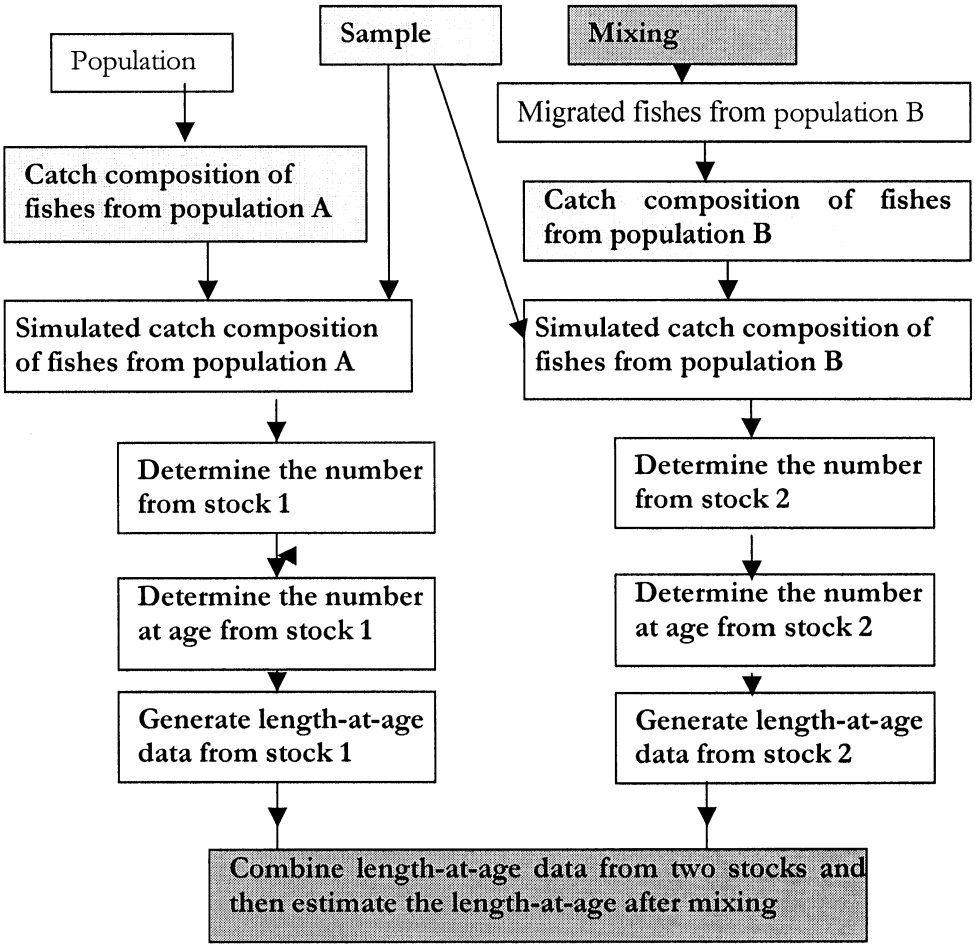

Figure 5.3. The growth curves of population A and B.

Figure 5.4. The simulation result of the growth parameter estimates under the scenario of the constant relative population size (i.e. scenario 1). Solid line for mixing fraction is constant; dash-dot line for mixing fraction is linearly decreasing; dotted line for mixing fraction is linearly increasing; and dotted line with a black dot is for mixing fraction is a function of yearly averaged temperature.

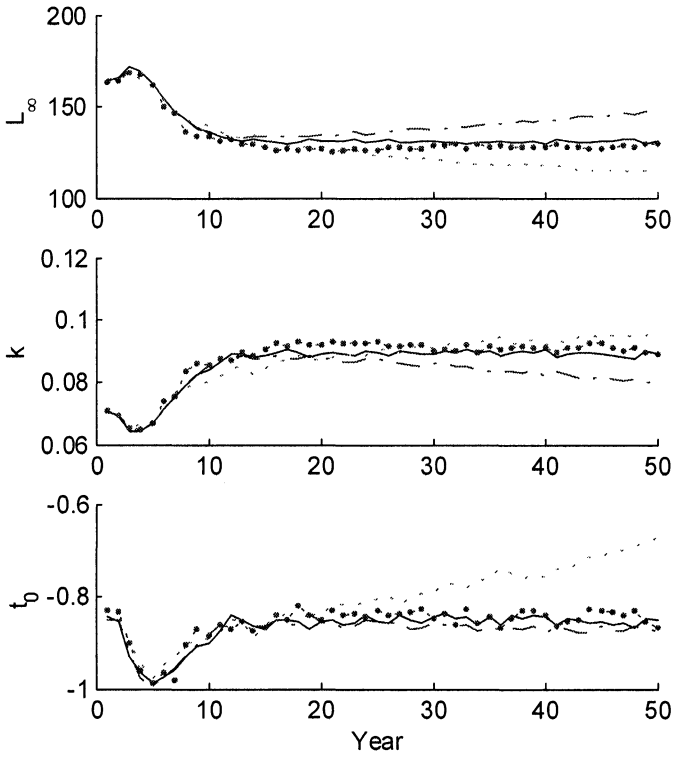

Figure 5.5. The simulation result of the length at age 5 estimates under population scenario 1 (i.e., the constant relative population size). (a) mixing fraction is constant; (b) mixing fraction is linearly decreasing; (c) mixing fraction is linearly increasing; and (d) mixing fraction is a function of yearly averaged temperature.

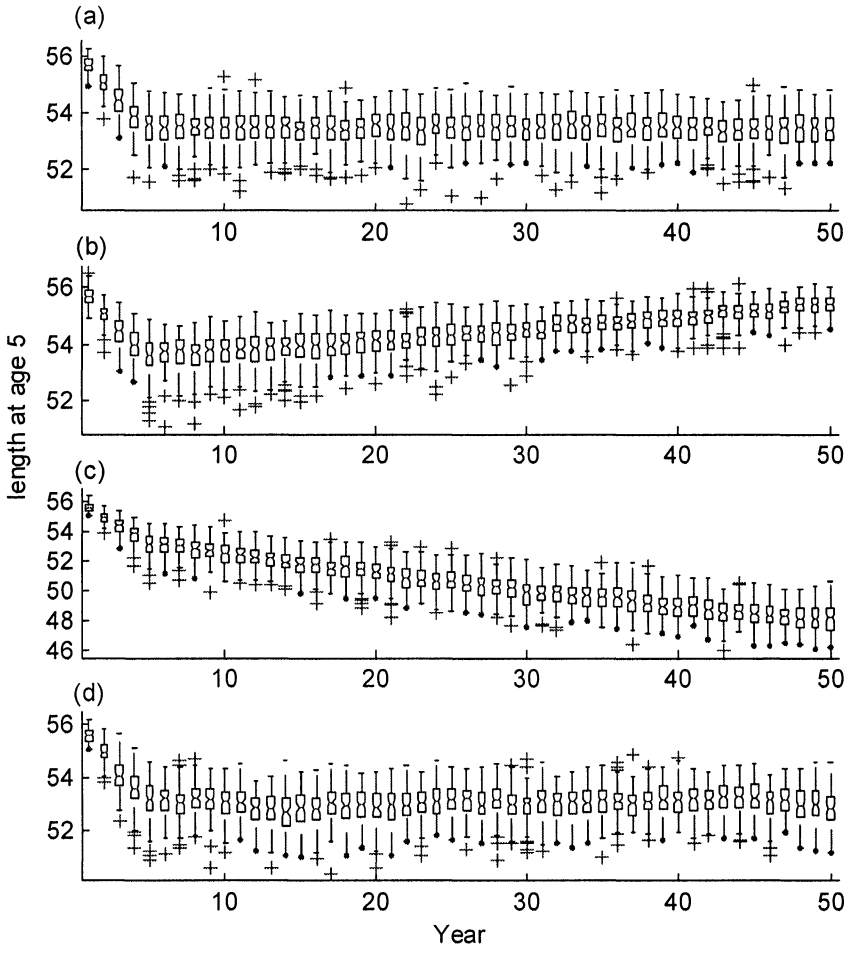

Figure 5.6. The simulation result of the growth parameter estimates under population scenario 2 (i.e., the size of population A is constant with random variations, while population B is linearly increasing with random variations). Solid line for mixing fraction is constant; dash-dot line for mixing fraction is linearly decreasing; dotted line for mixing fraction is linearly increasing; and dotted line with a black dot is for mixing fraction is a function of yearly averaged temperature.

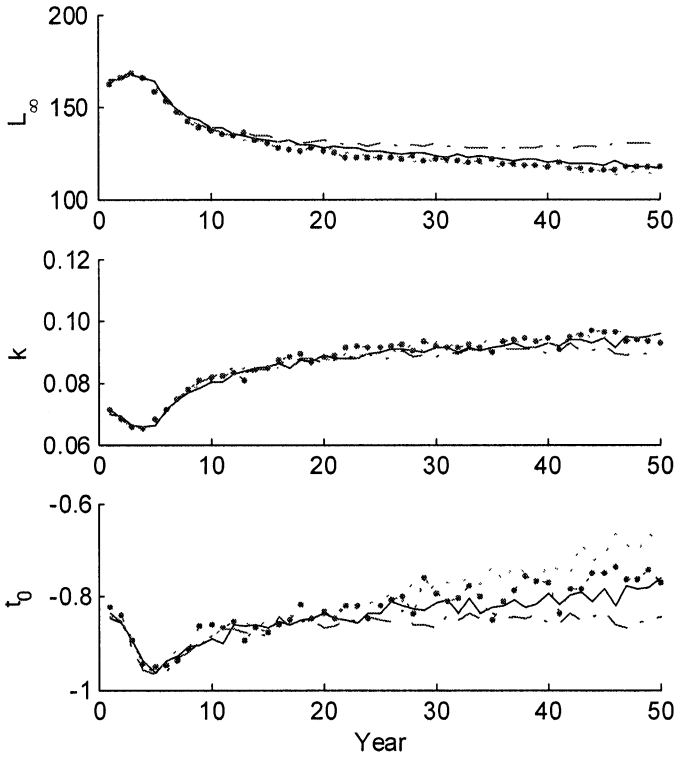

Figure 5.7. The simulation result of the length-at-age 5 estimates under population scenario 2 (i..e., the population size of A is constant with random variations, while population B is linearly increasing with random variations. (a) mixing fraction is constant; (b) mixing fraction is linearly decreasing; (c) mixing fraction is linearly increasing; and (d) mixing fraction is a function of yearly averaged temperature.

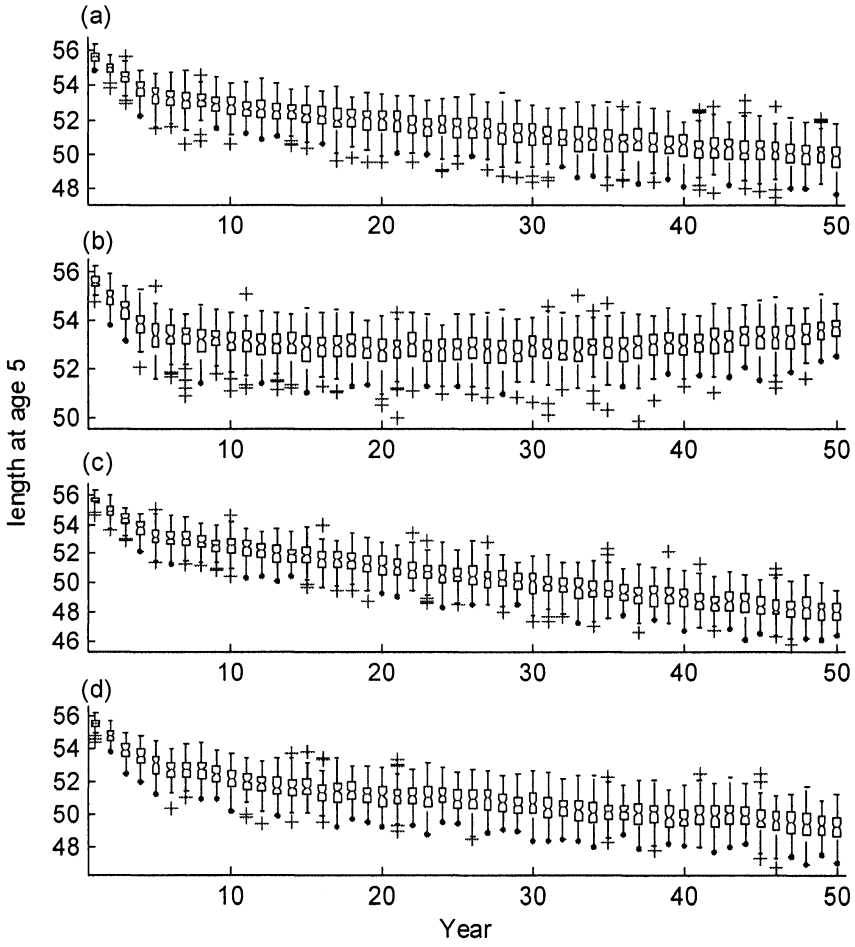

Figure 5.8. The simulation result of the growth parameter estimates under population scenario 3 (i.e., the population size of A is constant with random variations, while population B is linearly decreasing with random variations). Solid line for mixing fraction is constant; dash-dot line for mixing fraction is linearly decreasing; dotted line for mixing fraction is linearly increasing; and dotted line with a black dot is for mixing fraction is a function of yearly averaged temperature.

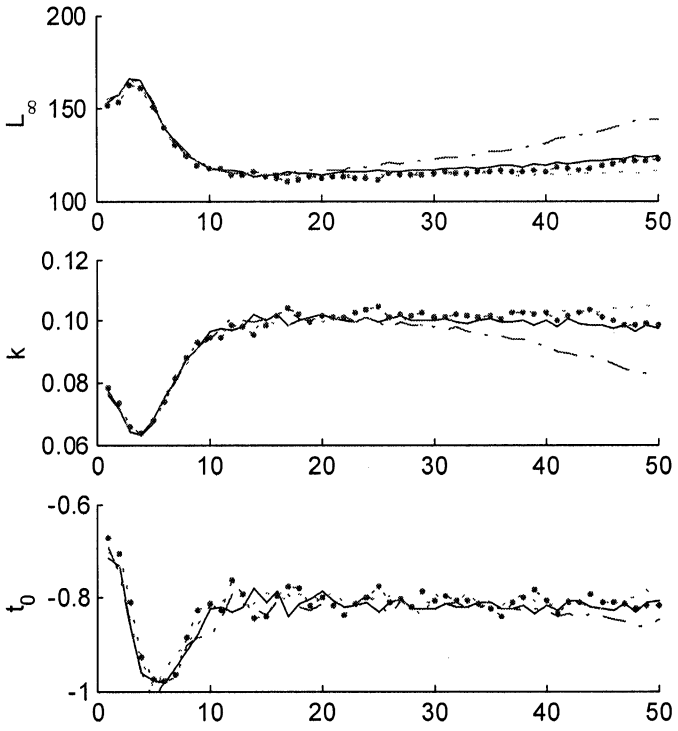

Figure 5.9. The simulation result of the length-at-age 5 estimates under population scenario 3 (i.e., the population size of A is constant with random variations, while population B is linearly decreasing with random variations). (a) mixing fraction is constant; (b) mixing fraction is linearly decreasing; (c) mixing fraction is linearly increasing; and (d) mixing fraction is a function of yearly averaged temperature.

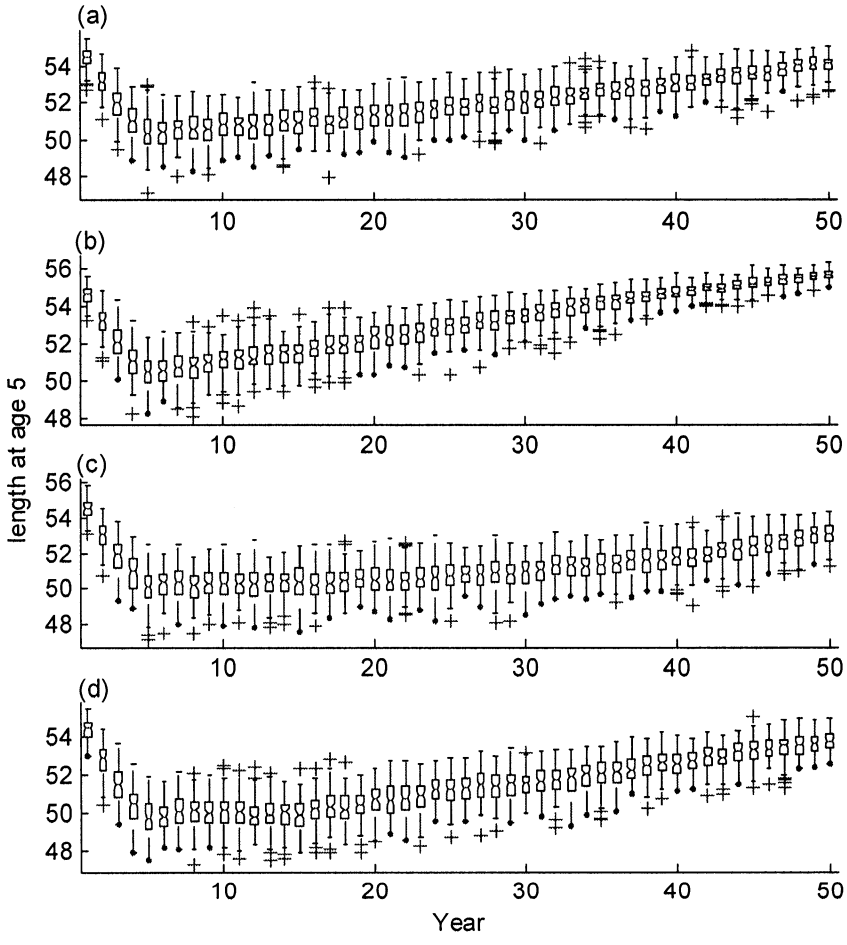

Figure 5.10. Plot of Coefficient of Variation (CV) and Relative Estimate Error (REE) of L_∞, k and t_0 versus sample size.

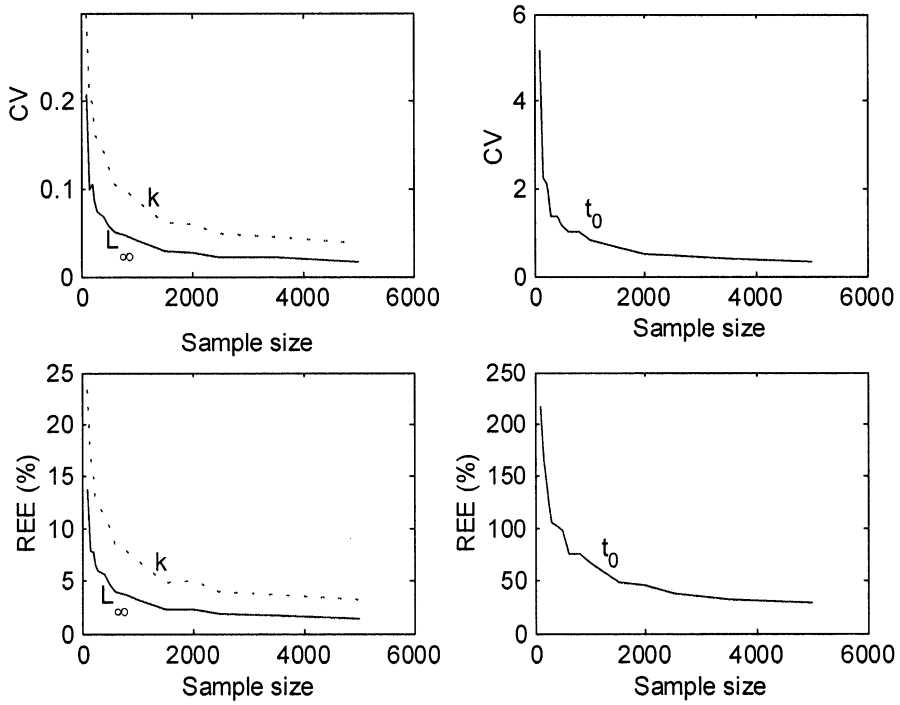

Figure 5.11. Plot of Coefficient of Variation (CV) and Relative Estimate Error (REE) of Length-at-age 5 and 10 against sample size.

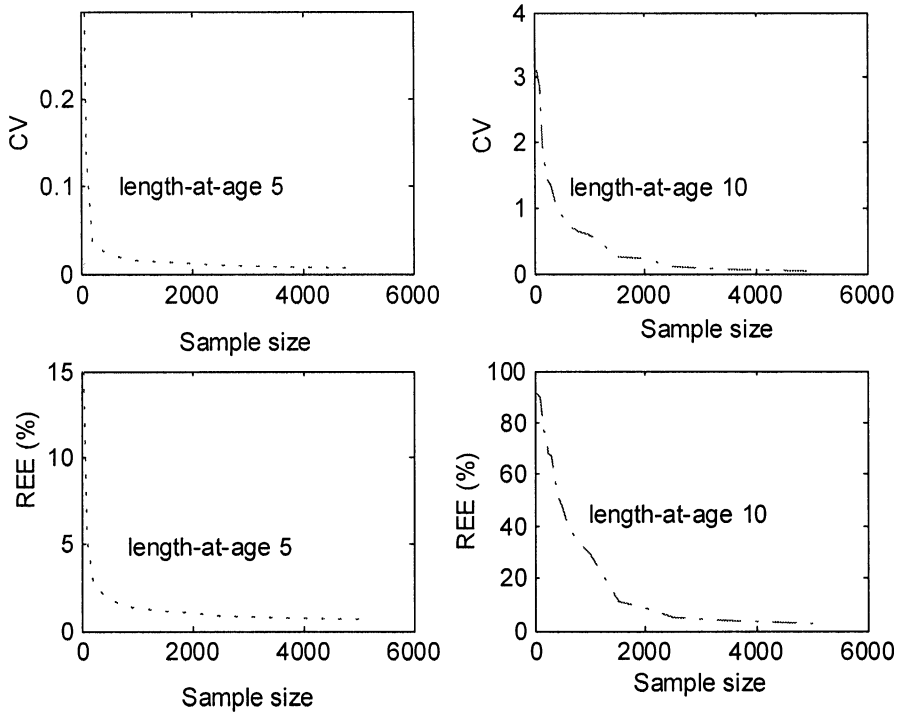

Figure 5.12. Comparison index (CI) of L_∞, k and t_0 (a) and proportion of catch-at-age (b) against sample size.

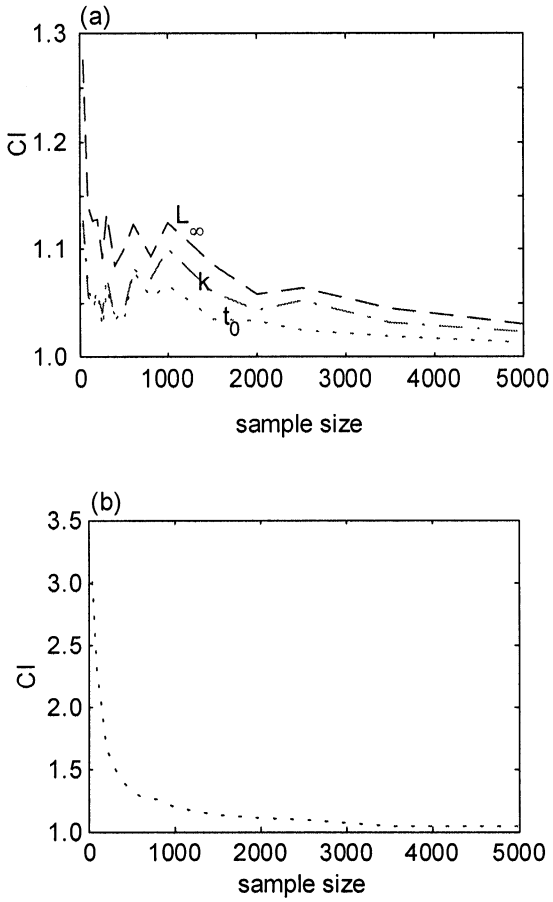

CHAPTER 6

AN APPLICATION OF COMPOSITE RISK ASSESSMENT METHOD IN ASSESSING FISHERIES STATUS

Abstract

The status of a fishery is often determined by comparing an indicator reference point (e.g. current fishing mortality) with a management reference point (e.g. $F_{0.1}$). Both references are likely subject to large uncertainty. Thus, it is necessary to incorporate such uncertainties in determining the status of fisheries. The composite risk assessment method, which is commonly used in civil engineering, can be used to quantify uncertainty associated with both indicator and management references in evaluating the status of a fishery. I applied this method to the Atlantic cod (*Gadus morhua*) fishery. The results suggest that the uncertainties in both indicator and current reference points can influence the evaluation of the fishery status. Uncertainty can come from different sources and is difficult to quantify. I suggest conducting a sensitivity analysis to evaluate the relative importance of uncertainties resulting from different sources. Such a study will enable us to identify key factors influencing the assessment of stock status in fisheries stock assessment and management.

6.1 Introduction

The collapse of many fisheries worldwide has been attributed to overexploitation resulting from gross overestimation of stock size and large scale discarding at sea, failed recruitment, and increased natural mortality due to changes in ecosystems. Ignoring or underestimating uncertainty in stock assessment and fisheries management is another important factor that may contribute to the decline of the fisheries (Hilborn and Walters, 1992; Ludwig et al., 1993; Walters and Maguire, 1996). The status of a fishery is often determined by comparing an indicator reference point estimated from stock assessment (e.g., current fishing mortality, current stock biomass) with a management reference point (e.g., $F_{0.1}$, B_{msy}; Caddy and Mahon, 1995). The declining trend in stock size as well as widely discussed impacts of uncertainty on stock assessment and management calls for a closer examination of the role of uncertainty plays in determining the status of a fishery (Ludwig et al., 1993; Myers and Worm, 2003). Replacing a currently used management reference point with a more conservative value to offset the impacts of uncertainty may bias the choice of the management reference points and cause distrust by fisheries stakeholders in fisheries management plans and stock assessment. A better approach would be to place emphasis on risk analysis and risk tolerance which incorporates the uncertainty in assessing the status of fisheries (Shelton and Rice, 2002).

Uncertainty in assessing a fishery may result from various sources such as measurement errors, process errors, model errors, and operating errors (Chen and Paloheimo, 1998; Patterson et al., 2001). An approach commonly used to incorporate

uncertainty in assessment is to estimate the empirical probability distribution of indicator reference points using methods such as the bootstrap and jackknife. The management reference points are calculated based on the fisheries data and life-history parameters using yield-per-recruit models, production models, and stock-recruitment models and are often assumed to be deterministic when they are compared with indicator reference points. Considering large variations that may exist in models, data and ecosystems, this assumption is rather unrealistic (Fogarty et al., 1996; Prager, 2003). Thus, management advisory statements derived using such an approach of comparing deterministic management reference points with stochastic indicator references do not reflect the fact that both the indicator and management reference points are subject to considerable uncertainty, and may yield erroneous conclusions about the status of fish stocks. A general approach should consider uncertainty in both indicator and management reference points (Helser et al., 2001; Chen and Wilson, 2002; Prager et al., 2003).

Composite risk analysis is a method of accounting for the risks resulting from various sources of uncertainty to produce an overall risk assessment for a particular decision-making problem (Yen, 1986). The composite risk analysis can allow for the incorporation of uncertainty in both indicator and management reference points in determining the status of a fishery. It provides an easy and direct estimate of the risk for overexploitation with full consideration of the uncertainties. Prager et al. (2003) used a similar approach to developing the target reference point based on the limit reference point. In Prager's approach, the risk assessment is regarded as a weighted integration,

while the weight is derived from the complementary cumulative distribution function. I used a similar approach by using a double integration function, which shows the exact scientific meaning of composite risk. I developed a discrete approach to estimate the composite risk, which is convenient to incorporate nontypical distributions and can avoid the influence from covariance between the two distributions of reference and management reference points. This approach is different from Prager's approach of REPAST (Ratio-Extended Probability Approach to Setting Targets).

For many fisheries there is a lack of understanding about the uncertainty in input data, variations in life history and population dynamics of fish stocks. Thus, it is important to evaluate the impacts of imprecise quantification of uncertainty of data in estimating reference points on the risk assessment and to identify key parameters influencing the determination of fisheries status. This calls for a sensitivity analysis which refers to the variation in the output of a mathematical model with respect to changes in the values of the model's input. A sensitivity analysis attempts to provide a ranking of the model's input assumptions with respect to their contribution to model output variability or uncertainty. In a broader sense, sensitivity can refer to how conclusions may change if models, data, or assessment assumptions are changed. A Monte Carlo simulation approach was used in this study for the sensitivity analysis, which allows for the systematic evaluation of model output with respect to uncertainty in input data. Uncertainty was incorporated into the simulation process in the forms of measurement and processing errors. All uncertainties in input data, and parameters were

examined to determine their effects on the output distributions through numerical experiments (scenarios). By comparing the differences in biological reference point (BRP) calculated under different uncertainty levels I could evaluate how a reference point responded to changes in a particular life-history process (growth, recruitment, or mortality). This helps identify important pathways and parameters for which assumptions about distributional functions contribute significantly to overall uncertainty and aid in focusing data gathering efforts.

The composite risk analysis and associated sensitivity analysis were applied to the Atlantic cod (*Gadus morhus*) fishery in divisions 2J3KL. The importance of incorporating uncertainty in both indicator and management reference points is discussed. Key factors that may influence the composite risk analysis were identified. This study provides an alternative approach for risk analysis in determining fisheries status.

6.2 Materials and Methods

Growth parameters and their variations are calculated from the DFO mean weight-at-age data (Lilly et al., 2001). The weight-age model, which combines the allometric weight-length model and von Bertalanffy length-age model, was used to estimate weight at age W_t and their corresponding variation (Quinn and Deriso, 1999),

(1) $$W_t = W_\infty [1 - e^{-k(t-t0)}]^b$$

where W_∞ is the maximum attainable weight; k is the Brody growth parameter, and t0 is the hypothetical age at which the weight is 0 (Ricker, 1975). A residual diagnostic analysis showed that the residuals of W_t in modeling followed lognormal distribution. Since the decline in cod abundance, studies have shown an increased variation in growth of cod, calling for the consideration of uncertainty of weight in stock assessment.

The information on proportion of cod caught at age t that are discarded at sea, D_t, for 2J3KL was from Kulka (1996). I modeled the relationship between age-specific discarding using the following logistic equation:

$$D_t = \frac{ND_t}{C_t} = \frac{1}{1+e^{d(t-d50)}}, \quad (2)$$

where ND_t is the number of fishes caught at age t that are discarded at sea, C_t is the catch number of fishes at age t, d is the shape parameter, $d50$ is the age at which 50% of the individuals are vulnerable to be discarded. d and $d50$ were assumed to be time-independent. Estimated parameters for D are shown in Table 6.1. The residual diagnostic analysis suggested that the residuals followed lognormal distribution in modeling. I thus defined D in equation 2 following a lognormal distribution with standard deviation shown in Table 6.1.

Age-specific selectivity was modeled using the following logistic equation:

$$s_t = \frac{1}{1+e^{-m(t-S50)}}, \quad (3)$$

where m is the shape parameter, $S50$ is the age at which 50% of the individuals are vulnerable to the fishing gear. m and $S50$ were assumed to be time-independent. Here, I used m =1.5, $S50$ =3.4 (Fu et al., 2001). I also assumed that S followed the lognormal distribution with standard deviation shown in Table 6.1.

Natural mortality (M) was assumed to follow a lognormal distribution with a mean of 0.2 and standard error of 0.1, 0.2, 0.4 to show low, median and high variations (Table 6.1). The lognormal distribution is often used for many fish life-history parameters including growth and mortality parameters (Hilborn and Walters, 1992; Shelton, 1992; Quinn and Deriso, 1999).

The exploitation rate estimated based on tagging data varied among areas and years. The averaged exploitation rates in 1999 and 2000 in 3KL area were estimated to be 43% and 12%, respectively (Cadigan and Brattey, 2002). These estimates were consistent with the exploitation rates estimated from landings and survey data in 1999 and 2000 (i.e. 0.29 for 1999 and 0.12 for 2000). The average exploitation rates in different tagging areas were weighted by experiment size (DFO, 2002). I used the weighted mean exploitation rate of all the areas as the mean exploitation rate during the year. The exploitation rate was assumed to follow a normal distribution defined by $N(0.24, 0.04^2)$ for 1999, $N(0.10, 0.01^2)$ for 2000, and $N(0.12, 0.01^2)$ for 2001 (DFO, 2002). The $N(\mu,\sigma^2)$ above define a normal distribution with the mean of μ and variance σ^2. The corresponding coefficients of variation of the exploitation rates were about 10% to 16%. The variance estimate did not consider variation in exploitation rate in unit tagging area and uncertainty resulting

from natural mortality, tagging loss, and gear selectivity. I then increased the coefficient of variation to 25%~30%. The corresponding fishing mortality would be drawn randomly from the distributions defined by N(0.30, 0.08^2) for 1999, N(0.12,0.03^2) for 2000, and N(0.14, 0.04^2) for 2001 based on the tag loss (2.8%) and natural mortality rate (9.5%). That is, exploitation rate $= \frac{C}{N} = \frac{F}{F+M}(1-e^{-F-M})$. From the above equation the fishing mortality rate can be estimated based on exploitation rate and natural mortality rate. For Scenario 8 of the simulation, a large natural mortality, 0.4, was used. The corresponding fishing mortality rate would then be drawn from N(0.34, 0.09^2) for 1999, N(0.13,0.03^2) for 2000, and N(0.16, 0.04^2) for 2001 for Scenario 8.

6.2.1 Composite risk analysis

Let X represent a management reference point (e.g., $F_{0.1}$) estimate and Y represent indicator reference point (e.g., current fishing mortality F_{cur}) estimate; then the corresponding *pdf* of X and Y are $f(x)$ and $g(y)$, respectively. If indicator Y is determined without uncertainty, then

(4) $$P(Y > X) = \int_{-\infty}^{y} f(x)dx .$$

If X is determined without uncertainty, then

(5) $$P(Y > X) = \int_{x}^{+\infty} g(y)dy .$$

Equation 5 is commonly used in assessing the status of the stock (Caddy and Mahon, 1995).

If both X and Y are not deterministic, and X and Y are independent, the probability of Y > X can be calculated as:

(6) $$P(Y > X) = \int_{-\infty}^{+\infty} \left\{ \int_{x}^{+\infty} g(y)dy \right\} f(x)dx$$

$$= \int_{-\infty}^{+\infty} G(y) \Big|_{x}^{+\infty} f(x)dx$$

$$= \int_{-\infty}^{+\infty} \{1 - G(x)\} f(x)dx$$

$$= \int_{-\infty}^{+\infty} f(x)dx - \int_{-\infty}^{+\infty} G(x) f(x)dx$$

$$= 1 - \int_{-\infty}^{+\infty} G(x) f(x)dx$$

Equation 6 can also be solved in the following way:

(6a) $$P(Y > X) = 1 - P(Y < X)$$

$$= 1 - \int_{-\infty}^{+\infty} \left\{ \int_{-\infty}^{x} g(y)dy \right\} f(x)dx$$

$$= 1 - \int_{-\infty}^{+\infty} G(x) f(x) dx$$

G(y) is the *cdf* of Y. This equation shows the risk of overexploitation, or the probability of the indicator (i.e., F_{cur}) being larger than the management BRP (i.e., $F_{0.1}$). In most of the cases the distribution of X and Y do not follow a standard distribution, and they are not continuous as in the above equation. One usually gets one or both of them from Monte Carlo simulations. In these cases, the above equation can be written as a discrete type.

$$(7) \qquad P(Y > X) = \sum_{-\infty}^{+\infty} \left\{ \sum_{x}^{+\infty} g(y) \Delta y \right\} f(x) \Delta x$$

$$= \sum_{-\infty}^{+\infty} G(y) \Big|_{x}^{+\infty} f(x) \Delta x$$

$$= \sum_{-\infty}^{+\infty} \{1 - G(x)\} f(x) \Delta x$$

$$= 1 - \sum_{-\infty}^{+\infty} G(x) f(x) \Delta x$$

Equation 7 can also be solved in the following way:

$$(7a) \qquad P(Y > X) = 1 - P(Y < X)$$

$$= 1 - \sum_{-\infty}^{+\infty} \left\{ \sum_{-\infty}^{x} g(y)\Delta y \right\} f(x)\Delta x$$

$$= 1 - \sum_{-\infty}^{+\infty} G(x) f(x)\Delta x$$

Replacing X and Y with $F_{0.1}$ and F_{cur} in the above equations, one can estimate the composite risk. Because both the $F_{0.1}$ and the current fishing mortality (F_{cur}) were estimated as a sample of random distribution generated from the Monte Carlo simulation (i.e., empirical distributions), I estimated the composite risk with equation 7a.

6.2.2 Yield-per-Recruit model

$F_{0.1}$ and F_{max} are estimated using the yield-per-recruit (YPR) model which calculates the average yield to be expected under a given pattern of fishing mortality over the life span of a cohort of fish. The YPR model is defined by parameters defining life history and fishery processes including growth, natural mortality, gear selectivity, and discarding. The uncertainty in estimating $F_{0.1}$ and F_{max} using the YPR model may come from the following sources: uncertainty in the model parameters, which are often estimated from other studies, and natural variability of life-history process resulting from variations in the biotic and abiotic environment. In this study some parameters and their variations (e.g., natural mortality, fishing selectivity) used in estimating $F_{0.1}$ and F_{max} were not derived from field data. Thus, the realism of these values could be questioned. Thus, one needs to run a simulation, which involves running a large range of values for the model parameters in deriving $F_{0.1}$ and F_{max}.

The commonly used discrete YPR model can be written as

$$Y = \sum_{t=t_r}^{t_l} C_t W_t (1 - D_t) \tag{8}$$

where Y is the attained yield, t_r is the age of entry into the fishery, and t_l is the maximum age of fish that could contribute to the fishery. The t_r was set at 3, and t_l =20 for the cod fishery. Given natural mortality, fishing mortality, and selectivity coefficients, catch-at-age C_t can be calculated from the catch equation as:

$$C_t = N_t \frac{s_t F}{s_t F + M}(1 - e^{-s_t F - M}), \tag{9}$$

where F is the fishing mortality. N_t is the number of fish at age t at the beginning of the year. N_t is estimated from recruitment R as follows:

$$N_t = \mathrm{Re}^{-\sum_{j=t_r}^{t-1}(s_t F + M)}. \tag{10}$$

Combining the equations 8, 9 and 10, one can get the YPR model as:

$$Y / R = \sum_{t=t_r}^{t_l} \left\{ \frac{W_t s_t F}{s_t F + M}(1 - e^{-s_t F - M}) e^{-\sum_{j=t_r}^{t-1}(s_j F + M)} (1 - D_t) \right\} \tag{11}$$

The $F_{0.1}$ was estimated from:

$$(12) \qquad \left.\frac{\partial(Y/R)}{\partial F}\right|_{F=F_{0.1}} = 0.1\left.\frac{\partial(Y/R)}{\partial F}\right|_{F=0}$$

The F_{max} was calculated from:

$$(13) \qquad \frac{\partial(Y/R)}{\partial F} = 0$$

I used the following procedure to estimate the uncertainty in $F_{0.1}$ and F_{max}: (1) identify the parameters that are likely to have uncertainties in the YPR model; (2) identify the magnitude and nature of errors for each model parameter identified in step (1); (3) randomly sample each parameter from its probability distribution; (4) apply the sampled model parameters to the YPR model to calculate $F_{0.1}$ and F_{max} (equation 12, 13); (5) repeat steps (3) and (4) for N times to yield N estimates of $F_{0.1}$ and F_{max}; (6) estimate the probability distribution of $F_{0.1}$ and F_{max} using the results derived in step (5).

Eight simulation scenarios were considered in this study (Table 6.1). Latin hypercube sampling was used to avoid unrealistically large or small values. The first three scenarios had medium, high, and low levels of variations for model parameters, respectively (Table 6.1). Scenarios 4 through 7 included high variations for selectivity coefficient, growth, discarding and natural mortality (the magnitudes of the corresponding parameters were the same as those for Scenario 2), while variations for other parameters were the same as those for Scenario 1. The difference in estimating $F_{0.1}$ and F_{max} between these scenarios and Scenario 1 illustrated the importance of variability in those parameters. Because of the speculations of a higher cod natural mortality possibly

resulting from climate changes and seal predation, a high natural mortality scenario was explored to identify possible impacts of increased natural mortality on composite risk analysis (i.e., Scenario 8; Table 6.1). The difference in the estimates of $F_{0.1}$ and F_{max} between the eighth and first scenarios thus reflected the relative importance of natural mortality in estimating uncertainty for $F_{0.1}$ and F_{max}.

For the first seven scenarios, 800 simulation runs were used to derive the stable probability distribution function for $F_{0.1}$ and F_{max}. For the high-natural mortality scenario (i.e., 8; Table 6.1), 1000 simulation runs were needed to yield stable probability distribution functions (*pdf*) for $F_{0.1}$ and F_{max}. The Kernel smoothing method was used to get a smooth *pdf* of $F_{0.1}$ and F_{max} (Bowman and Azzalini, 1997).

6.3 **Results**

The mean of the $F_{0.1}$ estimates using the data with a medium level of variation (i.e., scenario 1) was 0.1457 (Table 6.2). The probability distribution of $F_{0.1}$ in this scenario had 90% confidence intervals ranging from 0.1090 to 0.1980 (Table 6.2). The probability distributions for F_{cur} and $F_{0.1}$ did, however, share some overlaps (Figure 6.1). The composite risk assessment suggested that the probability of the current fishing mortality being higher than $F_{0.1}$ was 0.97 in 1999.

The distribution of $F_{0.1}$ derived for the high-variation scenario (i.e. Scenario 2) differed from that for the medium-variation scenario with long tails and different means.

Compared with those for the medium- and high-variation scenarios, variation in $F_{0.1}$ was lower for the low-variation scenario (i.e., Scenario 3; Table 6.2).

The high selectivity-variation, high growth-variation and high discarding-variation scenarios (i.e., Scenarios 4, 5 and 6, respectively) had levels of uncertainty for selectivity, growth and discarding as high as those in high-variation scenario (i.e., Scenario 2), while other parameters had uncertainty levels similar to those for medium-variation scenario (i.e., Scenario 1; Table 6.1). The probability distributions of $F_{0.1}$ for Scenarios 4, 5 and 6 were similar to that for Scenario 1 both in modes and in tails (Table 6.2 and Figure 6.1). The consistency of these scenarios with the medium-variation scenario suggests that the uncertainty in selectivity, growth, and discarding parameters is not the main contributor to the estimated uncertainty for $F_{0.1}$. Thus the estimate of $F_{0.1}$ is less sensitive to uncertainty in these parameters.

The level of uncertainty for natural mortality in Scenario 7 was the same as that for the high-variation scenario (i.e., scenario 2), while other parameters were same as those for the medium-variation scenario (i.e., Scenario 1). The probability distribution of $F_{0.1}$ for this scenario was different from that for Scenario 1 but similar to that for Scenario 2 (Figure 6.1). These results suggest that the uncertainty in natural mortality is the main contributor to the estimated uncertainty for $F_{0.1}$ and uncertainties of other parameters (growth, discarding, and selectivity) had limited influence on the estimated uncertainty of $F_{0.1}$.

When the higher natural mortality scenario was used, the probability distribution of $F_{0.1}$ for this scenario was different from the first seven scenarios both in the central tendency and in tails of the distributions (Figure 6.1). The estimated mean of the $F_{0.1}$ was 0.34, which was more than two times of the values estimated for other scenarios.

The risks of $F_{cur}>F_{0.1}$ in 1999 were close to 97% in scenarios 1, 4, 5 and 6. They were close to 92% ~ 93% in scenarios 2 and 7. This implied that the overexploitation risks were lower in the high-variation scenario and high M-variation scenario in this year. It also implied that the risk of overexploitation was sensitive to the variation of natural mortality.

The average of F_{cur} in 2000 was smaller than the mean and median of $F_{0.1}$ estimated for the first seven scenarios when natural mortality was assumed to be 0.2 (Tables 6.2 and 6.3 and Figure 6.1). The composite risk assessment suggested that there was a 37% to 45% probability of overexploitation. In the high-natural mortality scenario the $F_{0.1}$ estimate was larger, so the $P(F_{cur} > F_{0.1})$ was only 10%. The mean of F_{cur} in 2001 was similar to the mean and median of $F_{0.1}$ estimated from the first seven scenarios (Tables 6.2 and 6.3). The composite risk assessment suggested that there was a 54% to 61% of possibility of overexploitation. For 2000, the $P(F_{cur} > F_{0.1})$ was estimated as 13% for the high natural mortality scenario.

The pdf_S of F_{max} in different scenarios showed similar trend as $F_{0.1}$. The pdf_S of F_{max} for Scenarios 1, 4, 5 and 6 were also similar. The pdf_S of F_{max} in Scenarios 2 and 7, both

of which have larger variations, were similar (Figure 6.2). The $P(F_{cur} > F_{max})$ estimated using composite risk assessment suggested that when natural mortality was assumed to be 0.2, the $P(F_{cur} > F_{max})$ was about 70% to 80% for 1999; 8% to 25% for 2000, and 10% to 33% for 2001 (Table 6.3).

6.4 Discussion

This study suggests that incorporating uncertainty of indicator reference point and BRP into risk assessment of fisheries is important, and may influence the estimation of overexploitation risk and determination of stock status. Ignoring uncertainty may lead to incorrect conclusions about the status of the stock.

This study also suggests that the magnitude of the uncertainty in the parameters of the YPR model could influence the estimation of $P(F_{cur} > F_{0.1})$, thus affecting the conclusion as to whether the fishery is overfished. Higher uncertainty in the model parameters resulted in higher uncertainty in the estimates of $F_{0.1}$. By comparing the results of the medium-, high-, and low-variation scenarios considered in this study, I found that large uncertainty of parameters could reduce $P(F_{cur} > F_{0.1})$ when $\overline{F}_{cur} > \overline{F}_{0.1}$, thus making it less likely to conclude that the stock was overfished (the case for 1999). I also found that large uncertainty of parameters would increase $P(F_{cur} > F_{0.1})$ when $\overline{F}_{cur} < \overline{F}_{0.1}$, making it more likely to conclude that the stock was overfished (the case for 2000). The uncertainty associated with current fishing mortality F_{cur} is important in determining the status of a fish stock. It could be readily predicted that $P(F_{cur} > F_{0.1})$ decreases with increasing

uncertainty in F_{cur} when $\overline{F}_{cur} > \overline{F}_{0.1}$ and that $P(F_{cur} > F_{0.1})$ increases with increasing uncertainty in F_{cur} when $\overline{F}_{cur} < \overline{F}_{0.1}$. For example, if I increase variations associated with F_{cur} from current CV of 25%~ 30% to CV = 40%, for Scenario 1, $P(F_{cur} > F_{0.1})$ changed from 0.97 to 0.94 for 1999, and 0.38 to 0.41 for 2000, and 0.55 to 0.54 for 2001 , respectively (Table 6.4). To verify the above conclusion, the risk of $\overline{F}_{cur} > \overline{F}_{0.1}$ was calculated when both $F_{0.1}$ and F_{cur} followed normal distributions and had different CVs varying from 20% to 40% (Figure 6.3). The results were consistent with those derived for the cod fishery. In this study, I used F_{cur} from the tagging study. In many risk analyses, F_{cur} is estimated from sequential population analysis, in which situation F_{cur} is often over-estimated due to retrospective problems (Bishop and Shelton, 1997; Shelton and Rice, 2002). The consideration of this uncertainty should be the focus of future studies.

The sensitivity analysis suggested that uncertainty in natural mortality was most important in determining the uncertainty of $F_{0.1}$. This study indicated that uncertainty in $F_{0.1}$ was less sensitive to uncertainty in other parameters. This result is consistent with previous studies (Chen and Wilson, 2002). Reliable estimation of natural mortality and its associated uncertainty is thus critical in assessing the status of a fishery.

Quantification of uncertainty in life history and fishery parameters is an essential step for estimating uncertainty of $F_{0.1}$ and F_{cur}. Uncertainties can arise from the variation in the statistical estimation of the parameters and natural variability in the parameters among cohorts and geographic areas. However, it is unlikely that "correct" values can be

identified to define the uncertainty for the parameters. Sensitivity analysis through Monte Carlo simulation can help overcome this problem. In the simulation, different levels of uncertainty are considered for each parameter. The ranges of uncertainty for each parameter evaluated in the simulation were rather large, reflecting our efforts to cover all possible ranges of uncertainty within them. The comparison of results derived from different levels of uncertainty help us identify the sensitivity of the input parameters to the output reference point distribution and provide us with enough evidence in identifying impacts of uncertainty in reference points on the determination of the stock status and its possible management implications in decision making. In the situation of figure 6.3, when a risk of 5% is used in a precautionary approach and when $F_{0.1}$ is used as the BRP, the possible fishing mortality used as the management target (i.e., future F_{cur}) will differ when CVs of F_{cur} and $F_{0.1}$ were different. When CVs of both F_{cur} and $F_{0.1}$ were between 20% and 40%, the F_{cur} should be between (1/3 ~1/1.62) of $F_{0.1}$. Usually an estimate with CV of 30% is often considered to be a good estimate in fish stock assessment (Walters, 1998). A CV between 20% and 40% would be practical in fisheries. For a healthy fishery a target fishing mortality estimate with lower CVs assumed to both F_{cur} and $F_{0.1}$ can be used. For an overexploited fishery, a target fishing mortality estimate with higher CVs assumed to both F_{cur} and $F_{0.1}$ would be suggested.

I suggest using the composite risk analysis method to assess the risk resulting from uncertainty in developing precautionary approaches and in managing the fisheries. A precautionary approach considering uncertainty in both management reference point and

indicator reference point is needed to prevent overexploitation and to promote the recovery of the overexploited fisheries.

Table 6.1. Parameters and models with uncertainty considered in the $F_{0.1}$ and F_{max} estimate, and the simulation scenarios included in the study.

Scenarios	Parameter	Parameter value	Standard error
1	M	0.2	0.2
medium-variation	s	$m = 1.5; t50 = 3.4$	0.2
scenario (most realistic	W_t	W_∞=44.0597; k=0.0423;	0.28
scenario)		$t0$=-0.9955; b=2.5093;	
	D_t	d=4.0515; $td50$=2.5584	0.4
2	M	0.2	0.4
high-variation scenario	s	$m = 1.5; t50 = 3.4$	0.4
	W_t	See above	0.4
	D_t	See above	0.6
3	M	0.2	0.1
low-variation scenario	s	$m = 1.5; t50 = 3.4$	0.1
	W_t	See above	0.15
	D_t	See above	0.2
4	M	0.2	0.2
high selectivity	s	$m = 1.5; t50 = 3.4$	0.4
coefficient variation	W_t	See above	0.28
scenario	D_t	See above	0.4
5	M	0.2	0.2
high growth-variation	s	$m = 1.5; t50 = 3.4$	0.2

scenario	W_t	See above	0.5
	D_t	See above	0.4
6	M	0.2	0.2
high discarding-	s	$m = 1.5; t50 = 3.4$	0.2
variation scenario	W_t	See above	0.28
	D_t	See above	0.6
7	M	0.2	0.4
high M-variation	s	$m = 1.5; t50 = 3.4$	0.2
scenario	W_t	See above	0.28
	D_t	See above	0.4
8	M	0.4	0.4
high M scenario	s	$m = 1.5; t50 = 3.4$	0.2
	W_t	See above	0.28
	D_t	See above	0.4

Table 6.2. Summary statistics for the estimated $F_{0.1}$ in the simulation study.

Scenario	mean	median	percentiles	
			5th	95th
1	0.1457	0.1400	0.1090	0.1980
2	0.1659	0.1340	0.0940	0.3060
3	0.1425	0.1410	0.1230	0.1670
4	0.1485	0.1420	0.1090	0.2060
5	0.1465	0.1380	0.1060	0.2160
6	0.1400	0.1350	0.1050	0.1900
7	0.1652	0.1380	0.0980	0.3080
8	0.3432	0.3045	0.1880	0.6380

Table 6.3. Summary of the statistics of the estimated $P(F_{cur} > F_{0.1})$ and $P(F_{cur} > F_{max})$. $N(\mu, \sigma^2)$ describe a normal distribution with mean of μ and standard deviation of σ.

Year	F_{cur}	Scenarios	$P(F_{cur} > F_{0.1})$	$P(F_{cur} > F_{max})$
1999	$N(0.30, 0.08^2)$	1	0.97	0.73
		2	0.93	0.79
		3	0.98	0.75
		4	0.97	0.71
		5	0.97	0.77
		6	0.98	0.78
		7	0.92	0.74
	$N(0.34, 0.09^2)$	8	0.62	0.25
2000	$N(0.12, 0.03^2)$	1	0.38	0.15
		2	0.45	0.25
		3	0.37	0.08
		4	0.38	0.12
		5	0.41	0.19
		6	0.44	0.14
		7	0.42	0.20
	$N(0.13, 0.04^2)$	8	0.10	0.14
2001	$N(0.14, 0.04^2)$	1	0.55	0.19
		2	0.57	0.33
		3	0.57	0.10
		4	0.54	0.17
		5	0.57	0.25
		6	0.61	0.21
		7	0.54	0.27
	$N(0.16, 0.04^2)$	8	0.13	0.14

Table 6.4. Estimated $P(F_{cur} > F_{0.1})$ when increased uncertainty with F_{cur} was used for the medium-variation scenario (i.e., Scenario 1, Table 6.1). σ_1 is the standard deviation of F_{cur} with lower uncertainty, which is the same as in Table 6.3. σ_2 is the standard deviation of F_{cur} with higher uncertainty.

Year	$\overline{F}_{cur}$	σ	$P(F_{cur} > F_{0.1})$
1999	0.30	σ_1=0.08	0.97
		σ_2=0.12	0.94
2000	0.12	σ_1=0.03	0.38
		σ_2=0.048	0.41
2001	0.14	σ_1=0.04	0.55
		σ_2=0.056	0.54

Figure 6.1. Estimated *pdf* of $F_{0.1}$ for eight scenarios and *pdf* of F_{cur} in 1999, 2000 and 2001. S1 represents scenario 1, and so on.

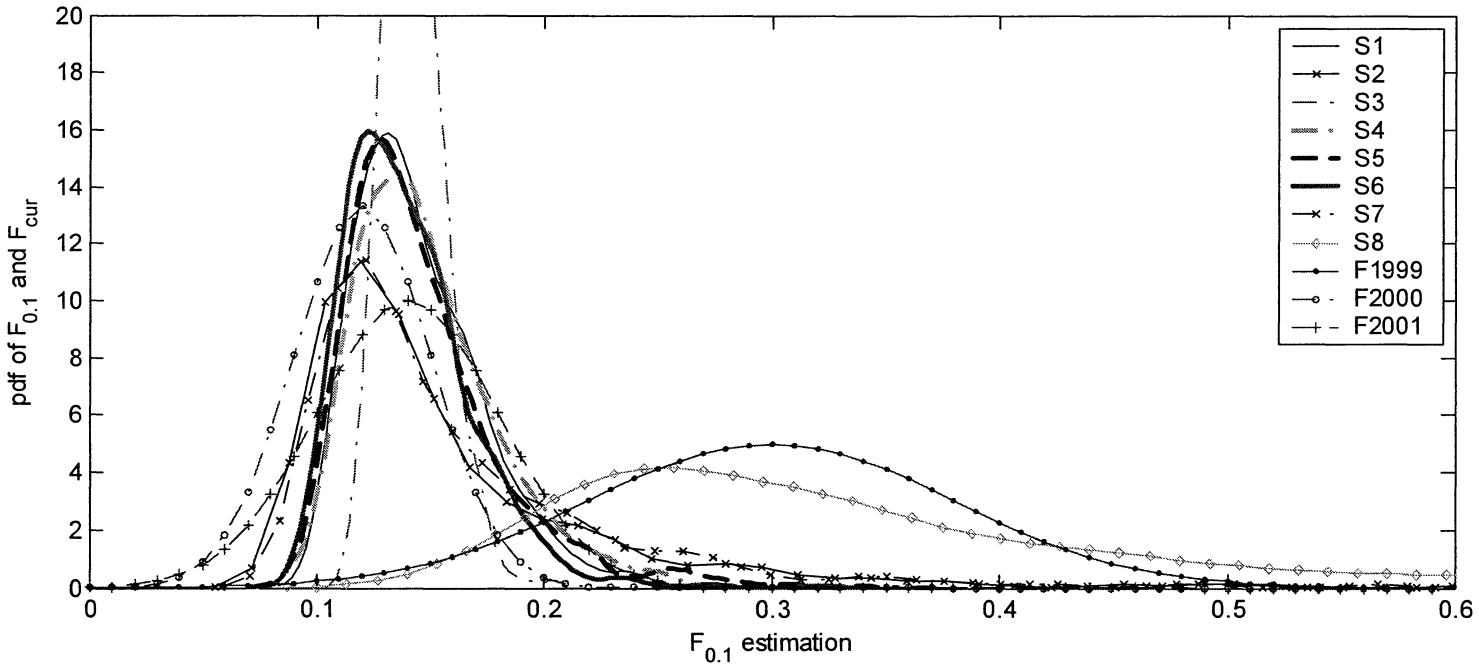

Figure 6.2. Estimated *pdf* of F_{max} for eight scenarios and *pdf* of F_{cur} in 1999, 2000 and 2001. S1 represents scenario 1, and so on.

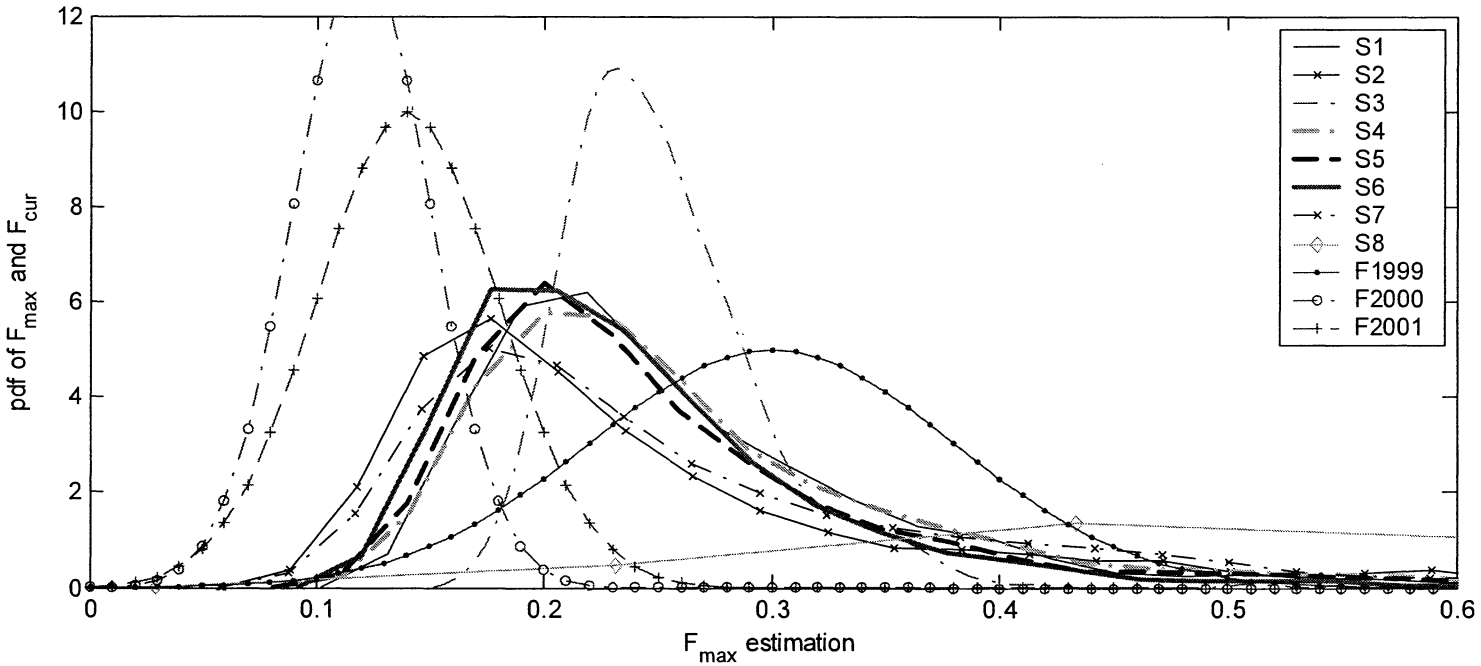

Figure 6.3. Risk of $F_{cur} > F_{0.1}$ when both $F_{0.1}$ and F_{cur} follow normal distribution and have different CVs changed from 20% to 40%.

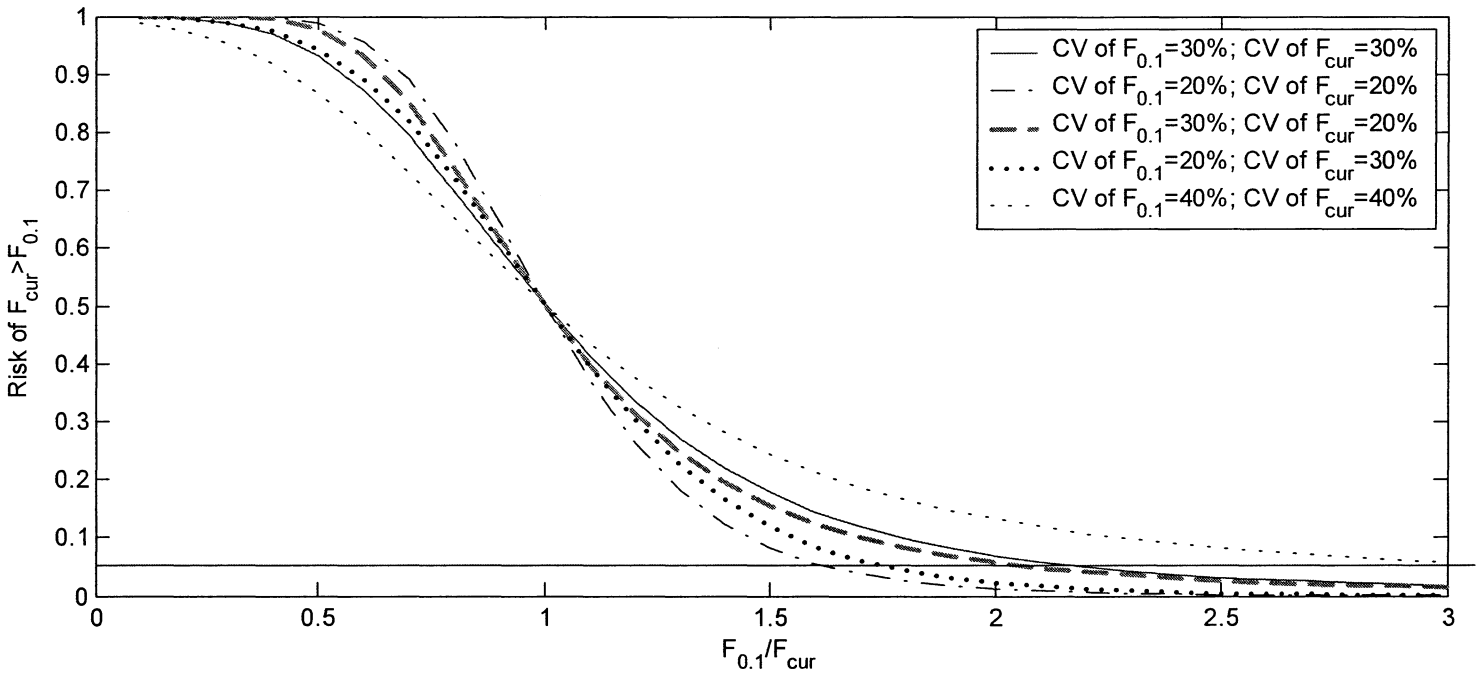

CHAPTER 7: SUMMARY

In this thesis I model uncertainties in stock-recruitment models, surplus production models and sequential age-structure population analysis by exploring their model error structures. The model error structures in those models were evaluated using generalized linear models which can deal with different error structures in the exponential family of probability distribution. The growth variations that may result from stock mixing were evaluated using a Monte Carlo simulation study. The impacts of sample size in subsampling catch on the observed length-at-age were evaluated through the simulation study. The total risk of overexploiting fisheries was quantified using a composite risk assessment method which includes uncertainties both from a management reference point and from an indicator reference point.

7.1 Model error structure in stock-recruitment models

The estimation of SR relationship is perhaps one of the most difficult works in fisheries stock assessment. Chapter 2 describes the impact of model error structure on modeling stock-recruitment data. A Monte Carlo simulation-estimation approach was used to evaluate the impact of the assumption of error structure on SR modeling. Data was first generated using the SR Ricker, Cushing and Beverton-Holt models along with known parameters. While estimating parameters, the generalized linear model, which can readily deal with different error structures, was used. Departure of the estimated parameters from the true values was measured by the relative estimation bias (REB) and

root mean square error (RMSE). With the simulation-estimation Monte Carlo approach, the effect of model errors was examined. In addition, because the number of SR data is often small and outliers are likely to be present in the SR data, the role of sample size and outliers in identifying appropriate error structure in SR modeling was also evaluated in the simulation study.

The results from the Monte Carlo simulation are encouraging and informative. The quality of SR parameter estimation, measured by estimation errors, can be influenced by the realism of error structure assumed in an estimation, number of SR data points, and number of outliers in modeling. A small number of SR data points and presence of outliers in SR data could increase the difficulty in identifying an appropriate error structure in modeling, which might lead to large biases in the SR parameter estimation. This study shows that generalized linear model methods can help identify an appropriate error distribution in SR modeling, leading to an improved estimation of parameters even when there are outliers and the number of SR data points is small.

Based on the simulation results in Chapter 2, using a generalized linear model approach, I explored and identified the appropriate model error structure in modeling SR data for gadoid stocks in Chapter 3. The result suggests that the appropriate SR model error structure can be normal and/or lognormal, which is widely assumed in SR modeling, but it can be gamma and/or Poisson also. In modeling SR data for gadoid stocks, the Ricker model was found to be more sensitive to the assumption of model error distribution than the Cushing model. The lognormal and gamma distribution had a higher

probability to be the appropriate model error distribution. Cluster analyses and summary statistics of error distributions in SR modeling did not show a consistent pattern in the identification of an appropriate model error structure among species, geographic distributions and sample sizes. However, stocks distributed in semi-enclosed water areas were found to have a higher probability of having symmetrical error distributions, such as a normal distribution. A better understanding of the factors and mechanisms resulting in differences in the choice of appropriate model error distributions for different populations is needed in future research. These two chapters imply that it is important to identify appropriate model error structures in quantifying SR relationships, the generalized linear model could be used as a tool to explore the SR model error structure.

7.2 Observation-model error structure in the surplus production model and population dynamic models

Assumptions on observation-model error structure play an important role in the parameter estimation of fishing mortality and population size in the surplus production model and age-structured population models. Commonly used lognormal error structure, without testing for its appropriateness for a given set of data, may result in estimation biases. Chapter 4 developed a generalized linear model approach to diagnose the model error structure when using the production and the population dynamic models. With an acceptable model error structure, the quality of the parameter estimation will be improved, which will then further improve the stock assessment and management.

7.3 Mixing among populations or stocks can result in large growth variations

A Monte Carlo simulation approach was used to explore the possibility of large growth variation resulting from large areas of migration and mixing among stocks of Atlantic Cod in Chapter 5. It addresses the question as to how observed variations in cod length-at-age can be influenced by stock mixing, and how a change in mixture rates may influence growth analyses. The 2J3KL and 3Ps cod stock growth parameters were used. The simulation includes some assumptions to simplify the simulation. Although some assumptions may not be realistic, such a study shows how the observed variations in growth can be explained by the hypothesis of mixing of fish of one population with another. The simulation study suggests that stock mixing can have great impacts on the growth modeling and stock assessment especially when the relative population composition varied greatly. The sample size effect on the estimation of length-at-age and length-at-age model parameters was also explored through a Monte Carlo simulation. The result suggests that a large sample size is needed in subsampling catch in order to clearly identify growth variations resulting from stock mixing. I suggest that stock mixing be incorporated into stock assessment models to improve the estimation of key fisheries parameters in stock assessment.

7.4 The importance of considering uncertainty in management BRP estimate and in the indicator BRP

Chapter 6 explored the uncertainty related to the BRP of $F_{0.1}$ and F_{max} estimation. The first step was to explore the key parameters and models with uncertainties. The following parameters and models were considered: gear selectivity, natural mortality,

growth and discarding. The second step was to set up a Monte Carlo simulation approach used in estimating biological reference point $F_{0.1}$ and F_{max} for the Atlantic cod fishery. The third step was to evaluate the sensitivities of $F_{0.1}$ and F_{max} to the magnitudes of uncertainties in those parameters and models. The last step was to estimate the risk. The composite risk assessment method was used to evaluate the risk of overexploitation in the cod fishery, which considered the uncertainties in both the biological reference point and current fishing mortality. The result suggests that the uncertainty in estimation of BRP greatly influence the risk estimate, while the uncertainty in management BRP also greatly influence the risk estimate. This implies that in decision making the uncertainty in management BRP should be considered.

My results suggested that the $F_{0.1}$ estimate was sensitive to natural mortality variations, but relatively robust to uncertainties in other parameters. I suggest using composite risk assessment in evaluating the status of the Atlantic cod fishery. A higher level of uncertainty was suggested when evaluating the fishery status and in future management BRP decision making for an exploited fishery.

7.5 Further improving fisheries stock assessment by better quantifying uncertainty

Life-history processes such as growth and mortality are pertinent to stock assessment and fishery management. A full understanding of these factors, appropriately modeling them and taking these factors into account of fisheries management is necessary. From this study I can see that natural mortality estimate is important in the Atlantic cod stock assessment. Considering that many fisheries stock assessments are

sensitive to variations in natural mortality and how little I know about reliability of estimated natural mortality, future research should focus on the evaluation of uncertainties in natural mortality and how they may be better quantified and evaluated.

The effect of uncertainty arising from the spatial distributions and migrations needs to be further studied through simulation study based on practical fisheries.

Availability of the uncertainty level of these life-history factors will further improve the stock assessment and fishery management. Because the variation of the life-history processes observed does not always covaries with the climate ocean variables and there are a large number of environmental variables, it is difficult to model those variations by including climate variables in fishery models. The commonly used ecosystem models also have the same problem. In this case, considering the levels of the uncertainty caused by the environmental changes and incorporate them into stock assessment will provide a better solution in stock assessment.

In many cases, the information on uncertainty of the life-history parameters are not available. A sensitivity analysis of the responses of population dynamics to different levels of variability in parameters will help improve the understanding of the roles the uncertainty plays in stock assessment modeling. A risk assessment including uncertainties from different sources will lead to an improved risk analysis, and subsequently improved management.

BIBLIOGRAPHY

Anscombe, F.J., and Tukey, J. W. 1963. The examination and analysis of residuals. Technometrics. 5:141-160.

Armstrong. M.J., and Shelton, P.A. 1988. Bias in estimation of stock-recruit function parameters caused by nonrandom environmental variability. Can. J. Fish. Aquat. Sci. 45:554-557.

Atkinson, D. B., and Bennett, B. 1994. Proceeding of a Northern Cod Workshop held in St. John's, Newfoundland, Canada, January 27-29, 1993. Can. Tech. Rep. Fish. Aquat. Sci. No. 1999.

Atkinson, D. B., Rose, G.A., Murphy, E.F. and Bishop, C.A. 1997. Distribution changes and abundance of northern cod (Gadus morhua), 1981-1993. Can. J. Fish. Aquat. Sci. 54 (Suppl. 1): 132-138

Baird, J.W., Bishop, C.A., Brodie, W.B., and Murphy, E.F. 1992. An assessment of the cod stock in NAFO Division 2J3KL. NAFO SCR Doc. 92/18.

Bajdik, C.D. and Schneider, D.C. 1991. Models of the fish yield from lakes: does the random component matter? Can. J. Fish. Aquat. Sci. 48:619-622.

Beacham, T.D. 1983. Growth and maturity of Atlantic cod (*Gadus morhua*) in the southern Gulf of St. Lawrence. Can. Tech. Rep. Fish. Aquat. Sci.

Bishop, C.A. and Shelton, P. 1997. A narrative of NAFO Divs. 2J3KL cod assessments from extension of jurisdiction to moratorium. Canadian Technical Report of fisheries and Aquatic Sciences 2199.

Bowman, A.W. and Azzalini, A. 1997. Applied Smoothing Techniques for Data Analysis. Oxford University Press. 208pp.

Brander, K.M., 1994. Patterns of distribution, spawning, and growth in North Atlantic cod: the utility of inter-regional comparisons. ICES Marine Science Symposia, 198, pp. 406-413.

Brander, K.M., 1996. Effects of climate change on cod (*Gadus morhua*) stocks. In Global Warming: Implications for freshwater and marine fish. Society for Experimental Biology Seminar Series 61. Edited by C.M. Wood and D.G. McDonald. Cambridge University Press, pp. 255-278.

Brattey, J. 2000. Stock structure and seasonal movements of Atlantic Cod (*Gadus morhua*) in NAFO Div. 3KL inferred from recent tagging experiments. Working paper. 2J-3KL cod assessment meeting.

Brattey, J., Cadigan, N.G., Healey, B.P., Lilly, G.R., Murphy, E.F., Shelton, P.A., Stansbury, D.E., Morgan, M.J. and Mahé, J.-C. 2001. An assessment of the cod stock in NAFO Subdivision 3Ps in October 2001. DFO CSAS Research Document. 2001/099.

Caddy, J.F. and Mahon, R. 1995. Reference points for fisheries management. FAO fisheries technical paper 347. 83pp.

Cadigan, N. and Brattey, J. 2002. Updated estimates of exploitation rates and biomass for cod (*Gadus morhua*) in NAFO Divisions 3KL and Subdivision 3Ps during 1997-2000 from tagging experiments in these years. DFO Canadian Science Advisory Secretariat Research Document 2002/021. 26pp.

Cadigan, N.G., and Myers, R.A. 2001. A comparison of gamma and lognormal maximum likelihood estimators in a sequential population analysis. Can. J. Fish. Aquat. Sci. 58:560-567.

Campana, S.E., Chouinard, G.A., Hanson, J.M., and Frechet, A. 1999. Mixing and migration of overwintering Atlantic Cod (*Gadus morhua*) stocks near the mouth of the Gulf of St. Lawrence. Can. J. Fish. Aquat. Sci. 56: 1873-1881

Carroll, R.J. and Ruppert, D. 1984. Power transformations when fitting theoretical models to data. J. Amer. Stat. Assoc. 79:321-328.

Chen, Y. 1996. A Monte Carlo study on impacts of the size of subsample catch on estimation of fish stock parameters. Fish. Res. 26:207-223

Chen, Y. and Mello, L.G.S. 1999. Growth and maturation of cod (*Gadus morhua*) of different year classes in the Northwest Atlantic, NAFO subdivision 3Ps. Fish. Res. 42:87-101

Chen, Y. and Wilson, C. 2002. A simulation study to evaluate uncertainty associated with biological reference point $F_{0.1}$ for the American lobster (*Homarus americanus*) fishery in the Gulf of Maine and some possible management implications. Can. J. Fish. Aquat. Sci. 59:1394-1403.

Chen, Y., and Paloheimo, J.E. 1995. A robust regression analysis of recruitment in fisheries. Can. J. Fish. Aquat. Sci. 52:993-1006.

Chen, Y., and Paloheimo, J.E. 1998. Can a more realistic model error structure improve parameter estimation in modeling the dynamics of fish populations? Fish. Res. 38: 9–17.

Chen, Y., Jackson, D.A. and Paloheimo, J.E. 1994. Robust regression analysis of fisheries data. Can. J. Fish. Aquat. Sci. 51:1420-1429.

Chen, Y., Jiao, Y. and Chen, L. 2003. Developing robust frequentist and Bayesian fish stock assessment methods. Fish and Fisheries. 3:1-16.

Clarke, W.G. 1991. Groundfish exploitation rates based on life history parameters. Can. J. Fish. Aquat. Sci. 48:734-750.

Dalley, EL; Anderson, JT. Age-dependent distribution of demersal juvenile Atlantic cod (*Gadus morhua*) in inshore/offshore Northeast Newfoundland. Can. J. Fish. Aquat. Sci. 54 (Suppl. 1): 168-176

Deriso, R.B., Quinn, T.J., and Neal, P.R. 1985. Catch-age analysis with auxiliary information. Can. J. Fish. Aquat. Sci. 42: 815-824.

deYoung, B. and Rose, G.A. 1993. On recruitment and distribution of Atlantic cod (*Gadus morhua*) off Newfoundland. Can. J. Fish. Aquat. Sci. 50:2729-2741.

DFO, 2002. Northern (2J3KL) cod stock status update. DFO science stock status report A2-01 (2002). 15pp.

DFO. 2000. Northwest Atlantic Harp Seals. DFO science stock status report E1-01 (2000).

Dickson, B., Yashayaev, I., Meincke, J., Turrell, B., Dye, S., Holfort, J. 2002. Rapid freshening of the deep North Atlantic Ocean over the past four decades. Nature. 416:832-837.

Dobson, A.J. 1990. An Introduction to Generalized Linear Models. Chapman & Hall,

Drinkwater, K.F. 2002. A review of the role of climate variability in the decline of northern cod. Pages 113-130 *in* N.A. McGinn editor. Fishing in a Changing Climate. American Fisheries Society, Symposium 32, Bethesda, Maryland.

Everitt, B.S., Landau, S., and Leese, M. 2001. Cluster Analysis. Arnold, London.

FAO. 1995. Reference points for fisheries management. FAO fisheries technical paper 347. 83pp.

FAO. 1996. Precautionary approach to fisheries. Part 2: Scientific papers. FAO fisheries technical paper 350/2. 210pp.

FAO. 1997. Bycatch management and the economics of discarding. FAO fisheries technical paper 370. 137pp.

Firth, D. 1988. Multiplicative errors: log-normal or gamma? J. Roy. Statist. Soc. Ser. B, **50**: 266–268.

Fogarty, M. J., Hilborn, R. and Gunderson, D. 1997. Chaos and parametric management. Marine Policy. 21:187-194

Fogarty, M.J. 1993. Recruitment distributions revised. Can. J. Fish. Aquat. Sci. 50:2723-2728.

Fogarty, M.J., R.K. Mayo, L. O'Brien, F. M. Serchuk, and A.A. Rosenberg. 1996. Assessing uncertainty and risk in exploited marine populations. Reliability Engineering and System Safety, 54:183-195.

Fu, C., Mohn, R., and Fanning, L.P. 2001. Why the Atlantic cod (*Gadus morhua*) stock off eastern Nova Scotia has not recovered. Can. J. Fish. Aquat. Sci. 58:1613-1623.

Garrod, D.J., and Schumacher, A. 1994. North Atlantic cod: the broad canvas. ICES Mar. Sci. Symp. 198:59-76.

Gilbert, D.J. 1997. Towards a new recruitment paradigm for fish stocks. Can. J. Fish. Aquat. Sci. 969-977

Giske, J. Huse, G. and Fiksen, Ø. 1998. Modeling spatial dynamics of fish. Reviews in Fish Biology and Fisheries. 8:57-91.

Gomes, M.C., Haedrich, R.L., Villagarcia, M.G. 1995. Spatial and temporal changes in the groundfish assemblages on the northeast Newfoundland/Labrador Shelf, Northwest Atlantic. Fish. Oceanogr. 4(2): 85-101

Haedrich, R. L., and Hamilton, L.C. 2000. The fall and future of Newfoundland's cod fishery. Society Nat. Resources. 13:359-372.

Hanson, J.M., Chouinard, G.A. 1992. Evidence that size-selectivity mortality affects growth of Atlantic cod (*Gadus morhua* L.) in the southern Gulf of St. Lawrence. J. Fish. Biol. 41: 31-41

Harrison P.J., and Parson, T.R. 2000. Fisheries Oceanography: An Integrative Approach to Fisheries Ecology and Management. Blackwell Science.

Helser, T.E., Sharov, T., and Kahn, D. M. 2001. A stochastic decision-based spproach to assessing the Delaware Bay blue crab (*Callinectes sapidus*) stock. In Incorporating Uncertainty into Fishery Models (Berkson, J.M., L.L. Kline, and D.J. Orth, eds.) American Fisheries Society Publication, Bethesday, MD. 208pp.

Hennemuth, R.C., Palmer, J.E., and Brown, B.E. 1980. A statistical description of recruitment in eighteen selected fish stock. J. Northwest Atl. Fish. Sci. 1:101-111.

Hilborn, R. and Walters, C. 1992. Quantitative Fisheries Stock Assessment: Choice, Dynamics, and Uncertainty. Chapman and Hall, New York. 570pp.

Hinrichsen, R.A. 2001. High variability in spawner-recruitment data hampers learning. Can. J. Fish. Aquat. Sci. 58: 769-776.

Houghton Milflin Co. 1992. The American Heritage Dictionary of English Language. Third Edition.

Hutchings, J. A. 1996. Spatial and temporal variation in the density of northern cod and a review of hypotheses for the stock's collapse. Can. J. Fish. Aquat. Sci. 53:943-962.

Hutchings, J. A., and R. A. Myers. 1994. What can be learned from the collapse of a renewable resource? Atlantic cod, *Gadus morhua*, of Newfoundland and Labrador. Can. J. Fish. Aquat. Sci. 51:2126-2146.

Hutchings, J.A., and Myers, R.A. 1994. Timing of cod reproduction: interannual variability and the influence of temperature. Mar. Ecol. Prog. Ser. 108, 21-31.

Hutchings, J.A., and Myers, R.A. 1995. The biological collapse of Atlantic cod off Newfoundland and Labrador: An explanation of historical changes in exploitation, harvesting technology, and management. The North Atlantic Fisheries: successes, failures and challenges. 3:37-93.

Hutchings, J.A., Myers, R.A., and Lilly, G.R., 1993. Geographic variation in the spawning of Atlantic cod, *Gadus morhua*, in the Northwest Atlantic. Canadian Journal of Fisheries and Aquatic Science, 50, pp. 2457-2467.

Iles, T.C. 1994. A review of stock-recruitment relationships with reference to flatfish populations. Neth. J. Sea Res. 32:399-420.

Iles, T.C. and Beverton, R.J.H. 1998. Stock, recruitment and moderating processes in flatfish. J. Sea. Res. 39:41-55.

Jiao, Y. Chen, Y. Schneider, D., and Wroblewski, J. 2003. A simulation study of impacts of error structure on modeling stock-recruitment data using generalized linear model. Can. J. Fish. Aquat. Sci. (in press)

Koslow, I.A., Thompson, K.R., and Silvert, W. 1987. Recruitment of Northwest Atlantic cod (*Gadus morhua*) and Haddock (*Melanogrammus aeglefinus*) stocks: influence of stock size and climate. Can. J. Fish. Aquat. Sci.

Koster, F. W., Hinrichsen, H.-H., St. John, M.A., Schnack, D., MacKenzie, B.R. Tomkiewicz, J., Plikshs, M. 2001. Developing Baltic cod recruitment models. II. Incorporation of environmental variability and species interaction. Can. J. Fish. Aquat. Sci. 58:1534-1556.

Krohn, M., Kerr, S. 1997. Declining weight-at-age in northern cod and the potential importance of the early years and size-selcvtive fishing mortality. Northwest Atlantic Fisheries Organization Scientific Council Studies. 29:43-50.

Krohn, M., Reidy, S., Kerr, S. 1997. Bioenergentic analysis of the effects of temperature and prey availability on growth and condition of northern cod (*Gadus morhua*). Can. J. Fish. Aquat. Sci. 54(1): 113-121

Kulka, D.W. 1996. Discarding of cod (*Gadus morhua*) in the Northern Cod and Northern Shrimp directed fisheries from 1980-1994. NAFO SCR Doc. 96/46. Serial No. N2721, 15pp.

Kurlansky, M., 1997. Cod: A Biography of the Fish That Changed the World. Alfred A. Knopf, Toronto.

Lande, R., Engen, S., and Sther, B.E. 2003. Stochatic population dynamics models in ecology and conservation: an introduction. Oxford University Press, Oxford.

Lapointe, M.F., Peterson, R.M. and Rothschild, B.J. 1992. Variable natural mortality rates inflate variance of recruitment estimated from virtual population analysis (VPA). Can. J. Fish. Aquat. Sci. 29: 2020-2027.

Lawson, G.L., and Rose, G.A. 2000. Seasonal distribution and movements of coastal cod (*Gadus morhua* L.) in Placentia Bay, Newfoundland. Fish. Res. 49: 61-75

Lear, W.H. and Parsons, L.S. 1993. History and management of the fishery for northern cod in NAFO Divisions 2J, 3K and 3L. in Parsons, L.S. and Lear, W.H. eds. Perspectives on Canadian Marine Fisheries Management. Can. Bull. Fish. Aquat. Sci. No. 226. 55-89.

Lear, W.H., 1993. Atlantic Cod. In Underwater World. Department of Fisheries and Oceans.

Lilly, G.R. 1996. Growth and condition of cod in Subdivision 3Ps as determined from trawl surveys (1972-1996) and sentinel surveys (1995). DFO Atlantic Fish. Res. Doc. 96/69

Lilly, G.R. 1998. Size-at-age and condition of cod in Division 2J+3KL. Zonal Assessment of Atlantic Cod Stocks. Working Paper (98)5-7

Lilly, G.R., Shelton, P.A., Brattey, J., Cadigan, N.G., Healey, B.P., Murphy, E.F., and Stansbury, D.E. 2001. An assessment of the cod stock in NAFO Divisions 2J+3KL. DFO Canadian Science Advisory Secretariat Research Document 2001/044. 148pp.

Lindsey, J.K. 1997. Applying Generalized Linear Models. Springer, New York.

Ludwig, D., Hilborn, R., and Walters, C. 1993. Uncertainty, resource exploitation and conservation: Lessons from history. Science (Washington, D.C.), 260:17-36.

McCullagh, P., and Nelder, J.A. 1989. Generalized Linear Models. Chapman and Hall, New York.

Megrey, B.A. 1989. Review and comparison of age-structured stock assessment models from theoretical and applied points of view. Am. Fish. Soc. Symp. **6**: 8–48.

Mohn, R. and Bowen, W.D. 1996. Grey seal predation on the eastern Scotian Shelf: Modelling the impact of Atlantic cod. Can. J. Fish. Aquat. Sci. 53:2722-2738

Mohn, R.K., and Cook, R. 1993. Introduction to sequential population analysis. NAFO Sci. Counc. Stud. No. 17.

Myers, R. A., and Worm, B. 2003. Rapid worldwide depletion of predatory fish communities. Nature, 423: 280-283.

Myers, R.A. 1989. Estimating bias in growth caused by size-selective fishing mortality. ICES COUNCIL MEETING.

Myers, R.A. and Barrowman, N.J. 1996. Is fish recruitment related to spawner abundance? Fish. Bull. 94:707-724.

Myers, R.A., and Mertz, G. 1998. The limits of exploitation: a precautionary approach. Ecol. Appl. 8 (Suppl. 1):165-169.

Myers, R.A., and Pepin, P. 1990. The robustness of lognormal based estimators of abundance. Biometrics, **46**: 1185–1192.

Myers, R.A., Bridson, J., and Barrowman, N.J. 1995. Summary of worldwide spawner and recruitment data. Can. Tech. Rep. Fish. Aquat. Sci. No. 2024.

Myers, R.A., Hutchings, J,A., Barrowman, N.J. 1996. Hypotheses for the decline of cod in the North Atlantic. Mar. Ecol. Prog. Ser. 138:293-308

Myers, R.A., Hutchings, J.A., and Barrowman, N.J., 1997. Why do fish stocks collapse? The example of cod in Atlantic Canada. Ecological Applications, 7, pp. 91-106.

Myers, R.H., Montgomery, D.C. and Vining, G.G. 2001. Generalized Linear Models: with Application in Engineering and the Science. John Wiley & Sons, Inc., New York.

Nelder, J.A. and Wedderburn, R.W.M. 1972. Generalized Linear Models. J. R. Statist. Soc. A. 135:370-384.

Ottersen, G. and Loeng, H., 2000. Covariability in early growth and year class strength of Barents Sea cod, haddock and herring: The environmental link. ICES J. Mar. sci., 57(2): 339-348.

Parsons, L.S. 1993. Management of Marine Fisheries in Canada. Can. Bull. Fish. Aquat. Sci. No. 225.

Patterson, K., Cook, R., Darby, C., Gavaris, S., Kell, L., et al. 2001. Estimating uncertainty in fish stock assessment and forecasting. Fish and Fisheries 2:125-157.

Pierce, D. A., and Schafer, D. W. 1986. Residuals in generalized linear models. J. Am. Statist. Assoc. 81: 977-986.

Polacheck, T., Hilborn, R., and Punt, A.E. 1993. Fitting surplus production models: comparing methods and measuring uncertainty. Can. J. Fish. Aquat. Sci. 50:2597-2607.

Power, M. 1996. The testing and selection of recruitment distributions from North Atlantic fish stocks. Fish. Res. 25:77-95.

Prager, M. H., Porch, C. E., Shertzer, K.W., and Caddy, J. F. 2003. Target and limits for management of fisheries: A simple probability-based approach. North American Journal of Fisheries Management, 23: 349-361.

Punt, A.E. 1988. Model selection for the dynamics of Southern African hake resources. Report Benguela Ecology Program of South Africa. 15:395.

Quinn, T.J. and Deriso, R.B. 1999. Quantitative Fish Dynamics. Oxford University Press, New York. 542pp.

Restrepo, V.R. and Powers, J.E. 1997. Application of high-breakdown robust regression to tuned stock assessment models. Fish. Bull. 95:149-160.

Rice, J. and Rivard, D. 2002. Proceedings of the DFO workshop in implementing the precautionary approach in assessments and advice. CSAS Proceeding Series 2002/009.

Ricker, W.E. 1975. Computation and Interpretation of Biological Statistics of Fish Populations. Fish. Res. Board Can. No. 191.

Rigler, F. H. (1982) The relation between fisheries management and limnology. Trans. Am. Fish. Soc. 111:121-132.

Rose, G.A., 1993. Cod spawning on a migration highway in the north-west Atlantic. Nature, 366, pp. 458-461.

Rose, G.A., Atkinson, B.A., Baird, J., Bishop, C.A., and Kulka, D.W., 1994. Changes in distribution of Atlantic cod and thermal variations in Newfoundland waters, 1980-1992. ICES Marine Science Symposia, 198, pp. 542-552.

Rose, G.A., deYoung, B., Kulka, D.W., Goddard, S.V., and Fletcher, G.L. 2000. Distribution shifts and overfishing the Northern Cod (*Gadus morhua*): a view from the ocean. Can. J. Fish. Aquat. Sci. 57: 644-663

Rosenberg, A.A. and Restropo, V.R. 1994. Uncertainty and risk evaluation in stock assessment advice for U.S. marine fisheries. Can. J. Fish. Aquat. Sci. 51:2715-2720

Schnute, J.T. 1989. The influence of statistical error in stock assessment: illustrations from Schaefers's model. *In* Effect of Ocean variability on recruitment and an evaluation of parameters used in stock assessment models. *Edited by* R.J. Beamish and G. A. McFarlane. Can. Spec. Publ. Fish. Aquat. Sci. No. 108. pp 101-109.

Schnute, J.T. 1991. The importance of noise in fish population models. Fish. Res. 11:197-223.

Schnute. J.T. and Richards, L.J. 2001. Use and abuse of fishery models. Can. J. Fish. Aquat. Sci. 58:10-17.

Scott, W.B., and Scott, M.G., 1988. Atlantic Fishes of Canada. Can. Bull. of Fish. and Aquat. Sci. 219. University of Toronto Press, Toronto.

Shelton, P. and Rice, J. 2002. Limits to overfishing: reference points in the context of the Canadian perspective on the precautionary approach. CSAS 2002/084. 28pp.

Shelton, P.A. 1992. The shape of recruitment distribution. Can. J. Fish. Aquat. Sci. 49: 1754-1761.

Shelton, P.A. 1998. A comparison between a fixed and a variable fishing mortality control rule used to manage the cod stock off southern Labrador and the east coast of Newfoundland. Fisheries Research. 37:275-286.

Shelton, P.A. and Healey, B.P. 1999. Should depensation be dismissed as a possible explanation for the lack of recovery of the northern cod (*Gadus morhua*) stock? Can. J, fish. Aquat. Sci. 56:1521-1524

Shelton, P.A., Stansbury, D.E., Murphy, E.F., Lilly, G.R. and Bratty, J. 1996. An assessment of the cod stock in NAFO Divisions 2J+3KL. DFO Atlantic Fisheries Research Document 96/80.

Shelton, P.A., and Lilly, G.R. 2000. Interpreting the collapse of the northern cod stock from survey and catch data. Can. J. Fish. Aquat. Sci. 57:2230-2239.

Shelton, P.A., Lilly, G.R., Colbourne, E. 1999. Patterns in the annual weight increment for Div. 2J+3KL cod and possible prediction for stock projection. J. Northwest Atl. Fish. Sci. 25:151-159

Shepherd, J.G. 1988. Fish stock assessments and their data requirements. *In* Fish population dynamics. *Edited by* J.A. Gulland. Wiley, New York. pp. 35–62.

Shertzer, K. and Prager, M. 2002. Least median of squares: a suitable objective function for stock assessment models? Can. J. Fish. Aquat. Sci. 59:1474-1481

Smith, S. J., Hunt, J.J., and Rivard, D. (ed.) 1993. Risk evaluation and biological reference points for fisheries management. Can. Spec. Publ. Fish. Aquat. Sci. 120.

Stansbury, D.E. Shelton, P.A., Stenson, G.B., Sjare, B. and Lilly, G.R. 1998. Catch at age of 2J3KL cod in the diet of harp seals. DFO CSAS Res. Doc. 1998/75.

Steele, JH. 1998. Regime shifts in marine ecosystems. Ecological Applications. 1 suppl. S33-S36.

Swain, D.P. 1993. Age- and density-dependent bathymetric pattern of Atlantic cod (*Gadus morhua*) in the southern Gulf of St. Lawrence. Can. J. Fish. Aquat. Sci. 50, 1255-1264

Taggart, C.T., Anderson, J., Bishop, C., Colbourne, E., Hutchings, J., Lilly, G., Morgan, J., Murphy, E., Myers, R., Rose, G., and Shelton, P., 1994. Overview of cod stocks, biology, and environment in the Northwest Atlantic region of Newfoundland, with emphasis on northern cod. ICES Marine Science Symposia, 198, pp. 140-157.

Templeman, W., 1979. Migration and intermingling of stocks of Atlantic Cod, *Gadus morhua*, of Newfoundland and Adjacent Areas from Tagging in 1962-66.

The Math Works Inc. 2002. MATLAB --- the language of technical computing. Natick, M.A.

The Math Works Inc. 1999. MATLAB Reference Guide.

Tripple, E.A. 1995. Age at maturity as a stress indicator in fisheries. BioScience. 45(11), 759-771

Walters, C. and Maguire, J.J. 1996. Lessons for stock assessment from the northern cod collapse. Rev. Fish Biol. Fish. 6:125-137.

Walters, C. J. 1998. Evaluation of quota management policies for developing fisheries. Can. J. Fish. Aquat. Sci. 55:2691-2705.

Walters, C.J. 1986. Adaptive Management of Renewable Resources. MacMillan, New York.

White, G.C. and Bennetts, R.E. 1996. Analysis of frequency count data using the negative binomial distribution. Ecology. 77: 2549-2557.

Xiao, Y. 1997. Subleties in, and practical problems with, the use of production models in fish stock assessment. Fish. Res. 33: 17-36.

Xiao, Y. 2000. A general theory of fish stock assessment models. Ecol. Model. 128: 165-180.

Yen, B.C. 1986. Stochastic and risk analysis in hydraulic engineering. Water resources publication, Littleton, Colorado.

Zhang, C.I., Gunderson, D.R., and Sullivan, P.J. 1991. Using data of biomass and fishing mortality in stock production modeling of flatfish. Neth. J. Sea Res. 27: 459-467.

Appendix

Table 1A: Summary of the simulations when the model error distributions used in the GzLM analyses were the same as those used in simulating SR data. The Ricker model and the first set of data which had S values randomly drawn from 1000 to 10000 were used in the simulation.

Model error distribution in simulating SR data	Number of Observations	% of simulations with homogeneous residuals	REB for $\ln(\alpha)$ (%)	REB for β (%)	RMSE for $\ln(\alpha)$	RMSE for β (10^{-5})
Normal	10	88.8	0.04	0.21	0.07	1.34
	20	90.3	0.12	0.53	0.05	0.90
	40	89.6	0.01	0.04	0.03	0.61
Lognormal	10	88.6	0.19	0.29	0.45	10.44
	20	88.7	1.39	9.52	0.30	6.70
	40	89.5	0.22	0.77	0.20	4.72

Gamma	10	85.8	0.01	0.34	0.06	1.42
	20	83.1	0.02	0.06	0.04	0.94
	40	79.7	0.01	0.03	0.03	0.64
Poisson	10	89.6	0.04	0.20	0.01	0.23
	20	89.6	0.004	0.01	0.01	0.15
	40	90.3	0.01	0.05	0.01	0.10

Table 2A: Summary of the simulations when the model error distributions used in the GzLM analyses were not the same as those used in simulating SR data. The Ricker model and the first set of data which had S values randomly drawn from 1000 to 10000 were used in the simulation.

Model error distribution		Number of SR observations	% of simulations with homogeneous residuals	REB for $\ln(\alpha)$ (%)	REB for β (%)	RMSE for $\ln(\alpha)$	RMSE for β (10^{-5})
In simulating SR data	In GzLM						
Normal	Lognormal	20	35.4	0.47	1.27	0.07	1.29
		40	8.8	1.1	3.79	0.05	0.95
	Gamma	20	35.8	0.22	0.86	0.06	1.27
		40	7.6	0.34	1.41	0.05	0.91
	Poisson	20	66.9	0.21	0.84	0.05	0.99
		40	48	0.13	0.58	0.04	0.68
Lognormal	Normal	20	52.9	6.72	17.07	0.44	9.10
		40	24.9	10.69	1.62	0.32	6.48
	Gamma	20	91.7	9.49	8.23	0.33	7.02
		40	91.9	11.45	0.66	0.25	5.05
	Poisson	20	78.4	9.74	6.82	0.35	7.36
		40	65.5	11.84	2.33	0.26	5.36
Gamma	Normal	20	62.2	0.04	0.09	0.05	1.04

		40	33.5	0.08	0.34	0.04	0.74
	Lognormal	20	82.9	0.31	0.45	0.04	0.94
		40	78.3	0.31	0.49	0.03	0.64
	Poisson	20	84.7	0.01	0.06	0.04	0.93
		40	83.1	0.04	0.19	0.03	0.65
Poisson	Normal	20	78.3	0.01	0.03	0.01	0.16
		40	60.0	0.02	0.06	0.01	0.11
	Lognormal	20	70.5	0.01	0.03	0.01	0.17
		40	49.2	0.02	0.07	0.01	0.11
	Gamma	20	71.5	0.004	0.01	0.01	0.15
		40	50.5	0.01	0.04	0.01	0.11

Table 3A: Summary of the simulations when the Ricker model and the second set of data which had true S values of pink salmon were used in the simulation.

Model error distribution		% of simulations with homogeneous residuals	REB for ln(α) (%)	REB for β (%)	RMSE for ln(α)	RMSE for β (10^{-5})
In simulating SR data	In GzLM					
Normal	Normal	90.6	0.13	0.52	0.03	0.58
	Lognormal	33.8	0.59	1.93	0.04	0.93
	Gamma	38.3	0.01	0.08	0.04	0.92
	Poisson	68.3	0.10	0.41	0.03	0.64
Lognormal	Normal	82.7	14.22	15.32	0.32	7.52
	Lognormal	92.1	0.31	1.13	0.23	6.59
	Gamma	94.2	12.70	6.69	0.28	6.86
	Poisson	90.9	14.22	14.74	0.29	6.90
Gamma	Normal	88.7	0.10	0.47	0.04	0.93
	Lognormal	83.2	0.38	0.86	0.03	0.84
	Gamma	84.8	0.06	0.34	0.03	0.84
	Poisson	94.8	0.07	0.34	0.03	0.84
Poisson	Normal	94.1	0.03	0.15	0.01	0.13
	Lognormal	73.8	0.01	0.05	0.01	0.14
	Gamma	76.8	0.01	0.07	0.01	0.14
	Poisson	91.8	0.02	0.11	0.01	0.13

Table 4A: Summary of simulations when the model error distributions used in the GzLM analyses were the same as those used in simulating SR data. The Ricker model and the first set of data which had S values randomly drawn from 1000 to 10000 were used in the simulation. Sample size was 40.

Model error distribution in simulating SR data	Distribution that outliers follow	% of data being outliers	% of simulations with homogeneous residuals	REB for $\ln(\alpha)$ (%)	REB for β (%)	RMSE for $\ln(\alpha)$	RMSE for β (10^{-5})
Normal	Lognormal	10	80.5	1.39	0.34	0.11	2.34
		20	73.4	1.68	2.99	0.15	3.38
		40	60.5	4.42	1.37	0.22	4.68
Lognormal	Normal	10	90.1	1.53	7.04	0.19	4.49
		20	90.3	0.10	2.39	0.18	4.23
		40	89.4	0.65	2.15	0.16	3.66
Ga	Normal	10	71.7	0.08	0.52	0.03	0.66
		20	61.6	0.04	0.16	0.03	0.69

		40	45.8	0.11	0.27	0.04	0.74
Poisson	Normal	10	84.0	0.04	0.21	0.02	0.23
		20	81.6	0.09	0.34	0.02	0.31
		40	74.2	0.03	0.13	0.02	0.44

Table 5A: Summary of the simulations when the model error distributions used in the GzLM analyses were not the same as those used in simulating SR data. The Ricker model and the first set of data which had S values randomly drawn from 1000 to 10000 were used in the simulation. Sample size was 40.

Model error distribution		% of data being outliers	% of simulations with homogeneous residuals	REB for $\ln(\alpha)$ (%)	REB for β (%)	RMSE for $\ln(\alpha)$	RMSE for β (10^{-5})
In simulating SR data	In GzLM						
Normal	Lognormal	10	68.1	0.42	1.62	0.08	1.73
		20	79.1	0.93	3.82	0.10	2.26
	Gamma	10	68.3	1.35	0.01	0.09	1.91
		20	76.9	2.14	1.43	0.11	2.58
	Poisson	10	82.0	1.51	0.69	0.09	1.98
		20	81.0	2.20	1.17	0.12	2.76
Lognormal	Normal	10	29.9	10.19	1.99	0.31	6.17
		20	37.6	8.14	0.64	0.28	5.87
	Gamma	10	93.2	11.49	6.34	0.24	4.72
		20	92.2	9.37	3.40	0.22	4.52
	Poisson	10	65.1	11.67	7.16	0.25	5.01
		20	71.8	9.48	4.00	0.24	4.83
Gamma	normal	10	39.4	0.10	0.18	0.03	0.72

		20	49.4	0.02	0.04	0.03	0.72
	Lognormal	10	71.3	0.42	1.13	0.03	0.67
		20	60.6	0.44	1.00	0.03	0.71
	Poisson	10	85.2	0.02	0.12	0.03	0.64
		20	88.8	0.02	0.04	0.03	0.66
Poisson	Normal	10	78.6	0.03	0.19	0.01	0.22
		20	84.6	0.05	0.21	0.02	0.29
	Lognormal	10	62.2	0.05	0.05	0.02	0.30
		20	56.4	0.05	0.04	0.02	0.40
	Gamma	10	62.5	0.04	0.21	0.01	0.30
		20	56.9	0.12	0.47	0.02	0.40

Table 6A: Summary of the simulations when the model error distributions used in the GzLM analyses were the same as those used in simulating SR data. The Ricker model and the second set of data which had true S values of pink salmon were used in the simulation.

Model error distribution in simulating SR data	Distribution that outliers follow	% of data being outliers	% of simulations with homogeneous residuals	REB for $\ln(\alpha)$ (%)	REB for β (%)	RMSE for $\ln(\alpha)$	RMSE for β (10^{-5})
Normal	Lognormal	10	87.5	1.86	1.42	0.06	0.84
		20	77.2	1.15	17.22	0.26	7.49
		40	43.6	2.35	15.94	0.27	7.36
Lognormal	Normal	10	88.5	1.22	2.41	0.23	6.35
		20	81.6	0.47	0.52	0.17	4.03
		40	39.9	0.09	0.77	0.17	3.65
Gamma	Normal	10	84.0	0.10	0.58	0.03	0.84
		20	82.6	0.03	0.22	0.03	0.71

		40	74.7	0.06	0.01	0.03	0.70
Poisson	Normal	10	93.1	0.04	0.14	0.01	0.17
		20	89.5	0.02	0.03	0.01	0.42
		40	66.3	0.08	0.44	0.02	0.42

Table 7A: Summary of the simulations when the model error distributions used in the GzLM analyses were not the same as those used in simulating SR data. The Ricker model and the second set of data which had true S values of pink salmon were used in the simulation.

Model error distribution		% of data being outliers	% of simulations with homogeneous residuals	REB for $\ln(\alpha)$ (%)	REB for β (%)	RMSE for $\ln(\alpha)$	RMSE for β (10^{-5})
In simulating SR data	In GzLM						
Normal	Lognormal	10	93.2	0.62	2.25	0.05	1.66
		20	82.4	0.74	3.04	0.15	5.13
	Gamma	10	93.4	0.20	8.16	0.06	1.95
		20	81.0	0.54	15.72	0.15	5.22
	Poisson	10	91.5	0.94	2.43	0.05	1.24
		20	79.9	0.62	16.02	0.21	6.47
Lognormal	Normal	10	92.8	13.44	18.29	0.33	7.97
		20	94.3	14.75	33.32	0.21	2.95
	Gamma	10	90.3	14.12	19.44	0.28	6.64
		20	84.3	12.43	21.71	0.23	4.54
	Poisson	10	94.4	14.46	21.64	0.29	7.11
		20	94.4	14.19	31.06	0.21	3.48
Gamma	Normal	10	90.9	0.15	0.85	0.04	0.94

		20	93.6	0.05	0.32	0.03	0.58
	Lognormal	10	82.9	0.21	0.04	0.03	0.84
		20	80.3	0.29	0.40	0.03	0.70
	Poisson	10	93.3	0.15	0.84	0.03	0.85
		20	95.1	0.05	0.32	0.03	0.58
Poisson	Normal	10	87.0	0.04	0.14	0.01	0.15
		20	84.2	0.03	0.01	0.02	0.49
	Lognormal	10	94.8	0.06	0.10	0.01	0.21
		20	95.0	0.01	0.003	0.01	0.35
	Gamma	10	95.3	0.04	0.14	0.01	0.21
		20	94.8	0.01	0.06	0.01	0.35

Table 8A: Summary of the simulations when the model error distributions used in the GzLM analyses were the same as those used in simulating SR data. The Beverton-Holt model and the first set of data which had S values randomly drawn from 1000 to 10000 were used in the simulation.

Model error distribution in simulating SR data	Number of Observations	% of simulations with homogeneous residuals	REB for $\ln(\alpha)$ (%)	REB for β (%)	RMSE for $\ln(\alpha)$	RMSE for β (10^{-5})
Normal	10	77.1	0.31	0.38	0.09	2.43
	20	78.1	0.21	1.68	0.06	1.68
	40	81.1	0.07	0.59	0.04	1.10
Lognormal	10	79.7	0.15	0.41	0.07	0.09
	20	82.4	5.43	1.35	0.06	0.08
	40	89.2	5.06	1.32	0.04	0.07
Gamma	10	74.6	0.04	1.92	0.08	2.16
	20	70.8	0.05	0.82	0.05	1.45

	40	70.2	0.08	0.42	0.04	0.99
Poisson	10	74.6	0.03	0.23	0.01	0.37
	20	79.1	0.01	0.07	0.01	0.25
	40	79.9	0.003	0.03	0.01	0.16

Table 9A: Summary of the simulations when the model error distributions used in the GzLM analyses were not the same as those used in simulating SR data. The Beverton-Holt model and the first set of data which had S values randomly drawn from 1000 to 10000 were used in the simulation.

Model error distribution		Number of SR observations	% of simulations with homogeneous residuals	REB for $\ln(\alpha)$ (%)	REB for β (%)	RMSE for $\ln(\alpha)$	RMSE for β (10^{-5})
In simulating SR data	In GzLM						
Normal	Lognormal	20	23.8	5.43	1.35	0.06	0.08
		40	15.2	5.43	1.35	0.06	0.08
	Gamma	20	24.6	0.09	1.61	0.08	2.02
		40	3.8	0.14	1.28	0.05	1.35
	Poisson	20	53.4	0.20	1.60	0.06	1.59
		40	34.4	0.12	0.93	0.04	1.05
Lognormal	Normal	20	29.9	12.98	69.23	0.45	27.95
		40	10.2	13.39	36.23	0.32	13.02
	Gamma	20	59.2	15.20	73.00	0.41	24.85
		40	61.4	14.47	39.01	0.30	11.84
	Poisson	20	66.3	15.01	71.85	0.37	24.97
		40	49.1	14.47	39.01	0.29	13.13
Gamma	Normal	20	38.7	0.12	1.12	0.05	1.51

		40	16.7	0.04	0.19	0.04	1.01
	Lognormal	20	37.9	15.13	4.15	0.16	0.98
		40	15.7	10.29	2.78	0.14	0.67
	Poisson	20	75.0	0.12	1.15	0.05	1.46
		40	68.6	0.07	0.35	0.04	0.98
Poisson	Normal	20	57.2	0.02	0.12	0.01	0.26
		40	36.1	0.003	0.02	0.01	0.18
	Lognormal	20	60.0	0.003	0.13	0.06	0.18
		40	35.6	0.01	0.02	0.01	0.19
	Gamma	20	52.8	0.03	0.15	0.02	0.27
		40	37.3	0.001	0.01	0.01	0.18

Table 10A: Summary of the simulations when the Beverton-Holt model and the second set of data which had true S values of pink salmon were used in the simulation.

Model error distribution		% of simulations with homogeneous residuals	REB for $\ln(\alpha)$ (%)	REB for β (%)	RMSE for $\ln(\alpha)$	RMSE for β (10^{-5})
In simulating SR data	In GzLM					
Normal	Normal	81.7	0.02	1.13	0.03	1.19
	Lognormal	30.5	0.05	1.35	0.05	1.59
	Gamma	31.1	0.05	1.41	0.05	1.58
	Poisson	57.0	0.05	1.03	0.04	1.10
Lognormal	Normal	33.5	14.70	103.94	0.44	36.76
	Lognormal	89.7	13.48	101.35	0.35	30.81
	Gamma	86.1	14.52	109.10	0.42	31.78
	Poisson	82.6	19.92	109.16	0.43	31.32
Gamma	Normal	37.9	0.10	0.25	0.04	1.56
	Lognormal	36.0	0.08	0.27	0.04	1.45
	Gamma	72.7	0.01	0.29	0.04	1.40
	Poisson	85.0	0.05	0.63	0.04	1.41
Poisson	Normal	51.2	0.04	0.22	0.01	0.26
	Lognormal	52.4	0.03	0.19	0.01	0.25

Gamma	56.9	0.03	0.18	0.01	0.24
Poisson	81.1	0.02	0.15	0.01	0.21

Table 11A: Summary of simulations when the model error distributions used in the GzLM analyses were the same as those used in simulating SR data. The Beverton-Holt model and the first set of data which had S values randomly drawn from 1000 to 10000 were used in the simulation. Sample size was 40.

Model error distribution in simulating SR data	Distribution that outliers follow	% of data being outliers	% of simulations with homogeneous residuals	REB for $\ln(\alpha)$ (%)	REB for β (%)	RMSE for $\ln(\alpha)$	RMSE for β (10^{-5})
Normal	Lognormal	10	74.8	1.32	3.69	0.11	3.45
		20	53.7	1.82	3.72	0.14	4.32
		40	40.3	4.91	11.81	0.20	6.43
Lognormal	Normal	10	84.2	12.37	30.62	0.21	8.83
		20	81.0	11.54	26.43	0.27	8.56
		40	80.7	5.74	6.35	0.22	6.78
Gamma	Normal	10	69.2	0.07	0.13	0.04	1.03
		20	47.9	0.02	0.28	0.04	1.09

		40	41.9	0.10	1.27	0.04	1.21
Poisson	Normal	10	70.5	0.01	0.06	0.01	0.38
		20	66.8	0.06	0.23	0.02	0.49
		40	62.6	0.03	0.25	0.03	0.69

Table 12A: Summary of the simulations when the model error distributions used in the GzLM analyses were not the same as those used in simulating SR data. The Beverton-Holt model and the first set of data which had S values randomly drawn from 1000 to 10000 were used in the simulation. Sample size was 40.

Model error distribution		% of data being outliers	% of simulations with homogeneous residuals	REB for $\ln(\alpha)$ (%)	REB for β (%)	RMSE for $\ln(\alpha)$	RMSE for β (10^{-5})
In simulating SR data	In GzLM						
Normal	Lognormal	10	69.4	0.13	3.69	0.11	3.42
		20	56.7	1.97	5.42	0.14	4.30
	Gamma	10	54.3	1.27	3.71	0.10	3.37
		20	65.9	2.27	5.88	0.13	4.24
	Poisson	10	70.8	1.51	1.90	0.02	4.92
		20	69.2	2.30	3.35	0.03	5.51
Lognormal	Normal	10	15.9	12.33	31.71	0.30	9.19
		20	19.7	11.01	26.80	0.28	8.84
	Gamma	10	83.1	13.09	34.80	0.29	8.95
		20	81.0	11.64	28.93	0.27	8.24
	Poisson	10	53.2	13.25	30.86	0.21	11.19
		20	57.7	11.87	31.18	0.27	9.11
Gamma	normal	10	22.8	0.09	0.01	0.04	1.03

		20	26.7	0.07	0.03	0.04	1.04
	Lognormal	10	50.9	0.07	0.14	0.04	1.03
		20	48.2	0.02	0.28	0.04	1.01
	Poisson	10	76.2	0.04	0.26	0.03	0.99
		20	77.6	0.02	0.20	0.04	1.01
Poisson	Normal	10	66.8	0.02	0.10	0.02	0.40
		20	71.4	0.05	0.21	0.02	0.51
	Lognormal	10	64.3	0.02	0.06	0.02	0.47
		20	71.4	0.05	0.21	0.02	0.61
	Gamma	10	49.9	0.01	0.06	0.02	0.48
		20	66.8	0.06	0.23	0.02	0.49

Table 13A: Summary of the simulations when the model error distributions used in the GzLM analyses were the same as those used in simulating SR data. The Beverton-Holt model and the second set of data which had true S values of pink salmon were used in the simulation.

Model error distribution in simulating SR data	Distribution that outliers follow	% of data being outliers	% of simulations with homogeneous residuals	REB for $\ln(\alpha)$ (%)	REB for β (%)	RMSE for $\ln(\alpha)$	RMSE for β (10^{-5})
Normal	Lognormal	10	59.8	0.91	7.57	0.12	4.81
		20	34.5	1.56	12.93	0.17	6.94
		40	22.1	41.3	25.15	0.23	10.38
Lognormal	Normal	10	72	3.51	14.77	0.09	2.11
		20	70.3	4.90	16.84	0.10	2.45
		40	50.1	6.10	22.27	0.20	6.39
Gamma	Normal	10	72.9	0.05	1.09	0.04	1.32

		20	70.4	0.09	0.16	0.04	1.17
		40	61.0	0.21	1.31	0.04	1.18
Poisson	Normal	10	78.7	0.02	0.17	0.01	0.28
		20	70.1	0.004	0.30	0.02	0.67
		40	47.3	0.11	0.82	0.02	0.70

Table 14A: Summary of the simulations when the model error distributions used in the GzLM analyses were not the same as those used in simulating SR data. The Beverton-Holt model and the second set of data which had true S values of pink salmon were used in the simulation.

Model error distribution		% of data being outliers	% of simulations with homogeneous residuals	REB for $\ln(\alpha)$ (%)	REB for β (%)	RMSE for $\ln(\alpha)$	RMSE for β (10^{-5})
In simulating SR data	In GzLM						
Normal	Lognormal	10	54.8	1.54	1.95	0.07	1.60
		20	36.2	0.75	11.77	0.18	6.84
	Gamma	10	82.7	0.27	3.13	0.08	3.15
		20	76.3	0.46	6.69	0.16	6.79
	Poisson	10	73.8	0.74	0.97	0.08	2.81
		20	66.6	0.05	7.91	0.24	9.25
Lognormal	Normal	10	44.5	4.72	21.05	0.16	6.06
		20	52.1	3.86	15.32	0.15	5.16
	Gamma	10	82.3	4.93	22.21	0.15	5.65
		20	70.2	4.48	17.71	0.13	4.16
	Poisson	10	87.2	5.53	27.62	0.17	6.23
		20	87.2	4.81	17.59	0.11	3.13
Gamma	Normal	10	39.3	0.001	0.79	0.04	1.42

		20	61.5	0.17	1.21	0.04	1.46
	Lognormal	10	37.9	0.07	1.32	0.04	1.35
		20	62.1	0.26	1.44	0.03	0.95
	Poisson	10	85.4	0.09	1.36	0.04	1.36
		20	87.6	0.28	1.60	0.03	1.00
Poisson	Normal	10	31.7	0.04	0.33	0.01	0.51
		20	36.1	0.05	0.52	0.02	0.64
	Lognormal	10	56.2	0.01	0.18	0.01	0.39
		20	60.4	0.04	0.59	0.02	0.81
	Gamma	10	79.2	0.01	0.14	0.01	0.35
		20	80.1	0.06	0.53	0.01	0.52